DESIGN AND ANALYSIS OF THE VERTICAL CONTROL FOR THE SUPERCONDUCTING SUPER COLLIDER PROJECT IN TEXAS

P. W. DeKROM

September 1995

GEODESY AND GEOMATICS ENGINEERING
UNB

TECHNICAL REPORT
NO. 173

PREFACE

In order to make our extensive series of technical reports more readily available, we have scanned the old master copies and produced electronic versions in Portable Document Format. The quality of the images varies depending on the quality of the originals. The images have not been converted to searchable text.

DESIGN AND ANALYSIS OF THE VERTICAL CONTROL FOR THE SUPERCONDUCTING SUPER COLLIDER PROJECT IN TEXAS

Peter W. DeKrom

Department of Geodesy and Geomatics Engineering
University of New Brunswick
P.O. Box 4400
Fredericton, N.B.
Canada
E3B 5A3

September 1995

PREFACE

This technical report is a reproduction of a thesis submitted in partial fulfillment of the requirements for the degree of Master of Science in Engineering in the Department of Geodesy and Geomatics Engineering, August 1994. The research was supervised by Dr. Adam Chrzanowski, and funding was provided partially by the Natural Sciences and Engineering Research Council of Canada, and John E. Chance and Associates.

 The citation to this work should appear as follows:

DeKrom, P. W. (1995). *Design and Analysis of the Vertical Control for the Superconducting Super Collider Project in Texas.* M.Sc.E.. report, Department of Geodesy and Geomatics Engineering Technical Report No. 173, University of New Brunswick, Fredericton, New Brunswick, Canada, 101 pp.

Abstract

The stringent accuracy requirements of the Superconducting Super Collider (SSC) have required a rigorous approach in designing and analyzing the vertical control required for the construction of the tunnel. All possible sources of errors are estimated to determine a realistic value for the achievable accuracy.

This thesis deals with the design of the network and the development of standards, specifications and procedures, unique to the SSC Project. All forms of vertical control were included in the standards, specifications and procedures, such as surface control (Primary Vertical Control Network), densification on the service areas where the shafts are located, elevation transfer techniques, and propagation of control in the tunnels.

Geodetic effects that are deemed important in the Primary Vertical Control Network are analyzed to ensure the adjusted elevations are accurate and reliable. The use of a correct weighting scheme is analyzed through the use of the Minimum Norm Quadratic Estimation (MINQE) and adjusted accordingly. Densification, elevation transfers, tunnel control and the initial tunnel breakthroughs are analyzed to be all within the tunneling requirements. The final tunnel elevations are calculated by the combined adjustment of all densification and shaft transfer surveys. The improvement of accuracy of the combined adjustment with that of the adjustment prior to breakthrough shows an increase of up to 2.8 mm at the 99 percent level of confidence.

The determination of an appropriate geoidal model was performed using a combination of Global Positioning System (GPS) and levelling to acquire a micro-geoid for accurate final invert elevations. The geoid undulations were determined to an accuracy of 13 mm at the 99 percent level of confidence.

Final estimated accuracy of 14 mm to 17 mm at the 99 percent level of confidence can be achieved for the invert elevations of the main tunnel.

Acknowledgements

I wish to express my deepest gratitude and sincere thanks to my supervisor, Dr. A. Chrzanowski. His constructive suggestions were invaluable and highly appreciated.

In addition, I would like to thank Greg Robinson, Vicky Labrecque and Trevor Greening for their constructive criticism of this thesis.

I would also like to thank all the office and field personnel of The PB/MK Geodetic Survey Department who helped in construction of the SSC. Finally, I would like to thank my family, especially Stacey and Matt, and my fellow employees of Measurement Science, Inc. for giving me the incentive and opportunity to finish this thesis.

Table of Contents

Table of Contents

Chapter Title Page

Table of Contents

List of Figures

List of Figures

List of Tables

Table	Title	Page

CHAPTER 1
INTRODUCTION

The Superconducting Super Collider (SSC)[1], being built south of the City of Dallas near Waxahachie, Texas, is designed to be the largest atomic particle accelerator in the world (Figure 1.1). By accelerating counter-rotating beams of protons to very high energy levels, it is hoped that the particle collisions will result in physical evidence of sub-atomic particles, some not yet discovered, that will advance our understanding of fundamental properties of energy and matter. To ensure that protons collide, stringent design requirements must be met for the construction of the tunnels in which the SSC will be located.

The components of the SSC consist of the Linear Accelerator facility (LINAC), the Low Energy Booster (LEB), the Medium Energy Booster (MEB), the High Energy Booster (HEB) and the main collider ring. The first accelerator, LINAC, is 0.148 km in length. The protons are passed from the LINAC to the LEB, which is 0.54 km in circumference, and then to the MEB, 3.96 km circumference, before being passed on to the HEB, circumference of 10.96 km (Figure 1.2). The protons then reach the main collider ring where they are accelerated in opposite directions around the main collider ring which is composed of more than 10 000 superconducting magnets. The main collider tunnel is designed to be oval in shape with a maximum diameter of about 30 km and a circumference of approximately 87 km. There will be approximately 50 magnet delivery, utility, ventilation and personnel shafts located around the main collider ring (Figure 1.3), through which horizontal and vertical survey control will be transferred down to the tunnel. These shafts are constructed on service area sites located at intervals of approximately 4.2 km along the main collider ring. The depths of the shafts range from 22 to 76 m. The main collider tunnel will be bored with up to six tunnel boring machines (TBMs) simultaneously, in a clockwise direction, at various 4.2 km sections between the sites of the vertical shafts which will be sunk in advance. After the protons have reached full energy, they are brought into collision at experimental halls, one located on the west campus and one on the east campus. The experimental halls will be 100 m long and 33 m wide by 60 m deep and

[1] At the time of writing this thesis, the SSC Project was well advanced. However in October of 1993, the U.S. Congress had voted to close the project. It is hoped that the SSC will eventually be completed with funding from other sources. At this time, the design, geodetic reductions and post-analysis of the vertical control have been completed for five tunnels.

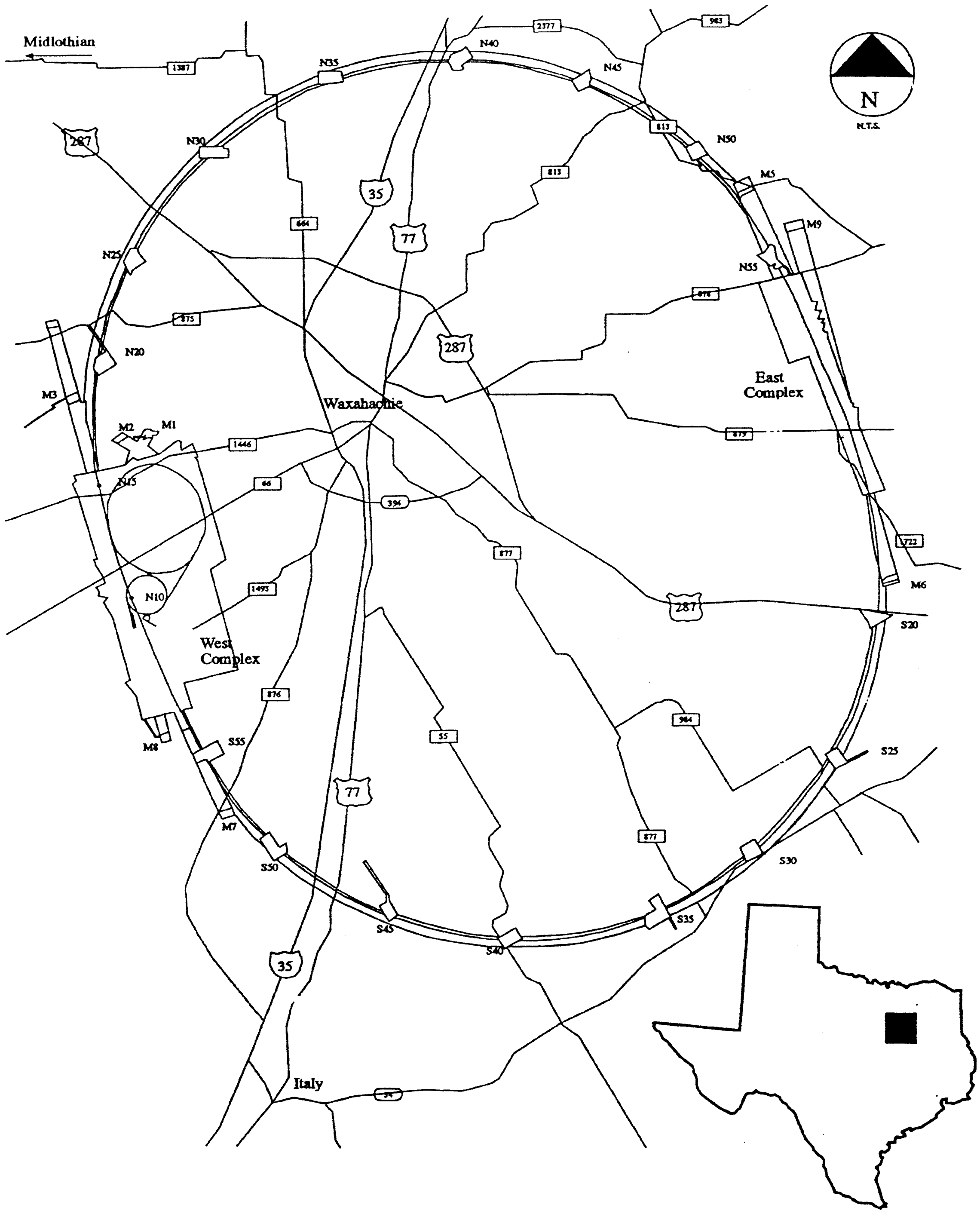

Figure 1.1
Location of SSC

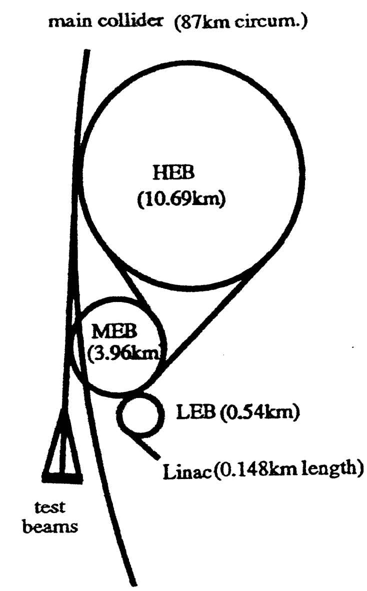

Figure 1.2
LINAC, LEB, MEB and HEB Accelerators

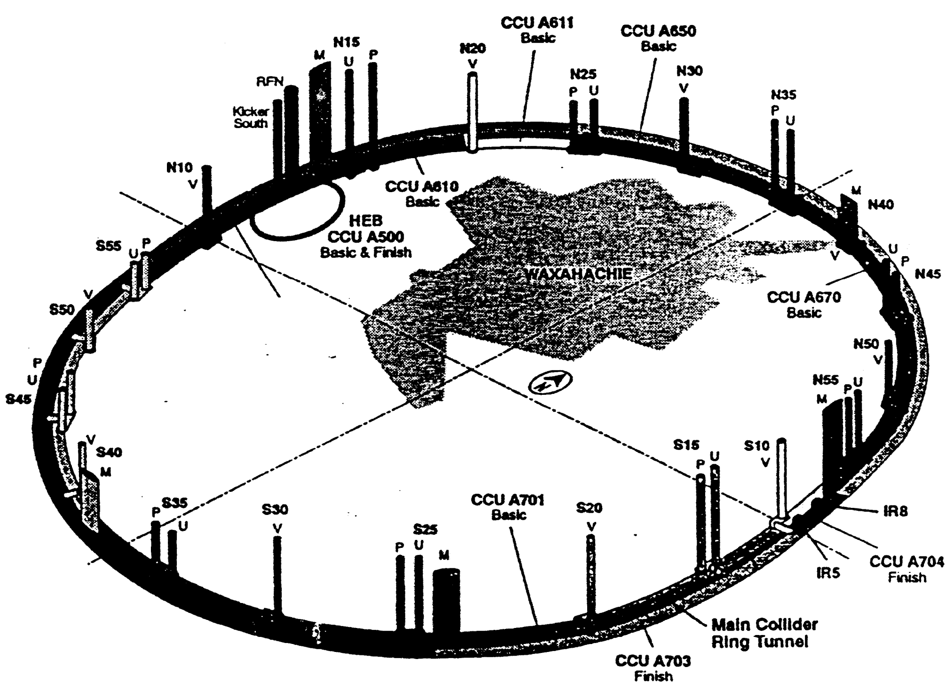

Figure 1.3
Shaft Locations Around Main Collider Ring of SSC

will house large detectors which will study the physical processes that occur when the high energy protons collide.

The contract for conventional construction for the tunnels and support facilities has been awarded to the joint venture of two engineering firms, Parsons Brinkerhoff (PB), and Morrison Knudsen (MK). The responsibilities of the joint venture, known as The PB/MK Team, include the construction of all tunnels and surface facilities for the SSC Laboratory (SSCL). Initial construction of the tunnel and its facilities commenced in 1991 and the SSC is expected to be completed early in the next century. Geodetic surveying services for the tunnel construction have been contracted to John E. Chance, and Associates (JECA) and its subcontractor Measurement Science, Inc. (MSI). Consultation to the project has been provided by the Engineering Surveys Research Group at the University of New Brunswick. It is the responsibilty of the PB/MK Geodetic Survey Division to ensure that geodetic control is supplied to the tunneling subcontractor to within 1000 ft (330 metres) of the head of the tunnel boring machine (TBM).

Vertical control for the construction of the SSC tunnel is accomplished in four components. The primary vertical control on the suface is performed using precise levelling techniques. This surface control forms the backbone of the vertical control and is therefore required to be accurate and reliable throughout the duration of the construction of the project. Densification of the vertical control to the service areas and the shafts must be performed efficiently and accurately. Densification is also performed using precise levelling. Transfer of vertical control from the surface to the tunnel is performed using methods developed on this project. A precise electronic optical distance measurement instrument (EODMI) measures vertical distances, which after corrected for meteorological and instrumentation errors yields accurate results. Propagation of elevations through the tunnel is performed by precise levelling. This thesis deals with the design and analysis of the four components of the vertical control for the project.

The design of the vertical control has to take into consideration that the atomic particles which will pass through the SSC are not influenced by the effects of gravity and will rotate in a planar motion. The SSC tunnels must, therefore, be set out on a plane defined in space (not a horizontal plane). This thesis includes analysis of five major tunnel halfsectors, the N15 to N20, N20 to N25, N25 to N30, N30 to N35 and the N40 to N45 (N15, N20, N25, N30, N35, N40 and N45 are service areas of the SSC), which have been completed at the time of this thesis (Figure 1.4). Results of the vertical breakthroughs are included.

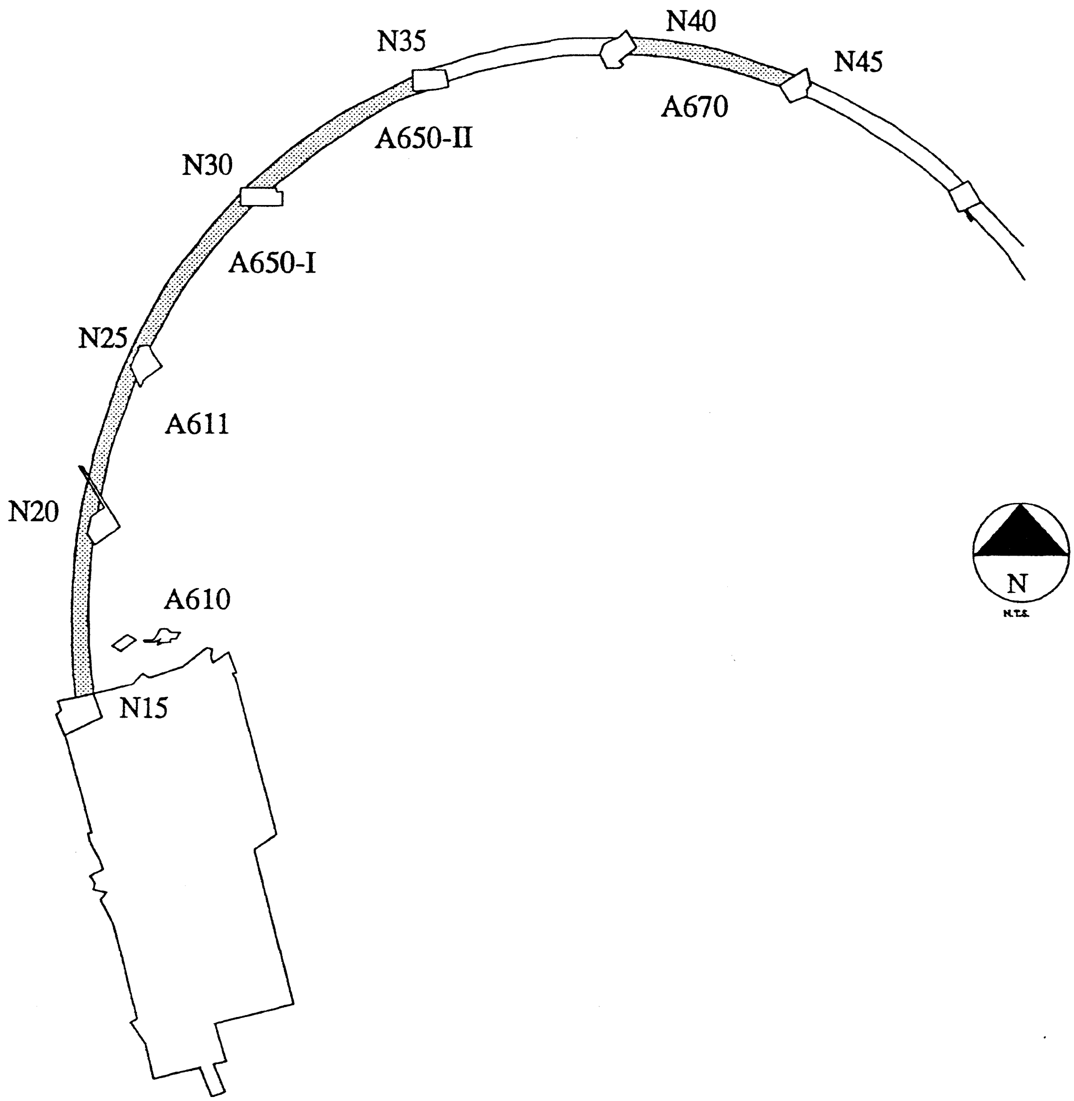

Figure 1.4
Completed Tunnel Half Sectors

CHAPTER 2
ACCURACY REQUIREMENTS OF THE VERTICAL CONTROL

The design requirements of the SSC must be correctly interpreted to ensure that vertical positioning accuracy is achieved. This is accomplished by an appropriate preanalysis to ensure the design requirements are achievable taking into account both the reliability and accuracy of the surface vertical control network, densification surveys, elevation transfer procedures and tunnel control.

2.1 Vertical Design Requirements of the SSC

According to initial design tolerances given to The PB/MK Team from the SSCL, the maximum departure of the excavated SSC tunnel from its theoretical position on a plane must not exceed an error envelope of eight inches (200 mm) (Figure 2.1). Five inches (126 mm) of this tolerance is reserved for construction (boring and lining) with the remaining three inches (76 mm) available for the surveying error budget. The maximum surveying error over the entire SSC plane (relative positional errors between any two points along the ring) can then be calculated from:

$$\varepsilon_{vert} = \sqrt{2}(76 \text{ mm}) = 108 \text{ mm}. \tag{2.1}$$

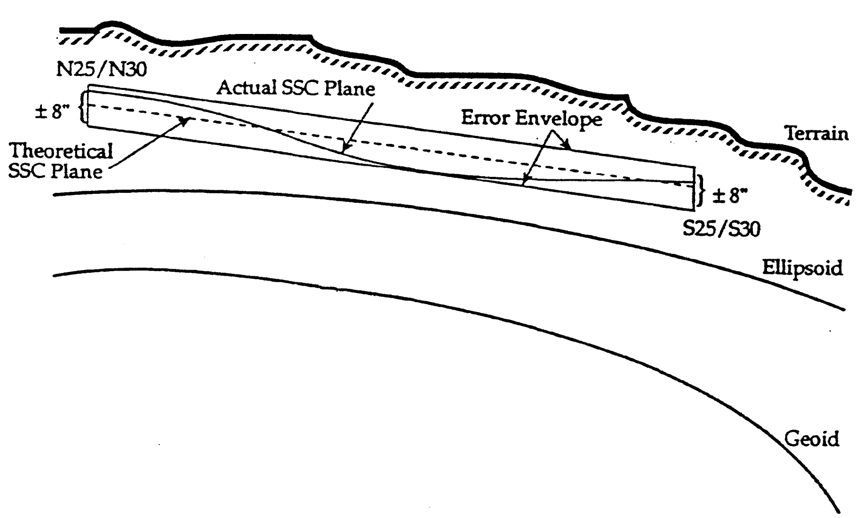

Figure 2.1
Visualization of Accuracy Requirements for SSC Plane

The initial design of the tunnel also requires that the final invert (floor) elevation be in the range 0" to -0.5" (0 mm to -12.5 mm). This is determined from factors such as the maximum adjustment range of the magnet stands and the degree of vertical "smoothness" required for the magnet alignment. All tolerances are assumed to be at the 99 percent level of confidence (99 percent level allows a safety factor of 2.6 which is close to three which is usual for large-scale engineering projects dealing with radiation or other hazards). The final invert elevation requirement is interpreted as the uncertainty of the difference in elevation between any two points anywhere along the collider being half of the allowable requirement, i.e., ±6.25 mm at 99 percent level of confidence.

The stringent requirements of the final invert require the most rigorous approach for vertical control for the SSC Project. It was then decided to determine if the existing Federal Geodetic Control Commission (FGCC) First Order Class I standards, specifications and procedures [FGCC, 1984] for precise levelling are sufficiently accurate for adaptation for the SSC Primary Vertical Control Network (PVCN).

2.2 Primary Vertical Control Network (PVCN) Design

The PVCN is designed to ensure stable surface control over a long period of time. The network design includes a large number of loops for reliability and accuracy.

Preliminary reconnaissance of the Primary Vertical Control Network was undertaken by the author during October, 1991. A total of 343 benchmark (BM) sites were identified in the preliminary design of the network. The benchmarks would be grouted into bedrock to ensure stability over the construction period of the SSC Project (Figure 2.2). In order to minimize costs without compromising the integrity of the network, it was decided that deep benchmarks would be installed only at junction points of level loops, and that at least two would be located in the vicinity of each primary point (fiducial monument) of the horizontal control network, and that three would be located near each service area. Control for densification and elevation transfers to the tunnel would only be transferred from deep benchmarks. This reduced the total number of deep benchmarks to 131. Temporary benchmarks or lower order control monuments would be used between deep benchmarks to ensure section lengths of under 3 km, as recommended by FGCC. Keeping section lengths under 3 km helps control the accumulation of systematic effects.

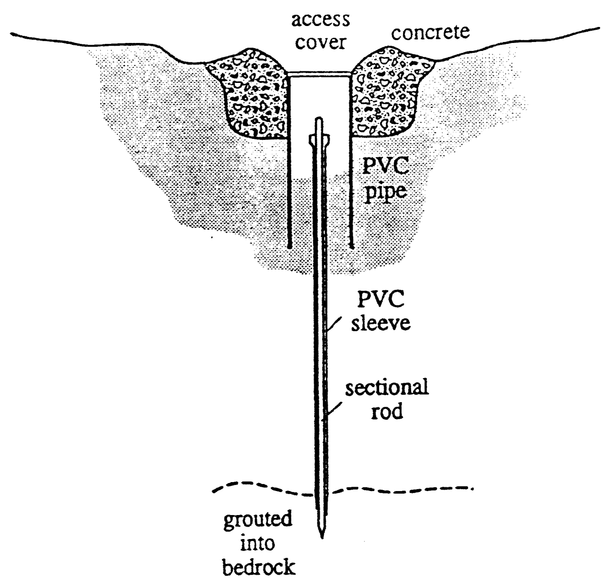

Figure 2.2
Deep Benchmark Design

The author performed a preanalysis of the proposed network (Figure 2.3) using the adjustment/simulation package Geolab^{tm} (Version 2.4c) with a weighting scheme for one way levellings adopted from FGCC specifications. According to FGCC First-Order Class I standards, the permissible difference between two runnings of a level section is given by [FGCC, 1984]:

$$\Delta_{max} = 3 \text{ mm} \sqrt{L}, \tag{2.2}$$

where L is the length of the section (km).

Since the tolerance is defined at the 95 percent level of confidence, the standard deviation of the expected misclosure can be estimated as follows:

$$\sigma_{\Delta} = \frac{3 \text{ mm} \sqrt{L}}{1.96} = 1.5 \text{ mm} \sqrt{L}. \tag{2.3}$$

Figure 2.3
Design of Primary Vertical Control Network After Optimization

If the direct and reverse runnings are assumed to be uncorrelated, then the standard deviation of a single-run section can be determined by:

$$\sigma = \frac{1.5 \text{ mm} \sqrt{L}}{\sqrt{2}} = 1.1 \text{ mm} \sqrt{L}. \tag{2.4}$$

The preanalysis results have shown that the relative accuracy across the main collider ring between two distant points (30 km apart) on the SSC ring (64130 and 64175) is 7 mm at the 99 percent confidence level.

The final design of the Primary Vertical Control Network was determined by mathematical optimization of the network without adversely affecting its accuracy. Optimization was accomplished using multi-objective design software developed by the Department of Surveying Engineering at the University of New Brunswick (UNB) [Kuang and Chrzanowski, 1992a]. The criteria for optimization was to eliminate as many levelling sections as possible without decreasing the overall accuracy across the SSC ring. Results of the optimization allowed for a total reduction from 686 km of double-run levelling from the preliminary design to 587 km which is a corresponding fifteen percent reduction in the field effort.

2.3 Accuracy Estimation of Tunnelling Surveys

Vertical accuracy of the SSC tunnel is determined by the estimation of the accuracy of four individual components, 1 - surface control, 2 - densification, 3 - elevation transfer, and 4- vertical tunnel control. The most conservative predicted vertical accuracy is defined by the vertical relative confidence interval between any two benchmarks located in the SSC tunnels. The highest predicted vertical error would occur between a benchmark at the end of a 4.6 km tunnel drive (which is the largest tunnel drive), just prior to breakthrough to the next shaft, and a similiar benchmark associated with a tunnel drive on the opposite end of the main collider tunnel, between service areas N25 to N30 and S25 to S30 (Figure 2.4).

Assuming no correlation exists between the four distinct components, the total variance at 99 percent is estimated from the sum of the variances of the components:

$$\sigma^2_{vert} = \sigma^2_{dH} + 2\,\sigma^2_{tun} + 2\,\sigma^2_{dens} + 2\,\sigma^2_{et}, \tag{2.5}$$

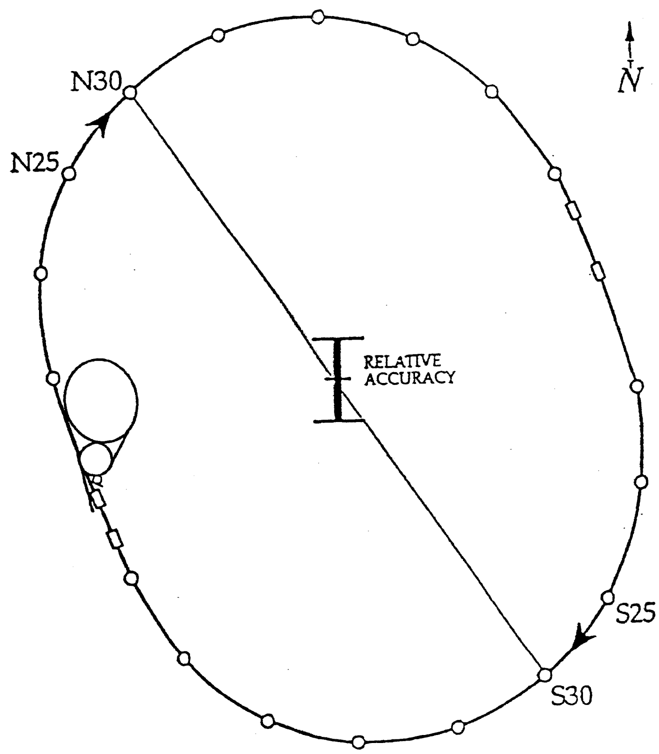

Figure 2.4

Vertical Relative Confidence Interval Between N25 to N30 and S25 to S30

where σ_{vert} is the vertical accuracy of positioning the main collider tunnel,
σ_{dH} is the accuracy across the ring of the surface network,
σ_{tun} is the vertical accuracy in each tunnel determined by precise levelling,
σ_{dens} is the accuracy of densification on the service areas, and
σ_{et} is the accuracy of transferring elevations down the shafts.

To ensure the accuracy of the vertical control is achievable, *a priori* accuracies of the densification, elevation transfer and tunnel control are estimated. The preanalysis of the surface network estimated an accuracy of 7 mm across the main collider ring after optimization is achievable at the 99 percent level of confidence (Section 2.2).

The accuracy of positioning temporary BMs on the shaft collar for the purpose of elevation transfer is estimated to be better than 4 mm at the 99 percent level of confidence. This estimation is based on the assumption that at least one deep BM is located within 2 km of the shaft and that similiar levelling procedures to the surface network are used in the densification. It is estimated that when using conventional methods for elevation transfers such as a steel tape, a standard deviation of 2 mm is achievable once proper corrections are applied.

Assuming that the levelling in the tunnel is carried out using the same methodology as with the surface control, then the standard deviation of vertical control in the tunnel can be estimated from:

$$\sigma_{tun} = 1.1 \text{ mm} \sqrt{4.6 \text{ km}} = 2.4 \text{ mm}. \tag{2.6}$$

The tunnel accuracy is then estimated to be 6.2 mm at the 99 percent level of confidence.

Substituting the estimated variances into Equation (2.5), an accuracy of 14.5 mm at the 99 percent level of confidence is achievable between stations in the tunnel across the diameter of the main collider ring. The tolerances for the tunnel construction allow an uncertainty of 108 mm. Therefore, assuming the algebraic summation of random and systematic errors, the application of geodetic corrections and reductions (vertical atmospheric correction, orthometric correction, etc.) may be safely ignored for tunnel construction requirements if their accumulated effect is below 93 mm. However, the afore-mentionned accuracy requirements for the final invert elevations cannot be achieved using FGCC standards for First-Order Class I.

Since the area of the SSC Project and the expected lengths of the levelling loops are not compatible with the large area of the national network, the direct application of the FGCC standards was considered inappropriate. Therefore, a deterministic approach for the development of standards and specifications, unique to the SSC Project, through a thorough analysis of random and systematic errors and geodetic reductions has been adopted for the PVCN. Basic specifications for instrumentation and field procedures for FGCC First-Order Class I work have been adopted but office tolerances will be based upon a deterministic approach.

Improved methodology for densification, elevation transfers down the shafts, and the propagation of tunnel control through each tunnel have been developed to improve the accuracy and reliability. These adaptations will increase the accuracy for tunnel control from the initial estimates.

CHAPTER 3
REVIEW OF OBSERVATIONAL ERRORS

Elevation differences are subject to observational uncertainty. These errors can be classified as either random or systematic. They are carefully reviewed in this chapter and their expected magnitudes in the SSC Project are estimated.

3.1 Random Errors

Random errors in levelling are caused by small unpredictable observational and instrumentation errors [FGCC, 1984]. Random errors can be classified according to the following categories [Chrzanowski, 1985]:

- Levelling of the line-of-sight, σ_l, and
- Pointing and reading of the instruments, σ_p and σ_r.

Random errors cannot be completely eliminated but may be controlled by adopting appropriate observing procedures.

3.1.1 Levelling of Line-of-Sight

A geodetic level should provide a consistent horizontal line-of-sight perpendicular to the direction of gravity at the vertical axis of the instrument. If the line-of-sight deviates from the horizontal, an error in the observation results. A deviation of the line-of-sight is caused by the limited sensitivity of the levelling instrument, atmospheric refraction, and by systematic collimation error (Section 3.2.6).

The sensitivity of the instrument depends primarily on the sensitivity of the level bubble or random influences of the compensator. Testing has shown that precision geodetic levels have a repeatibility of setting the line-of-sight of about 0.3". Thus over a distance the accuracy of levelling a line-of-sight can be estimated from [Chrzanowski, 1985]:

$$\sigma_l = \frac{0.3''}{206265''}\, s, \tag{3.1}$$

where s is the length of the line-of-sight, [m]. For a line-of-sight of 50 metres, the standard deviation of the levelling error is 0.07 mm.

3.1.2 Pointing and Reading of the Instrument

The pointing and reading error is mainly affected by the observer's inability to repeat the observation exactly. This is caused by the limited optical resolution of the instrument, and of the observer's pointing capability as well as other factors such as slight variations of atmospheric refraction (scintillation). In geodetic levelling, the pointing and reading errors are reduced by using precise, high magnification instruments with micrometers and wedge shaped reticules.

The error associated with pointing and reading depends primarily on the magnification of the instrument. Environmetal influences (refraction oscillations) and the limits of the optical resolution of the human eye also influence the pointing. The pointing error over a distance s, to a perfectly designed target, ranges from a minimum error of [Chrzanowski, 1985]:

$$\sigma_p = \frac{20''}{M \times 206265''} s, \tag{3.2a}$$

to:

$$\sigma_p = \frac{70''}{M \times 206265''} s, \tag{3.2b}$$

where M is the magnification of the instrument.

Assuming average atmospheric conditions and a magnification of 40X, the pointing error at the SSC Project is accepted as being equal to:

$$\sigma_p = \frac{45''}{M \times 206265''} s, \tag{3.2c}$$

which for line-of-sight lengths of 50 metres, gives an error of σ_p = 0.27 mm. This corresponds to an error of 0.19 mm from a mean reading of a double-scale rod, assuming there is no correlation between the two readings.

Random mislevelment of a level rod equipped with a box level results in a reading error which depends primarily on the sensitivity of the level bubble. This can be estimated from [Chrzanowski, 1985]:

$$\sigma_r = \frac{l\left(\frac{v''}{206265''}\right)^2}{2}, \tag{3.3}$$

where l is the height of the sighting on to the rod in [m], and

v" is the sensitivity of the bubble.

For rods used in geodetic levelling, the sensitivity of the bubble can amount to 600" (10'). When sighting to the top of the 3 metre rod, this can amount to an uncertainty of 0.01 mm in a single pointing. If the bubble is not properly adjusted then the rod tilt produces a systematic error (Section 3.2.4).

The combined effects of levelling, pointing and reading constitute the random component of the error associated with geodetic levelling. It should be pointed out that the residual effects of certain systematic errors may also be regarded as random errors.

3.2 Observational Systematic Effects

Systematic effects have a constant influence on measurements and reveal the limitations of the basic mathematical model. Systematic effects can be minimized to be within the noise level at every setup yet may accumulate over many level sections and result in unreliable elevation differences. The following systematic effects that have been considered in the SSC geodetic levelling operations [DeKrom, et al., 1992a]:

- Rod scale error,
- Rod index error,
- Rod temperature error,
- Error due to the systematic tilt of the rod,
- Level collimation error,
- Effect of instrument and turning point sinking and rebound,
- Effect of the earth's curvature, and
- Vertical atmospheric refraction.

3.2.1 Rod Scale Error

The calibrated length of the rod is provided on request by the manufacturer and can be checked by comparing the length of the invar strip with a length standard. The rods are calibrated for scale at the beginning and at the end of the survey campaign, and at any time the rod is mishandled. The error is determined at each setup as [Chrzanowski, 1985]:

$$\varepsilon_{scale} = \left[s_A B - s_B F\right] - \left[B - F\right], \tag{3.4}$$

where s_A is the scale factor of the first rod,
s_B is the scale factor of the second rod,
B is the back-sight reading in [m], and
F is the fore-sight reading in [m].

Using typical rod scale values of s_A =0.999991 and s_B = 1.000009, and over an elevation difference of 40 m, which is the approximate value across the ring, then an accumulation error across the ring of 8.5 mm can be expected.

3.2.2 Rod Index Error

The rod index error is caused by the constant offset of the zero gradient on the rod from the base of the plate. This error is eliminated by the observation procedure. The error cancels out if there is an even number of setups in the section or if in one setup sections, the same rod is used on both benchmarks.

3.2.3 Rod Temperature Error

The rod is calibrated at a specific temperature. If the coefficient of thermal expansion of the invar strip is known, the length of the rod at any temperature can be determined. The rod temperature correction is applied to the elevation difference of a level setup using the observed temperature of the invar. Under the assumption that the invar strips of both rods have similiar properties, then the error is computed from the following [Balazs and Young, 1982]:

$$\varepsilon_{temp} = (t_{setup} - t_{stand})\, \Delta h\, \alpha_{te}, \tag{3.5}$$

where t_{setup} is the temperature of the invar scale at each setup in [°C],
t_{stand} is the standardized temperature of invar in [°C],

Δh is the observed mean elevation difference over a setup in [m], and
α_{te} is the coefficient of thermal expansion of invar in [/1°C].

For example, typically for invar, α_{te} is 10^{-6}/1°C. Thus, for a Δh of 2.5 m and a $t_{setup} - t_{stand}$ of 20°C, then an error of 0.05 mm can be expected over a setup. This correction is dependent on the change of elevation over a setup and therefore insignificant on flat terrain.

3.2.4 Error Due to Tilt of the Rod

A systematic deviation of the level rods from the vertical causes a systematic error in levelling (Figure 3.1). The reading on the tilted rod is always larger than it should be. Even though this effect is within the noise level of the instrument, it will accumulate on sloping terrian. The error of an observation is determined from the difference of real rod reading and true rod reading [Balazs and Young, 1982]:

$$\varepsilon_{tilt} = RR - TR, \tag{3.6}$$

where RR is the real rod reading, and
TR is true rod reading.

Assuming a tilt of 10', the error over 30 km and 40 m elevation difference does not accumulate to more than 0.3 mm. This error is disregarded because the level rods are to be frequently checked for verticality and adjustments to the level bubbles are accomplished when necessary.

3.2.5 Level Collimation Error

The collimation error of the instrument results from a systematic deviation of the line-of-sight from the horizontal plane as defined by the gravity vector at the instrument (Figure 3.2). It can be minimized by balancing the lengths of the back- and the fore-sights. It is intended that the imbalance will not exceed 2 metres per setup or accumulate algebraically to more than 4 metres a section. If a level has a collimation error larger than 10" (0.05 mm/m), it will not be used in the survey. The error is determined from [Balazs and Young, 1982]:

$$\varepsilon_{coll} = \Delta s \, c_{coll}, \tag{3.7}$$

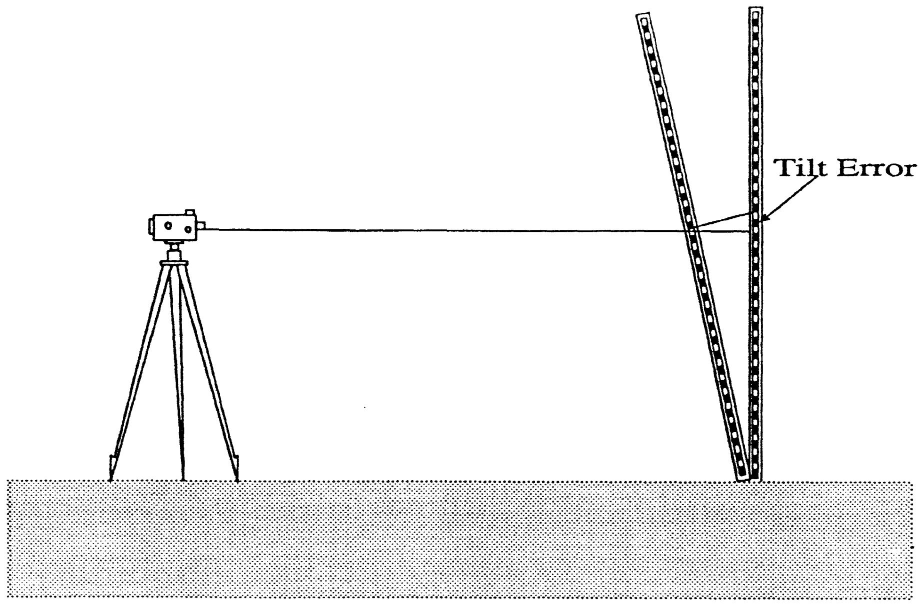

Figure 3.1
Rod Tilt Error

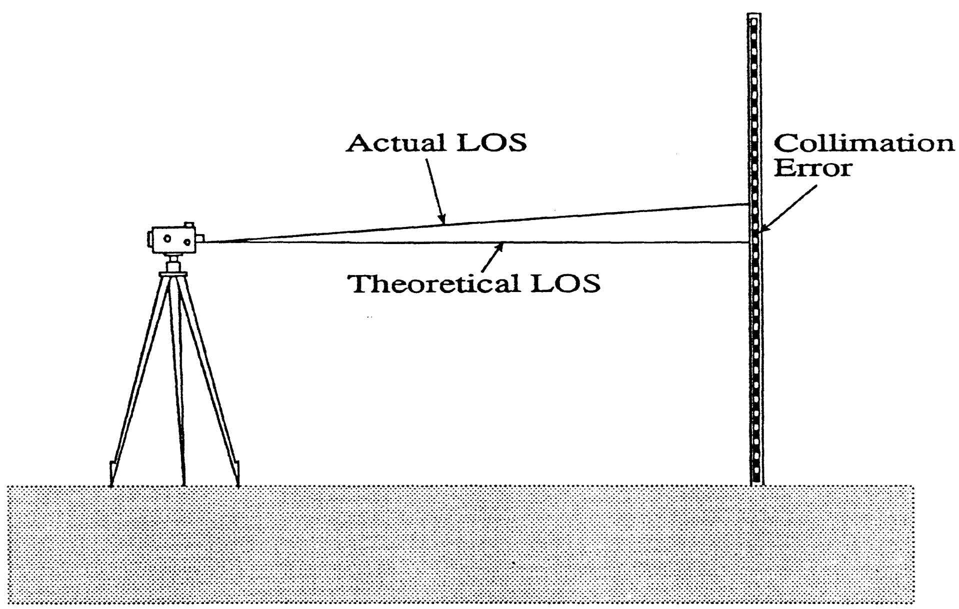

Figure 3.2
Level Collimation Error

where Δs is the difference in the length of the back- and fore-sights, in [m] [= s_b-s_a], and

c_{coll} is the collimation error of the instrument in [mm/m].

For example, if c_{coll} is 0.05 mm/m and Δs is 2 m, then the error over a setup is 0.1 mm. This correction is applied for every setup in a section when instruments other than those having a double-compensator are used. When double-compensator instruments are used, the c_{coll} is not expected to reach more than 0.02 mm/m or 0.08 mm/section length when the maximum discrepancy of Δs does not exceed 4 m.

3.2.6 Effect of Sinking and Rebound of the Instrument and Turning Points

Instrument sinking and rebound is minimized by the observation procedure. It is assumed that the instrument sinks or rebounds in a time dependent manner. Thus, by observing back-sight low scale (B_{low}), fore-sight low scale (F_{low}), fore-sight high scale (F_{high}) and then finally back-sight high scale (B_{high}), and taking the mean of the two elevation differences, high scale and low scale, the effect is minimized. This can be seen in Figure 3.3.

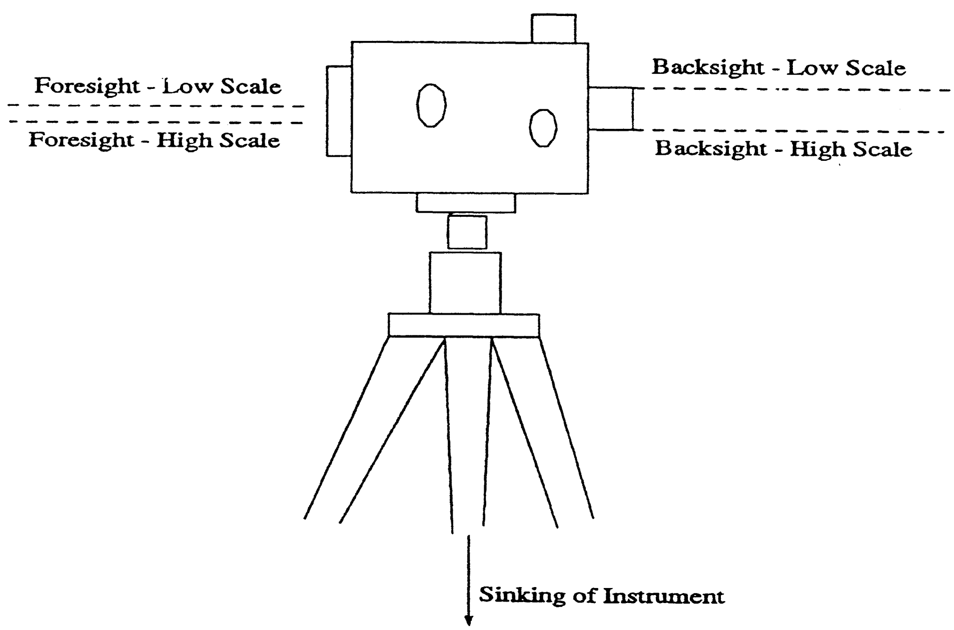

Figure 3.3
Minimizing Instrument Sinking Over a Setup

The effect can be further reduced by observing onto rod A (the rod with the lowest serial number) first at each setup. The sequence for observing is:

1st setup and every consecutive odd setup -

B_{low}, F_{low}, F_{high} then B_{high}

2nd setup and every consecutive even setup -

F_{low}, B_{low}, B_{high} then F_{high}

Figure 3.4 clearly shows that this observing procedure tends to reduce the effect of sinking and rebound.

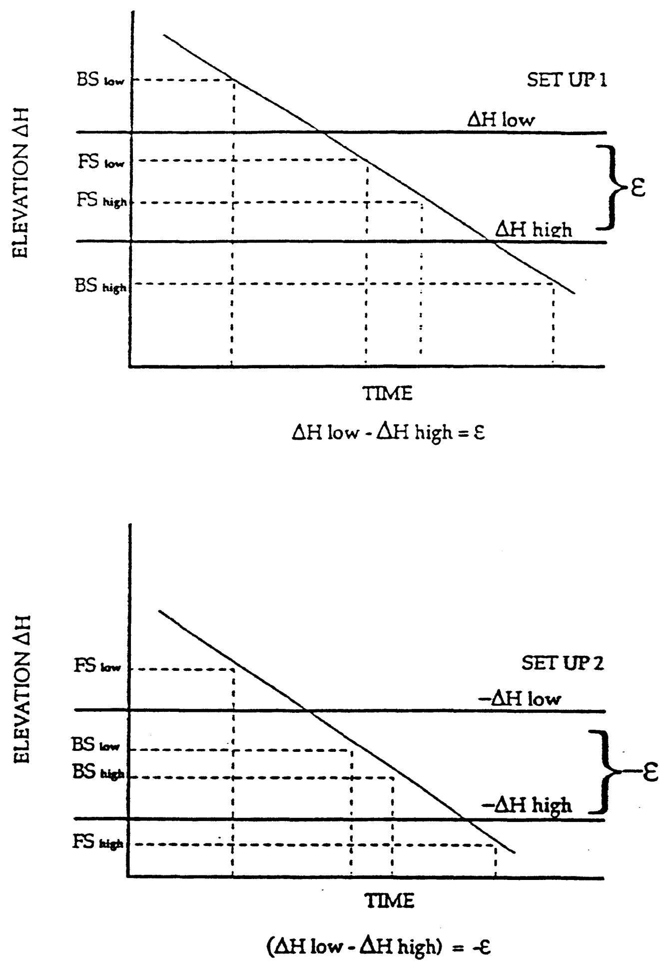

Figure 3.4

Minimizing Instrument Sinking Over Two Setups

The error associated with the sinking of turning points can amount to as much as 0.5 mm/setup [Chrzanowski, 1985] . The most serious error is sinking of the forward rod which becomes the backward rod when the instrument is moved to the next setup. This error may cause large loop misclosures and large differences between two way levellings.

Displacements of turning points (both spikes and turning plates) over time has been previously examined in Greening [1985]. Table 3.1 summarizes the results of these studies.

Table 3.1
Turning Point Displacement Over Time

Location of Turning Point	Type of Turning Point	Displacement [mm] In 20 secs.	Displacement [mm] In 2 mins.
Paved Highway	Spike Base Plate	-0.008 -0.038	-0.01 -0.046
Railroad	Spike Base Plate	-0.008 -0.032	-0.01 -0.041
Unpaved Road	Spike Base Plate	-0.011 -0.05	-0.016 -0.068
Sandy Ground	Spike Base Plate	-0.02 -0.119	-0.024 -0.135
Turfy Ground	Spike Base Plate	-0.13 -0.668	-0.168 -0.84

The analysis of the displacement of the turning points over time shows a systematic trend. Over a seven minute setup (the average length of a setup), the error is expected to be within the noise level of each setup but may accumulate significantly over a level section. Taking, for example, a systematic sinking of only 0.05 mm/setup, a realistic value, of the back rod (when waiting for a new setup of the instrument), the error may accumulate to 1.5 mm over a 3 km section (30 setups assuming 100 m/setup) which produces the difference of 3 mm between the two-way levellings.

It is estimated that for the purpose of developing appropriate tolerances, that with a specially designed turning plate, and with the proper observational procedures, the systematic effect of the sinking of the rods could be reduced to an average value not exceeding 0.03 mm/setup. Further analysis is required to confirm this value.

3.2.7 Effect of Earth's Curvature

The effect of earth curvature is minimized by balancing the back- and fore-sight lengths. The error occurs because the instrument and rods are setup with respect to the direction of gravity, which is normal to a curved equipotential surface, while the line-of-sight of a geodetic level describes a plane tangent to this surface (Figure 3.5). In order to minimize this effect, the imbalance of the back- and fore-sight lengths is not to exceed 2 metres/setup, or accumulate algebraically to more than 4 metres over a section. The error associated with the earth curvature is calculated from [Chrzanowski, 1985]:

$$\varepsilon_{curv} = \frac{s_F^2 - s_B^2}{2R}, \qquad (3.8)$$

where s_F and s_B is the back- and fore-sight lengths in [m], respectively, and
R is the radius of the earth in [m].

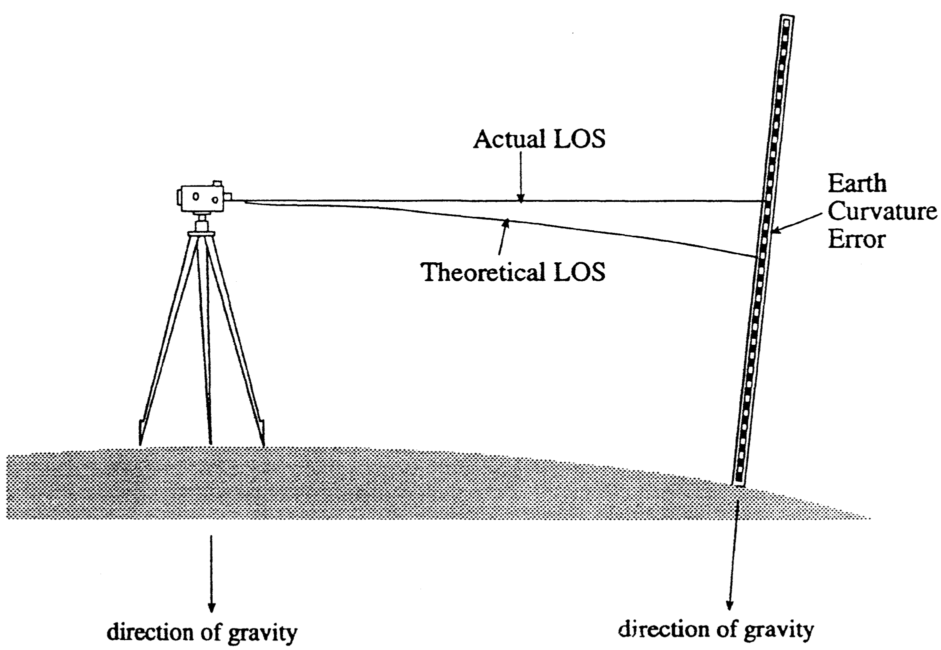

Figure 3.5
Effect of Earth's Curvature

Assuming a 2 m imbalance between the fore-sight and back-sight over a 98 m setup (s_F and s_B are 50 m and 48 m, consecutively), then the error is 0.015 mm over the setup.

3.2.8 Vertical Atmospheric Refraction

Atmospheric refraction has both random and systematic components. The random error which is manifested by shimmering or scintillation can be minimized by shortening the line-of-sight. The systematic effects are of two kinds:

- Effect due to the imbalance of the length of lines-of-sight at individual setups.
- Systematic accumulation of the refraction error over long inclined routes (sloping terrain) as shown in Figure 3.6.

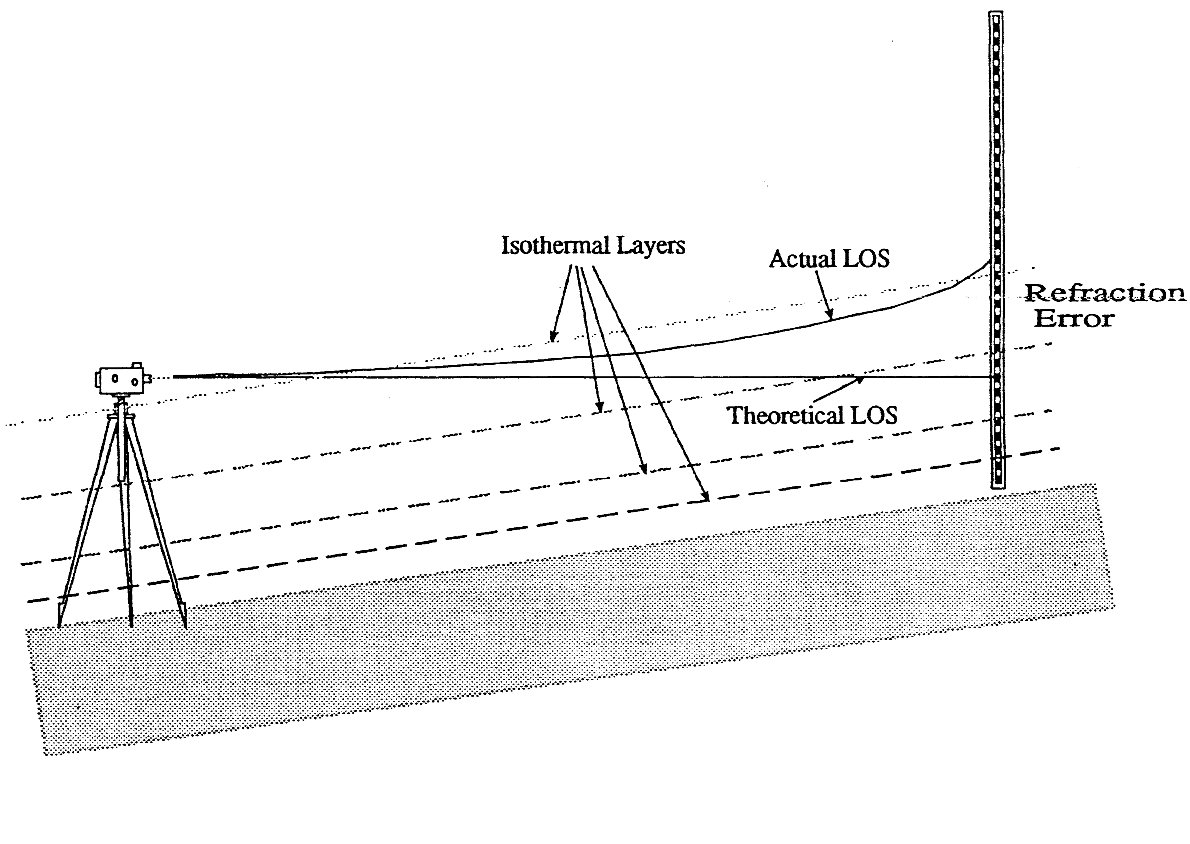

Figure 3.6
Effect of Vertical Atmospheric Refraction

The refraction error is calculated from the following formula by [Chrzanowski, 1985]:

$$\varepsilon_{ref} = \frac{k\, s^2}{2R}, \tag{3.9}$$

where s is the back- or fore- sight lengths in [m],

R is the radius of the Earth in [m], and

k is the coefficient of refraction, which may be computed from [Kharaghani, 1987]:

$$k = 78.83 \left(0.0342 + \frac{dT}{dz}\right) \frac{PR}{T^2}\, 10^{-6}, \tag{3.10}$$

where P is the pressure at the instrument in [mb],

T is the temperature at the height of instrument in [K], and

$\frac{dT}{dz}$ is the temperature gradient interpolated midway between the instrument setup and the level rod in /°C/m.

Isothermal layers are modelled by Kukkamaki's Equation [Kharaghani, 1987]:

$$t = a + bz^c. \tag{3.11}$$

At each height, z, above the terrain, there are three unknowns that describe the temperature profile (a, b, and c). The temperature gradient is determined by differentiating temperature in Equation (3.11) with respect to height above the terrain:

$$\frac{dT}{dz} = b\, c\, z^{c-1}. \tag{3.12}$$

To rigorously correct for the effect of refraction, certain assumptions are made:

- the ground slope is uniform at each setup,
- the sight distances are equal,
- the isothermal layers are parallel to the terrain, and
- the isobaric layers are horizontal with respect to gravity.

Equation (3.9) is based on a linear ray-path effect of refraction. It, however, does not behave in a linear fashion. To rigorously compute the effect of refraction, it is necessary to determine a realistic path of the line-of-sight as it passes through different isothermal layers. This can be approximated by differentiating the path over the line-of-sight based on the above assumptions. The error can be estimated for the fore-sight as:

$$\varepsilon_f = \cos\beta \int_0^S 78.83 \frac{P}{T^2}\left(0.0342+\frac{dT}{dy}\right)10^{-6}\,(S-x)dx, \tag{3.13a}$$

and over a back-sight length as:

$$\varepsilon_b = \cos\beta \int_0^{-S} 78.83 \frac{P}{T^2}\left(0.0342+\frac{dT}{dy}\right)10^{-6}\,(-S-x)dx, \tag{3.13b}$$

where S is the length of the line-of-sight and x is distance along the integral. Assuming that the pressure and temperature are constant during a setup, and applying the first integral results in the following:

$$\varepsilon_f = A\left[0.0342\frac{S^2}{2} + \int_0^{s} \frac{dT}{dy}\,(S-x)dx\right], \tag{3.14a}$$

and,

$$\varepsilon_b = A\left[0.0342\frac{S^2}{2} + \int_0^{-s} \frac{dT}{dy}\,(S+x)dx\right]. \tag{3.14b}$$

where,

$$A = 78.83 \cos\beta \frac{P}{T^2}10^{-6}. \tag{3.14c}$$

Subtracting Equation (3.14a) from (3.14b) results in the error over a setup of:

$$\varepsilon_s = -A\left[\int_0^{S} \frac{dT}{dy}(S+x)dx + \int_0^{S} \frac{dT}{dy}(S-x)dx\right]. \tag{3.15}$$

It is necessary to determine the height, z, of the optical path along the length of the integration. The height of the optical path at any distance, x, along the line-of-sight can be expressed by,

$$z = HI - \tan\beta\, x. \tag{3.16}$$

Equation (3.16) can then be substituted into Equation (3.12), resulting in:

$$\frac{dT}{dz} = -bc\left(HI - \tan\beta\, x\right)^{c-1}. \tag{3.17}$$

Substituting Equation (3.17) into Equation (3.15) results in:

$$\varepsilon_s = -Abc\left[\int_0^{-S} \left(HI-\tan\beta\, x\right)^{c-1}(S+x)dx + \int_0^{S} \left(HI-\tan\beta\, x\right)^{c-1}(S-x)dx\right]. \tag{3.18}$$

The approximation of Equation (3.18) can be determined through the use of McLaurin's Series [Greening, 1985]. Letting:

$$u(x) = \left(HI-\tan\beta\, x\right)^{c-1}(S+x), \tag{3.19a}$$

and

$$v(x) = \left(HI-\tan\beta\, x\right)^{c-1}(S-x). \tag{3.19b}$$

Equation (3.18) becomes:

$$\varepsilon_s = -Abc\left[\int_0^{-S} u(x)dx + \int_0^{S} v(x)dx\right], \tag{3.20}$$

where,

$$u(x) = u(0) + x\,u'(0) + \frac{x^2 u''(0)}{2!}, \tag{3.21a}$$

and

$$v(x) = v(0) + x\,v'(0) + \frac{x^2 v''(0)}{2!}. \qquad (3.21b)$$

The error of refraction can then be estimated over an instrument setup as:

$$\varepsilon_s = A\frac{S^2}{6}\left(D_2(\Delta H) + \frac{1}{80}D_4(\Delta H)^3\right), \qquad (3.22a)$$

where

$$D_2 = b\,(c-1)\,cI^{c-2}, \qquad (3.22b)$$

$$D_4 = b\,(c-3)(c-2)(c-1)\,cI^{c-4}, \qquad (3.22c)$$

and

$$\Delta H = 2S\,\tan\beta. \qquad (3.22d)$$

The parameters b and c can be determined from the above equations if the temperatures are measured at at least three different heights.

The author performed a simulation for determining the possible accumulation of refraction over the sloping terrain was performed using Equations (3.9) to (3.22d). To determine the maximum possible effect, the largest elevation difference across the diameter of SSC main collider ring is used in the simulation (Figure 3.7). The terrain slopes downwards from the north-west to south-east. A vertical profile is obtained using elevations and distances from the existing survey control. Unfavourable atmospheric conditions are assumed and hence values of 2.5 and -0.33 for constants b and c are adopted for the simulation, respectively. The error across the SSC ring is shown in Table 3.2.

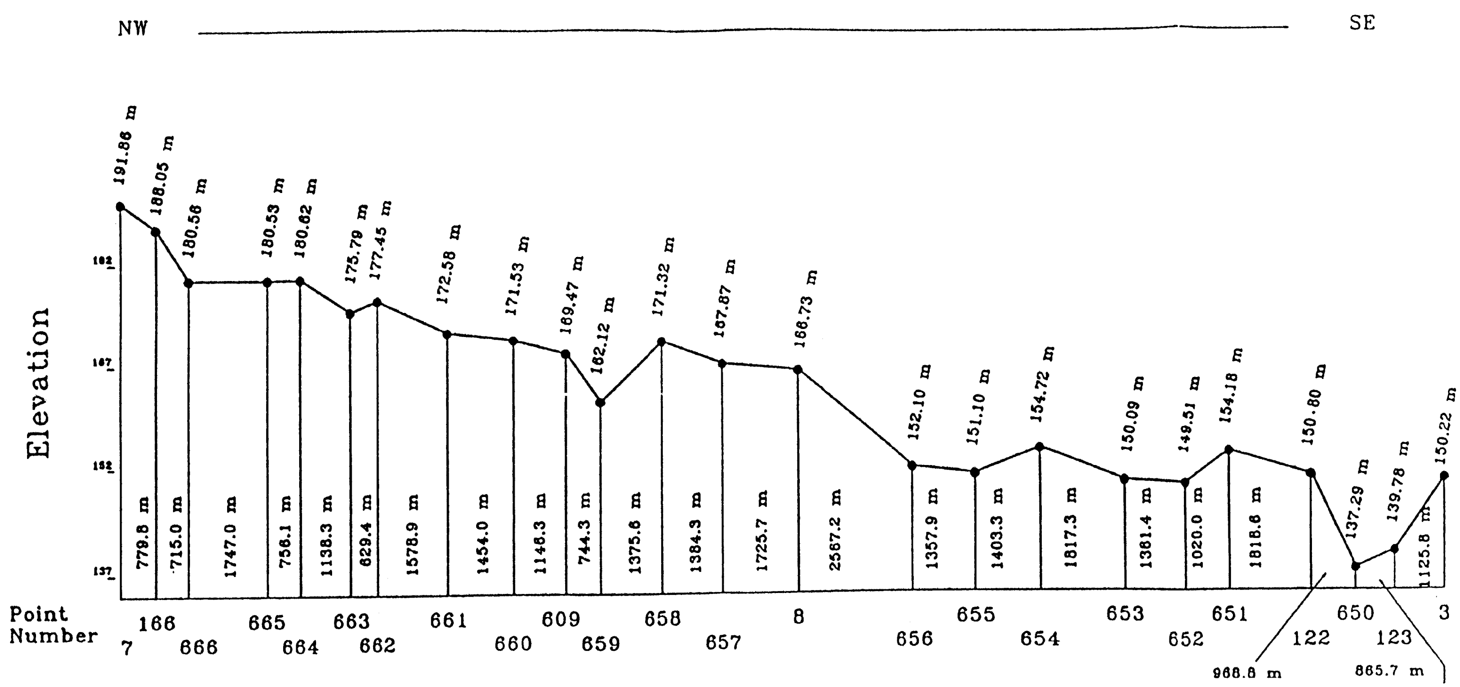

Figure 3.7
Vertical Profile From North-West to South-East
(Along U.S. 287)

Table 3.2
Refraction Error Simulation

From	To	Elev Diff (m)	Section (km)	No. of Setups	Error (mm)	Acc. Error (mm)
64007	64166	-3.81	0.78	8	-0.5	-0.5
64166	64666	-7.49	0.715	8	-0.8	-1.3
64666	64665	-0.03	1.747	18	0.0	0.0
64665	64664	0.09	0.756	8	0.0	0.0
64664	64663	-4.83	1.138	12	-0.6	-1.9
64663	64662	1.66	0.629	8	0.1	-1.8
64662	64661	-4.87	1.578	16	-0.6	-2.4
64661	64660	-1.05	1.454	16	-0.1	-2.5
64660	64609	-2.06	1.146	12	-0.2	-2.7
64609	64659	-7.35	0.744	8	-0.9	-3.6
64659	64658	9.2	1.376	14	1.2	-2.4
64658	64657	-3.45	1.384	14	-0.4	-2.8
64657	64008	-1.14	1.726	18	-0.1	-2.9
64008	64656	-14.63	2.567	26	-1.9	-4.8
64656	64655	-1	1.358	14	-0.1	-4.9
64655	64654	3.62	1.403	16	0.4	-4.4
64654	64653	-4.63	1.817	20	-0.5	-4.9
64653	64652	-0.58	1.361	14	-0.1	-5.0
64652	64651	4.67	1.02	12	0.4	-4.6
64651	64122	-3.38	1.819	20	-0.4	-5.0
64122	64650	-13.51	0.969	10	-0.4	-5.4
64650	64123	2.49	0.867	10	0.2	-5.2
64123	64003	10.44	1.126	12	0.9	-4.1

A refraction error of -4.1 mm accumulated in a north-west to south-east direction over a distance of 30 km which has the maximum elevation difference. This error can be reduced by at least half by observing temperature gradients and modelling the effect. The residual systematic error accumulation may be estimated to be within 0.1 mm/km.

A summary of the random and systematic errors analyzed by the author and their expected effect on the SSC vertical control is shown in Table 3.3.

Table 3.3
Summary of Random and Systematic Errors

Error		Cause	Estimated Magnitude (mm)	Equation
Random	Levelling of line-of-sight	Nonperpendicularity of line-of-sight	0.07 mm	3.1
	Pointing	Imperfections of instrument, observer and residual atmospheric effects	0.27 mm each scale	3.2c
	Reading	Limits of sensitivity of level bubble	0.01 mm	3.3
Systematic	Rod scale error	Difference in standard scale	8.5 mm over 30 km	3.4
	Rod temperature	Expansion of invar at different temperatures	0.05 mm per setup	3.5
	Rod tilt error	Systematic deviation of rod from vertical	0.3 mm over 30 km	3.6
	Level collimation error	Deviation of line-of-sight from horizontal plane	0.08 mm per section	3.7
	Sinking of turning point	Sinking of back-sight turning plate between setups	0.03mm per setup	-
	Effect of earth's curvature	Nonperpendicularity between line-of-sight and rod	0.015 mm per setup	3.8
	Vertical atmospheric refraction	Deviation of line-of-sight due to refraction	4.1 mm over 30 km	3.9 to 3.22d

CHAPTER 4
ANALYSIS OF GEODETIC REDUCTIONS

The effects of geodetic reductions must be carefully investigated to ensure the vertical design accuracy is achieved. For the SSC Project, the following geodetic reductions have been analyzed [Grodecki, et al., 1992a; Grodecki, et al., 1992b]:

- Effect of Tidal Forces, and
- Orthometric Correction.

4.1 Analysis of the Effect of Tidal Forces

Astronomic effects are due to the lunar and solar body's uplift of the earth's gravity equipotential surfaces. The tidal forces also cause the redistribution of the mass of the earth, which in turn results in additional uplift of the equipotential surfaces. The tilt of the terrain, and therefore the levelled height differences, are affected by the distortion of the equipotential surfaces.

The component of the moon's influence on elevation is [Balazs and Young, 1982]:

$$h_m = (3m\, Mr)(\sin 2q)/2d^3 + (3m\, Mr^2)(5\cos^2 q - 1)(\sin q)/2d^4, \tag{4.1}$$

and the corresponding effect of the sun is [Balazs and Young, 1982]:

$$h_s = (3m\, Sr)(\sin 2r)/2D^3, \tag{4.2}$$

where h_m is the component of tidal acceleration due to the moon, [sec. m s^{-2}],
h_s is the component of tidal acceleration due to the sun, [sec. m s^{-2}],
μ is Newton's gravtational constant, [N m^2 s^{-2}],
r is the distance from the point on the surface to the center of the earth, [m],
M is the mass of the moon, [kg],
m is the mass of the sun, [kg],
d is the distance between the centers of the earth and moon, [m],
D is the distance between the centers of the earth and the sun, [m],
θ is the zenith distance of the moon, [sec], and
ρ is the zenith distance of the sun, [sec].

The values, h_m and h_s, are converted to deflections by dividing h_m and h_s by a constant gravity value.

The total effect of the sun and the moon's tidal accelerations is then computed from the effects of the components:

$$e_{tidal} = -(\tan e_m \cos(A_m - \alpha) + \tan e_s \cos(A_s - \alpha))\, S, \tag{4.3}$$

where S is the section length in [m],
α is the azimuth of the section in [sec],
A_m is the azimuth of the Moon in [sec], and
A_s is the azimuth of the Sun in [sec].

The effect and magnitude of the tidal forces at the SSC Project is simulated on two levelling lines [Grodecki, et al., 1992a], one level line in the north-south direction and the other in an east-west direction (Figure 4.1).

Analysis of the effect of the solar component was performed by the Engineering Surveys Research Group at the University of New Brunswick. The mean longitude of the sun, H, is approximated using the form of a truncated polynomial [Grodecki, et al., 1992b]:

$$H = L + dL + sL + \psi, \tag{4.4}$$

where L is the geometric mean longitude of the ficticious mean sun, determined by:

$$L = 279°41'48.04" + 129602768.13" + 1.089"T^2, \tag{4.5}$$

and T is the Julian ephemeris date reduced to the fundamental epoch and expressed in centuries of 36525 days,
dL is the correction to get the mean longitude of the true sun:

$$dL = (6910.057" - 17.24"T) \sin g, \tag{4.6}$$

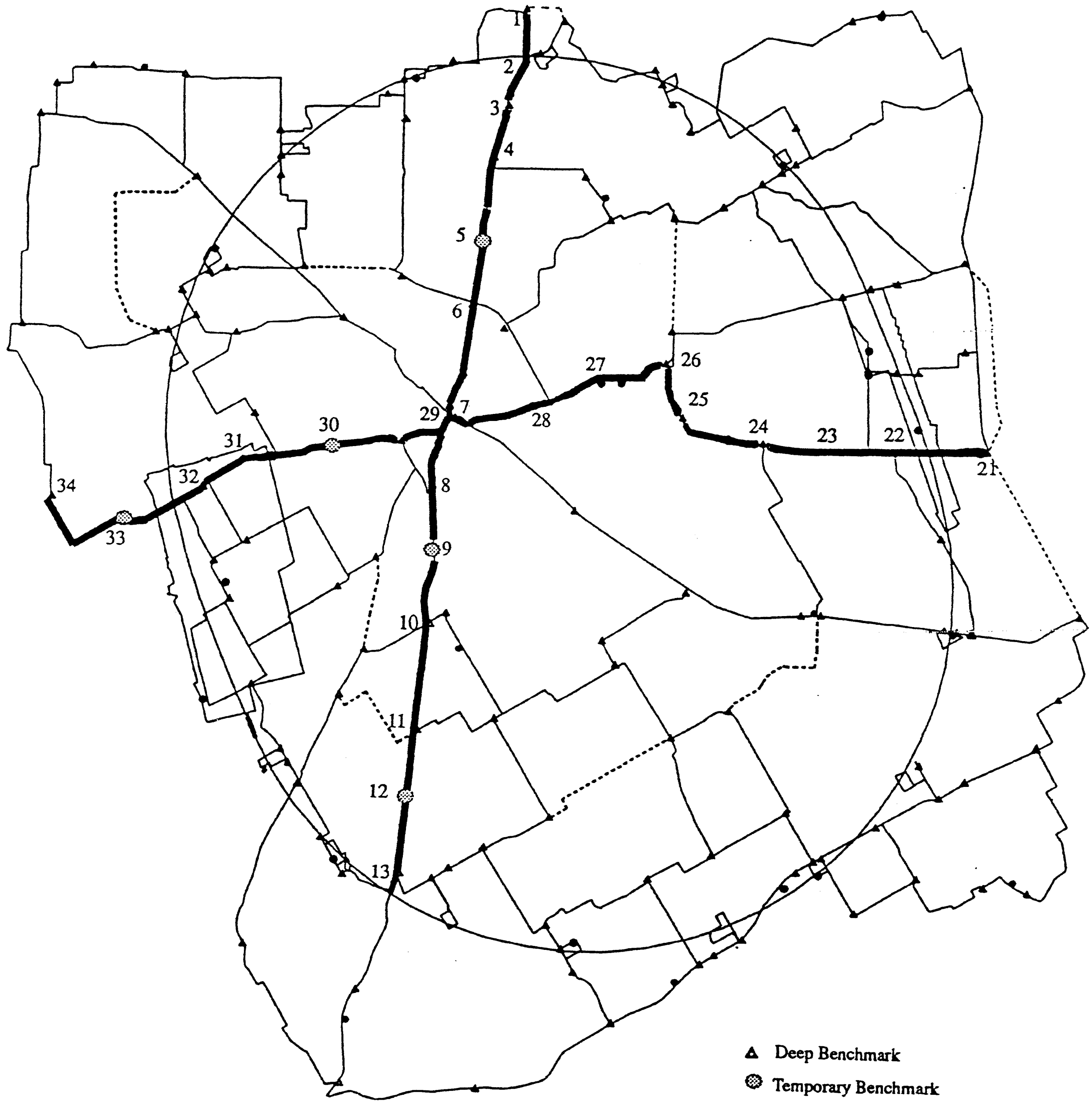

Figure 4.1
North-South and East-West Lines Chosen for Simulation

where g is the earth's mean anomaly:

$$g = 358°28'33" + 129596579.10"T - 0.54"T^2 - 0.012"T^3, \tag{4.7}$$

sL is the lunar pertubation of the mean longitude [Pagiatakis, 1982]:

$$sL = 6.4" \sin(231.19° + 20.20°T), \text{ and} \tag{4.8}$$

ψ is the nutation in longitude [Grodecki, et. al., 1992]:

$$\psi = -0.0048° \sin(279.9° - 0.053° \, d) - 0.0004° \sin(197.9° - 1.971° \, d), \tag{4.9}$$

$$d = jD - 2447891.5. \tag{4.10}$$

The declination δ, right ascension α, mean sidereal time st, and hour angle of the sun h, are calculated by the following [Pagiatakis, 1982]:

$$\delta = \arcsin(0.406 \sin\alpha + 0.008 \sin 3\alpha), \tag{4.11}$$

$$\alpha = x - 0.043° \sin 2x, \text{ and} \tag{4.12}$$

$$x = H + 0.034° \sin(H - pa), \tag{4.13}$$

where H is the geometric mean longitude of the sun, and
pa is the parallax (pa = 8.8").

The mean sidereal time at 00 hrs Universal Time is given by:

$$st = 99.69098333° + 36000.76892° \, T + 3.86708333 \times 10^{-4} \, T^2. \tag{4.14}$$

Finally, the hour angle of the sun is expressed as:

$$h = st + \lambda - \alpha. \tag{4.15}$$

The azimuth and zenith angle is determined from the following formulae [Thomson, 1978]:

$$Az = \arctan\left(\frac{\sin h}{\sin \varphi \cos h - \tan \delta \cos \varphi}\right), \tag{4.16}$$

and:

$$Z = \arctan\left(\frac{\dfrac{(-\cos \delta \sin h)}{\sin Az}}{\sin \varphi \sin \delta + \cos \varphi \cos h}\right). \tag{4.17}$$

The simulation, was performed by the Engineering Research Group [Grodecki, et al., 1992] for the date of 11 May 1992. Certain assumptions were made to achieve a realistic simulation. It was assumed that the survey crew would work a 6 hour day with a 1 hour break for lunch. Hourly progress of 0.5 km of levelling would be achieved. The mean astronomical correction was computed for each 0.5 km portion of a section and for the remainder of the section. The azimuth of the section was computed from the approximate coordinates of each potential location of a benchmark. Table 4.1 shows the results of the solar contribution of the tidal potential.

Table 4.1
Solar Tide Corrections

North-South Line			East-West Line		
From	To	Acc Corr (mm)	From	To	Acc Corr (mm)
1	2	-0.01	21	22	0.03
2	3	0.01	22	23	0.01
3	4	0.03	23	24	0.02
4	5	0.06	24	25	0.00
5	6	0.09	25	26	0.01
6	7	0.11	26	27	0.00
7	8	0.12	27	28	0.00
8	9	0.15	28	29	0.00
9	10	0.17	29	30	-0.02
10	11	0.22	30	31	0.02
11	12	0.23	31	32	0.03
12	13	0.25	32	33	0.00
			33	34	0.00

Analysis of the results given in Table 4.1 shows an accumulation of error in the north-south direction of 0.25 mm. In the east-west direction, there is no systematic accumulation.

A similiar analysis was performed for the contribution of the lunar effect, where it was estimated that the lunar contribution is twice that of the solar effect. The mean tropic longitude of the moon is given by:

$$s = 270.43659° + 481267.890057° \, T - 0.00198 \, T^2 + 0.000002 \, T^2 , \qquad (4.18)$$

and the mean tropic longitude of the lunar perigee is given by:

$$p = 334.32956° + 4069.03403° \, T - 0.01032° \, T^2 - 0.00001° \, T^3 , \qquad (4.19)$$

where T is Julian ephemeris date reduced to the fundemental epoch and expressed in centuries of 36525 days.

The mean tropic longitude of the sun is given by:

$$k = 1.0 + 0.0549 \cos(s-p) + 0.010 \cos(s-2h+p) + 0.008 \cos(2s-2h) . \qquad (4.20)$$

Table 4.2 shows the results of the lunar contribution of the tidal potential.

The values in Table 4.2 show an accumulation of error in the north-south direction of 0.59 mm which is slightly larger than twice the solar component. In the east-west direction there is once again no systematic accumulation.

The effect of ocean tide loading is expected to be no more than 1 to 2 mm per 1000 km, which is equivalent to 0.06 mm for a 30 km line and therefore can be safely ignored for the purpose of vertical control at the SSC Project.

Table 4.2
Lunar Tide Corrections

North-South Line			East-West Line		
From	To	Acc Corr (mm)	From	To	Acc Corr (mm)
1	2	0.10	21	22	-0.10
2	3	0.11	22	23	-0.14
3	4	0.18	23	24	-0.21
4	5	0.31	24	25	-0.25
5	6	0.38	25	26	-0.33
6	7	0.41	26	27	-0.37
7	8	0.40	27	28	-0.37
8	9	0.44	28	29	-0.36
9	10	0.44	29	30	-0.29
10	11	0.46	30	31	-0.19
11	12	0.53	31	32	-0.11
12	13	0.59	32	33	-0.05
			33	34	0.02

Considering the above analyses, the following recommendations were made. The effect of tidal accelerations in the north-south direction accumulates to a significant amount (up to 1mm) yet it is not necessary to correct for the effect because it will cause a small tilt of the whole plane of the SSC Project. The effect in the east-west direction can be safely ignored since it does not accumulate systematically. The observations should, however, be evenly distributed before and after local apparent noon when planning the schedule for field crews.

4.2 Analysis of the Effect of Orthometric Correction

The orthometric correction must be applied to compensate for the non-parallelity of potential surfaces to the reference surface or geoid. The variation of gravity must be eliminated from the observations to place elevation differences in a common frame of reference. To overcome this difficulty, levelled heights are converted to geopotential numbers by [Vanicek and Krakiwsky, 1986]:

$$C_j - C_i = \int_{P_i}^{P} g \; dh, \qquad (4.21)$$

where C_j and C_i are the geopotential numbers at points P_j and P_i, $[m^2 s^{-2}]$, respectively,
dh are the leveled height differences, [m], and
g is the gravity value, $[m^2 s^{-2}]$, corresponding to the levelled height difference, dh.

A potential difference, $C_j - C_i$, is independent of the route between the points. In order to give it dimensions of length, the geopotential is scaled by the value of normal gravity for an arbitrary standard latitude for the international ellipsoid [Heiskanen and Moritz, 1984]. As a result, the geopotential number is converted to a dynamic height. As both the geopotential number and dynamic heights express only potential differences, and do not have clear geometrical meaning, the concept of orthometric heights is introduced. The orthometric height of a point is defined as the geometrical distance between the geoid and the point measured along the plumbline. By definition, the relationship between the orthometric height and geopotential numbers is given by [Vanicek and Krakiwsky, 1986]:

$$H^o = \frac{C}{\bar{g}}, \tag{4.22}$$

where $\bar{g}$ is the mean gravity along the plumbline.

It is impossible to determine the exact value of the mean value of gravity, $\bar{g}$. It is therefore necessary to approximate the value of the gravity gradient. Different approximations lead to different orthometric height systems. The system used in the U.S.A. and on the SSC Project is the Helmert orthometric height system, which is defined as [Vanicek and Krakiwsky, 1986]:

$$H_i^H = \frac{C_i}{g_i^H}, \tag{4.23}$$

where g_i^H is the Helmert gravity gradient from:

$$g_i^H = g_i + 0.0424\, H_i, \tag{4.24}$$

and g_i is the gravity at the point P_i on the earth's surface.

The orthometric height differences can therefore be computed from levelled height differences combined with the orthometric corrections [Vanicek and Krakiwsky, 1986]:

$$\Delta H_{ij} = \Delta h_{ij} + OC_{ij}, \tag{4.25}$$

where OC_{ij} is the orthometric correction [m], determined from:

$$OC_{ij} = \sum_{k=i} \frac{g_k - g_r}{g_r} dh_k + H_i^D \frac{g_i' - g_r}{g_r} - H_j^D \frac{g_j' - g_r}{g_r}, \tag{4.26}$$

where dh_k is the levelled height difference between points k and k-1,

g_r is the reference gravity,

g_i' is the mean gravity along the plumbline at point i,

g_j' is the mean gravity along the plumbline at point j, and

H_i^D and H_j^D are the dynamic heights determined by:

$$H_i^D = \frac{C_i}{g_r}. \tag{4.27}$$

For projects requiring precise levelling such as the SSC, the accuracy of determining orthometric heights should be kept below 0.1 mm/km (ten percent of the total admissible error) [Grodecki, et al., 1992b]. This may be accomplished by applying corrections based on gravity measurements. An analysis of the accuracy of the existing National Geodetic Survey (NGS) gravity data was performed by the Engineering Surveys Research Group [Grodecki, et al., 1992b] to ensure the vertical control requirements were achievable using existing gravity and thus determine whether further densification of gravity is required.

Given the set of observed gravity values at points in a particular area, the prediction methods enable gravity to be estimated at other points in the area. The unknown gravity value at point P is generally approximated by the function [Heiskanen and Moritz, 1984]:

$$\widetilde{\Delta g}_P = F(\Delta g_1, \Delta g_2, \ldots, \Delta g_n). \tag{4.28}$$

In most practical applications, the function F is linear in terms of gravity anomalies Δg. In the analysis of gravity accuracy performed by UNB, least squares collocation was found to be the appropriate method for predicting gravity anomalies.

The least-squares prediction (collocation) method is derived by minimizing, in terms of coefficient a , the square of the prediction error expressed by:

$$\varepsilon_P = \Delta g_P - \widetilde{\Delta g}_P. \tag{4.29}$$

The least squares prediction gives optimum results and accuracy estimates. The final prediction formula is given by [Torge, 1980]:

$$\widetilde{\Delta g}_P = C_P^T (C + D)^{-1} \Delta g, \tag{4.30}$$

where:

$$C_P = \begin{pmatrix} C_{P_1} \\ \cdot \\ \cdot \\ \cdot \\ C_{P_n} \end{pmatrix} \tag{4.31}$$

$$C = \begin{pmatrix} C_{11} & \cdots & C_{1n} \\ \cdot & & \cdot \\ \cdot & & \cdot \\ \cdot & & \cdot \\ C_{n1} & \cdots & C_{nn} \end{pmatrix} \tag{4.32}$$

$$D = \begin{pmatrix} D_{11} & \cdots & D_{1n} \\ \cdot & & \cdot \\ \cdot & & \cdot \\ \cdot & & \cdot \\ D_{n1} & \cdots & D_{nn} \end{pmatrix} \tag{4.33}$$

$$\Delta g = \begin{pmatrix} \Delta g_1 \\ \cdot \\ \cdot \\ \cdot \\ \Delta g_n \end{pmatrix} \tag{4.34}$$

and where $C_{P_i} = M\{Dg_P\, Dg_i\}$ is the crosscovariance of the gravity anomaly at point P with the gravity anomaly at the observed point P_i,

$C_{ij} = M\{Dg_i\, Dg_j\}$ is the autocovariance of the gravity anomalies at the observed points,

$D_{ij} = M\{n_i\, n_j\}$ is the autocovariance of the observational errors n (noise), and

$M\{..\}$ stands for the averaging operator.

The variance-covariance matrix of the predicted anomalies can be determined from [Grodecki, et al., 1992b]:

$$E_{PP} = C_{PP} - C^T_{PP_i}(C + D)^{-1} C_{PP_i}, \tag{4.35}$$

where C_{PP} is the covariance matrix of the anomalies being estimated, and

C_{PP_i} is the crosscovariance matrix of the anomalies being estimated with the observed gravity anomalies.

Subsequently, the standard error of the predicted gravity anomaly for point P is given by the following formula [Heiskanen and Moritz, 1984]:

$$m_P^2 = C_0 - C_P^T (C + D)^{-1} C_P, \tag{4.36}$$

where C_0 is the expected mean square value of the gravity anomalies.

The least-squares prediction method takes advantage of the fact that the gravity anomalies can be considered as statistical quantities with a mean value of zero [Torge, 1980]. It is also assumed that the stochastic properties of the anomalies are homogeneous and isotropic. Under these assumptions, the stochastic properties of the anomalies can be described by a single covariance function $\operatorname{cov}(\Delta g_i, \Delta g_j, s)$ which depends only on the distance, s, between the points P_i and P_j. Such a covariance function can be expressed by the following [Grodecki, et. al, 1992b]:

$$\operatorname{cov}(\Delta g_i, \Delta g_j, s) = M\{\Delta g_i, \Delta g_j\}_s, \tag{4.37}$$

where M is the mean value operator, and
s is the ellipsoidal distance between the points P_i and P_j.

In general, the free-air gravity anomalies are correlated with elevation. Therefore, this correlation has to be removed before the covariance function is estimated. The functional relationship between free-air anomalies and the elevations is approximately linear [Grodecki, et al., 1992b]. To obtain the anomalies, which are independent of the elevations, a term that is proportional to the elevation must be added:

$$z = \Delta g - a\,\Delta h. \tag{4.38}$$

If z is a Bouguer anomaly, then for, the density $\rho = 2.67$ g/cm^3, the coefficient a, is equal to 0.112 mgal/meter [Heiskanen and Moritz, 1984] (Note: a and z have different representation than in refraction).

The least-squares collocation of the gravity anomalies for the SSC Project area was performed using the above mentioned numerical procedures. The data were provided by the National Geodetic Survey (NGS) Vertical Network Branch in the form of a computer file containing 5990 gravity points for the area enclosed by latitudes N31.00 to N34.00 degrees, and longitudes W95.50 to W98.50 degrees.

Each of the gravity points is described by its latitude and longitude of position, topographic height, observed gravity, estimated error of gravity, bore hole depth, free-air anomaly, estimated error of anomaly, terrain correction, and observation type.

In the first approximation, the correlation between the free-air anomalies and the elevations was neglected. Analysis was performed by UNB consultants to estimate the covariance function [Grodecki, et al., 1992b]. The Geodetic Reference System 1980 (GRS 80) was chosen to be the reference ellipsoid. The parameters describing the functional relationship between the gravity anomalies and heights were set to zero. The ellipsoidal distances between the gravity points were computed by means of the Puissant's solution to the inverse problem on the ellipsoid [Vanicek and Krakiwsky, 1986]. All 5990 data points were utilized, and the values of the covariance function were estimated for every 2 km interval, for the points up to 158 km apart. The result of the estimated covariance function is shown in Figure 4.2.

A straight line was used to estimate the functional relationship between the anomalies and elevations. It had been implicitly assumed that this relationship is of a linear nature. The functional relationship is:

$$\Delta g = a\,h + b, \tag{4.39}$$

where h is the topographic height.

All 5990 gravity points were used, and the estimation gave the following results:

$a = -0.11274 \pm 0.00322,$

$b = 22.55328 \pm 0.71644,$

$\sigma_o^2 = 426.23.$

The estimated parameter a, was found to be virtually identical to the theoretical coefficient defined for the Bouguer anomaly as shown in Equation (4.38). After removal of the correlation of gravity anomalies with elevations, the covariance function was re-computed. The results of this estimation are shown in Figure 4.3.

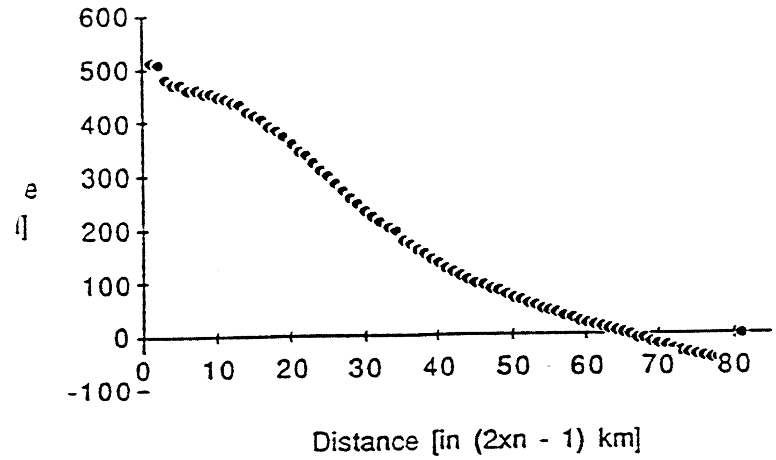

Figure 4.2
Estimated Covariance Function (Correlation with Heights Not Accounted For) [Grodecki, et. al., 1992b]

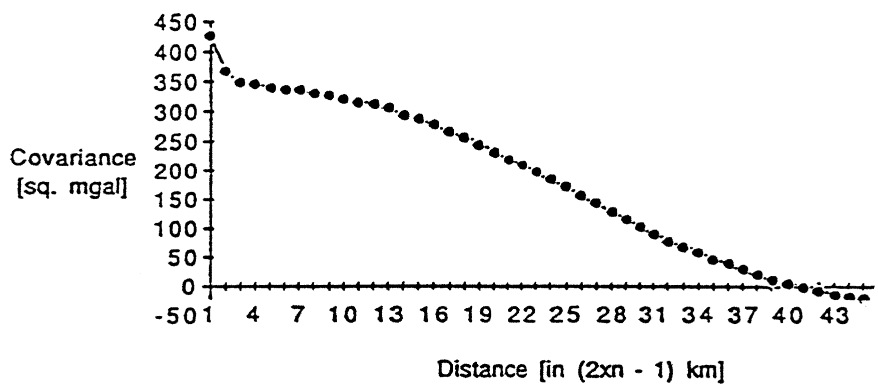

Figure 4.3.
Estimated Covariance Function (Correlation with Heights Removed) [Grodecki, et al., 1992b]

For the purpose of the least-squares prediction, the estimated covariance function has to be approximated by an algebraic formula. One of the most commonly used is the exponential function [Grodecki, et al., 1992b]:

$$\Delta g = a \exp(-b\, s). \tag{4.40}$$

In this analysis, two types of functions were used for the approximation of the covariance function: the exponential function given by Equation (4.36) and the following third degree polynomial.

$$\Delta g = a + bs + cs^2 + ds^3. \tag{4.41}$$

The main disadvantage of the exponential function is that it is unable to accurately approximate the shape of the covariance function. It is, however, relatively uncomplicated and provides a fairly good fit for the short portions of the covariance function. The polynomial provides a better fit to the overall shape of the function, but may result in oscillations, the amplitude and number of which increases with a degree of a polynomial.

The exponential function was fitted by UNB to the portion of the covariance function from 0 to 38 km. The fitting gave the following results [Grodecki, et al., 1992b]:

$a = 423.782 \pm 1.007$,
$b = 0.01586 \pm 0.00078$,
$\sigma_o^2 = 0.005$.

The difference between the covariance function and its approximating function is shown in Figure 4.4.

The third degree polynomial was fitted by the UNB consultants to the portion of the covariance function from 0 to 38 km. The approximation gave the following results [Grodecki, et al., 1992b]:

$a = 425.435 \pm 0.491$,
$b = -15.792 \pm 0.527$,
$c = 0.751 \pm 0.043$, and
$d = -0.013 \pm 0.001$.

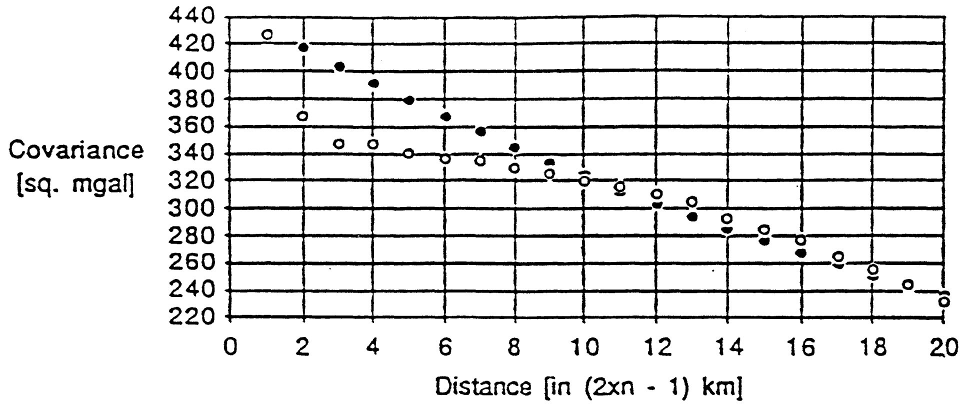

Figure 4.4
Approximating vs Estimating Covariance
Function (Exponential Function) [Grodecki, et al., 1992b]

The difference between the covariance function and its approximating function is shown in Figure 4.5.

As mentioned previously, the impact of gravity errors should not be larger than 0.1 mm√L (ten percent of the total admissible error for FGCC First-Order Class I). This is equivalent to about 100 [mGal m] √L. The maximum value of the combined error of interpolation and the gravity point error should therefore be smaller than this limit.

For the purpose of this analysis, the least-squares prediction of gravity anomalies was performed on the same two leveling lines as in the tidal analysis (Figure 4.1). The first level line runs from point 1 to point 13 and the second line runs from point 21 to point 34. The prediction method applied here takes both the accuracy of the gravity data and the interpolation error into account.

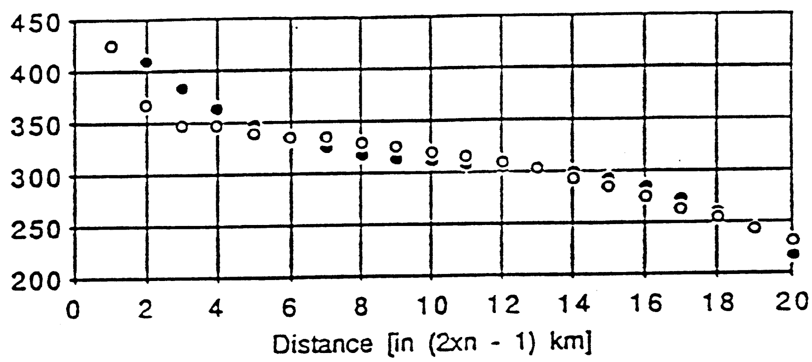

Figure 4.5
Approximating vs Estimated Covariance
Function (Polynomial) [Grodecki, et al., 1992b]

A simulation was performed by the UNB Engineering Surveys Research Group. Two types of functions approximating the covariance function were used: the exponential function (Equation 4.36) and the 3rd degree polynomial (Equation 4.37). The results of the gravity anomaly predictions are given in Tables 4.3 and 4.4.

Analysis of the results given in Tables 4.3 and 4.4 shows that there is generally good agreement between the two models. The third degree polynomial model gives slightly larger estimates of standard deviations of the predicted anomalies.

Table 4.3
Estimated Gravity Anomalies and Standard Deviations for Leveling Between 1 to 13

Point Number	Model	
	(Exponential Function)	(3rd Degree Polynomial)
[-]	[mgal]	[mgal]
1	-4.62 ± 4.03	-5.63 ± 6.18
2	-4.62 ± 3.86	-4.41 ± 5.85
3	-4.64 ± 2.41	-4.52 ± 3.62
4	-4.61 ± 3.86	-4.37 ± 5.88
5	-6.11 ± 3.63	-6.26 ± 5.52
6	-7.92 ± 2.73	-7.97 ± 4.12
7	-7.69 ± 3.54	-7.20 ± 5.37
8	-7.46 ± 4.40	-6.34 ± 6.68
9	-7.42 ± 2.86	-7.18 ± 4.33
10	-7.00 ± 2.40	-6.88 ± 3.63
11	-8.53 ± 3.85	-9.79 ± 5.87
12	-10.31 ± 3.24	-9.70 ± 4.91
13	-7.64 ± 2.00	-7.54 ± 2.98

Table 4.4
Estimated Gravity Anomalies and Standard Deviations for Leveling Between 21 to 34

Point Number	Model	
	(Exponential Function)	(3rd Degree Polynomial)
[-]	[mgal]	[mgal]
21	-10.48 ± 4.37	-10.66 ± 6.64
22	-7.59 ± 3.68	-7.59 ± 5.59
23	-7.54 ± 3.86	-7.48 ± 5.87
24	-7.85 ± 2.74	-7.84 ± 4.15
25	-7.88 ± 2.36	-7.87 ± 3.55
26	-7.23 ± 3.98	-6.78 ± 6.04
27	-7.69 ± 3.54	-7.20 ± 5.37
28	-7.92 ± 2.73	-7.97 ± 4.12
29	-7.01 ± 3.84	-6.73 ± 5.84
30	-5.48 ± 3.82	-5.40 ± 5.82
31	-2.90 ± 3.81	-1.95 ± 5.78
32	0.24 ± 2.77	1.51 ± 4.17
33	2.88 ± 3.54	3.14 ± 5.38

The correlation between the free-air gravity anomalies and the elevations had been estimated and removed, but only for the purpose of estimation of the covariance function.

The geopotential numbers can be expressed as:

$$\Delta C_{ij} = \sum_{k=i}^{j} g\,(\varphi,\lambda\,,h\,)_k\,\delta l_k + \sum_{k=i}^{j} g_k\,\delta l_k + \sum_{k=i}^{j} \Delta g_k \delta l_k, \qquad (4.42)$$

where $g(\varphi,\lambda\,,h\,)$ is the reference gravity (e.g., normal gravity),
Δg_k is the gravity anomaly, and
δl_k is the levelled height difference.

Differentiating Equation (4.42) results in:

$$d(\Delta C_{ij}) = \sum_{k=i}^{j} g\,(\varphi,\lambda\,,h\,)_k\, d\,(\delta l_k) + \sum_{k=i}^{j} \Delta g_k\, d\,(\delta l_k) + \sum_{k=i}^{j} d\,(\Delta g_k)\delta l_k, \qquad (4.43)$$

The first term of the differentiation does not depend on the density and accuracy of gravity data nor the error of gravity anomalies. The second term expresses the influence of the elevation difference error and is at least two to three orders of magnitude smaller than the third term, which gives the influence of the accuracy of the predicted gravity anomalies. Assuming that the errors propagate randomly, the accumulated effect of the errors of predicted gravity anomalies is estimated as [Grodecki, et al., 1992b]:

$$\sigma^2_{\Delta C} = \sum_{k=i}^{j} \sigma^2_{\Delta g_k}\, \delta l^2{}_k. \qquad (4.44)$$

The results for the two leveling test lines are given in Table 4.5.

Results from the UNB analysis of the available NGS gravity data concludes that the influence of the interpolation of gravity anomalies does not exceed 0.5 mm at the standard confidence level over 30 km. The error associated with gravity interpolation is lower than the estimated ten percent of the estimated error in the levelling, therefore no additional gravity measurements are required. The least squares collocation method provides a rigorous method for reducing levelled height differences to orthometric heights required for the SSC Project.

Table 4.5
Effect of Interpolated Gravity

Line From - To	Model Maximum [-]	Maximum Allowable Error [mm]	Error in Elevation Difference [mm]
1-13	Exponential	0.66	0.17
1-13	Polynomial	0.66	0.23
21-34	Exponential	0.63	0.32
21-34	Polynomial	0.63	0.49

CHAPTER 5
STANDARDS, SPECIFICATIONS AND PROCEDURES

The need for a small network with a large degree of redundancy resulted in the development of standards, specifications and procedures unique to the SSC Project as opposed to adapting existing FGCC guidelines which are suitable for large scale networks (National or Regional networks of over 100 km in length). A deterministic approach for developing standards for vertical control is required using the analysis of observational errors and geodetic reductions in the previous two chapters. Instrument specifications and field procedures are adopted from those of existing FGCC First-Order Class I with minor changes to ensure high accuracy is achieved. Procedures for densification of vertical control from the PVCN to the service areas, elevation transfers from the service areas to the the bottom of the shafts, and tunnel extension ensure the reliability and accuracy of elevations for the construction of the tunnels.

5.1 Accuracy Tolerances

Geodetic levelling tolerances for vertical control are developed to ensure that the accuracy requirements for the surface control network are met. They are easily adapted for densification as well as for tunnel control surveys. The tolerances for geodetic levelling are determined from a combination of random and systematic errors. Random errors include pointing, reading and levelling of the line-of-sight. They propagate proportionally to $\sqrt{L}$ where L is the length of the level section in kilometres.

Assuming a maximum line-of-sight of 50 m at each setup, which is possible at the SSC Project area since the terrain consists of gentle rolling hills, and using double pointings (two scales - high and low scales), the standard deviation of an elevation difference at each setup, Δh_i, due to random errors only, is estimated as:

$$\sigma^2_{\Delta h_i} = \frac{2\sigma_l^2 + 2\sigma_p^2 + 2\sigma_r^2}{2} = (0.28\ \text{mm})^2, \tag{5.1}$$

which can be translated into a standard deviation, σ_o, of a section length:

$$\sigma_o = 0.28\ \text{mm}\sqrt{10\ \text{setups/km}} = 0.88\ \text{mm}/\sqrt{\text{km}}\,. \tag{5.2}$$

Therefore, the random error component of the accuracy of a one-way measured levelling line of length, L, in kilometres is:

$$\sigma_l = 0.88 \text{ mm}\sqrt{L}. \tag{5.3}$$

The uncertainty is increased by the accumulation of residual systematic effects. Such effects that were previously discussed include the sinking of the turning plates (0.03 mm/setup) (Section 3.2.6), atmospheric refraction (0.1 mm/km) (Section 3.2.8) and the orthometric correction (0.1 mm/km) (Section 4.2). Since the systematic effects are taken as residual effects only (the major influences removed by proper survey methods), the systematic errors are accumulated in squares. The total accuracy can be expressed as a combination of random and systematic errors [Chrzanowski, 1985]:

$$\sigma_t^2 = \sigma_o^2 L + \varepsilon_o^2 L^2, \tag{5.4}$$

where ε_o is the systematic component of errors associated with one kilometre of levelling.

Applying the above estimations for these errors, one obtains [DeKrom, et al., 1992a]:

$$\sigma_t^2 = \left(0.88\text{mm}\sqrt{L}\right)^2 + \left(0.03\text{mm}\times n\, L\right)^2 + \left(0.1\text{mm}\, L\right)^2 + \left(0.1\text{mm}\, L\right)^2, \tag{5.5}$$

where n is the number of set ups in a kilometre.

If the maximum line-of-sight is assumed, then there are ten set ups (n = 10) in one kilometre, and Equation (5.5) simplifies to [DeKrom, et al., 1992a]:

$$\sigma_t = \sqrt{\left(0.77\text{mm}\, L\right) + \left(0.11\text{mm}\, L^2\right)}. \tag{5.6}$$

Equation (5.6) forms the basis of the derived allowable tolerances of the SSC geodetic levelling, which include:

- Section closures, $\Delta_{section}$,
- Loop closures, Δ_{loop},
- Setup tolerance, Δ_{setup}, and
- Rejection criteria, $\Delta_{relevel}$.

5.1.1 Section Closures

Section closures are the maximum allowable difference between two one-way levellings at the 95 percent confidence level. Initial investigations estimate a correlation of +0.1 [Torge, 1980] between direct and reverse levellings caused by turning plate sinking and atmospheric refraction. Since section closure tolerances for the SSC Project already consider turning plate sinking and refraction, it is assumed that no correlation exists between the two-way levellings. The allowable section closure may be determined from Equation (5.6), multiplied by 1.96 to increase to 95 percent confidence level, and multiplied by $\sqrt{2}$ for a two-way section (by the theory of error propagation) [DeKrom, et al., 1992a]:

$$\Delta_{section} = 1.96 \times \sqrt{2} \times \sqrt{(0.77 \text{ mm L}) + (0.11 \text{ mm L}^2)}, \tag{5.7}$$

which simplifies to [DeKrom, et al., 1992a]:

$$\Delta_{section} = \sqrt{(5.92 \text{ mm L}) + (0.84 \text{ mm L}^2)}, \tag{5.8}$$

where L is the length of the section in kilometres.

5.1.2 Loop Closures

The loop closures are the allowable misclosure of the single one-way levelling in a loop. The required closure maybe determined from Equation (5.6) [DeKrom, et al., 1992a]:

$$\Delta_{loop} = 1.96 \times \sqrt{(0.77\text{mm L}) + (0.11\text{mm L}^2)}, \tag{5.9}$$

which simplifies as [DeKrom, et al., 1992a]:

$$\Delta_{loop} = \sqrt{(2.96\text{mm L}) + (0.42\text{mm L}^2)}. \tag{5.10}$$

5.1.3 Setup Tolerances

The setup tolerance is the allowed difference at the 95 percent confidence level between high scale and low scale determinations of Δh at each set up. The value can be derived from Equation (5.1) [DeKrom, et al., 1992a]:

$$\Delta_{setup} = 0.28 \text{ mm} \times 1.96 \times \sqrt{2} = 0.78 \text{ mm}. \tag{5.11}$$

If one can assume that there is no correlation between the high scale and low scale readings, then Equation (5.1) would be appropriate. Since a strong correlation could be expected if the observations are taken almost simultaneously (same setup, same atmospheric conditions, and same observer), the tolerance can then be derived through the theory of error propagation:

$$\Delta_{setup} = 1.96 \times \left[\sigma^2_{high} + \sigma^2_{low} - 2\,\rho\sigma_{high}\sigma_{low}\right], \tag{5.12}$$

where σ^2_{high} and σ^2_{low} are the variances of the elevation difference, and
ρ is the correlation between high scale and low elevation differences.

The correlation can be assumed to be as high as +0.75 for double compensator instruments and +0.9 for single compensator instruments. The reason for the increase from +0.75 to +0.9 for single compensator instruments is due to the increase in systematic effects caused by the uncertainty of the compensator that are eliminated with the use of a double compensator system. Using Equation (5.12), the maximum allowable elevation difference for double compensator instruments for a set up becomes 0.4 mm, and for single compensator instruments, 0.3 mm.

5.1.4 Rejection Criteria

If either $\Delta_{section}$ or Δ_{loop} is not met, then the required vertical accuracy is not being achieved and the elevation difference is considered an outlier at the 95 percent level of confidence and must be re-observed. To ensure that the re-observation of the level section is acceptable, the rejection criteria is formulated from in-context statistical testing on the sample mean with known variance [Vanicek and Krakiwsky, 1986].

Statistical testing on the sample mean, $\bar{x}$, is performed to determine if outliers exist when three or more runnings, x_i, of a level section are measured. The rejection criterion, at the 95 percent level of confidence, of an observation from the sample mean is formulated as:

$$\Delta_{relevel} = \left|\bar{x} - x_i\right| = t\,\sigma_t. \tag{5.13}$$

where σ_t is formulated from Equation (5.6) and t is listed in Table 5.1.

Table 5.1

Rejection Criteria for Relevelling Sections

No. of Runnings	t
3	1.96
4	2.17
5	2.31
6	2.41

Any elevation difference that does not satisfy the above criteria is considered an outlier at the 95 percent level of confidence and is eliminated. Re-observations are necessary until at least one direct and one reverse running of a section agree. When another elevation difference is measured, a new mean, $\overline{x}$, is computed and each individual observation is tested against the new mean.

5.2 Procedures for Vertical Surface Control

The procedures are designed in order to minimize the influence of systematic effects mentioned previously. The procedures developed are similiar to those used by the FGCC, which are based on many years of data collection. Minor changes are required to accommodate the requirements of the limited area of the SSC Primary Vertical Control Network [DeKrom, et al., 1992b]. An abridged version of the field and office procedures is presented in Table 5.2.

Instrumentation for the Primary Vertical Control Network consists of JENA Zeiss Ni002A levels (double compensator levels) with Wild half-centimetre rods. This allows for high accuracy and efficient use of field crews. Field crews are found to average five minutes per setup as opposed to eight minutes with the Wild NA2 level with micrometer. It is expected that the shorter set-up time will reduce the effect of turning plate sinking to less than 0.03 mm/setup.

Rod verticality checks are performed by each crew on a daily basis to ensure that the rod are within 10' of the vertical. Collimation checks on the instruments are also performed daily. If the instrument is out of the allowed range of 0.02 mm/m, then it must be readjusted.

Table 5.2
Procedures for the PVCN

Field Procedures	
Setup Tolerances - Single compensator - Double compensator	 0.30 mm 0.40 mm
Sight Length - Maximum Allowable L-O-S - Maximum L-O-S Discrepancy	 50 m 2 m/setup 4 m/section
Observation Procedure - Odd setups - Even setups	 BS(low), FS(low), FS(high), BS(high) FS(low), BS(low), BS(high), FS(high)
Office Procedures	
Section Closures	$\Delta_{section} = \sqrt{(5.92\ \text{mm}\ L) + (0.84\ \text{mm}\ L^2)}$
Loop Closures	$\Delta_{loop} = \sqrt{(2.96\text{mm}\ L) + (0.42\text{mm}\ L^2)}$
Planning Procedures	
Sections are evenly distributed before and after local apparent noon	
Randomization of field crews, instruments, sections	
Observe temperature at five different heights	

To account for the effect of refraction, temperature gradients are measured in the field along the levelling line. To ensure rigorous determination of the effect, additional temperature gradients are observed from five temperature probes mounted on a rod at different heights above the terrain (0.3 m, 0.7 m, 1.2 m, 1.8 m and 3.0 m). The temperature meter was designed by the PB/MK Geodetic Survey Division. The thermistors and temperature collector were constructed by DEBAN Enterprises, Inc. Field tests show an accuracy of 0.1°C to be achievable using continuous measurements of temperature with the probes. Field tests show that the temperature collector has enough memory to continuously collect data at 20 second intervals for an 12 hour period. Data has to be downloaded and the memory cleared on a daily basis.

The effect of refraction can be rigorously determined through non-linear least-squares estimations for constants a, b, and c in Kukkamaki's Equation, Equation (3.11). By determining temperature differences, the unknown a, is eliminated then only constants b and c are necessary. Determining temperature differences results in:

$$\begin{aligned} \Delta t_{(1-2)} &= b\left(z_1^c - z_2^c\right), \\ \Delta t_{(2-3)} &= b\left(z_2^c - z_3^c\right), \text{ etc.} \end{aligned} \tag{5.14}$$

Differentiating Equation (5.14) with respect to the unknowns, b and c, is required for non-linear least squares estimations. The result are:

$$\begin{aligned} \frac{\partial}{\partial b}\left(\Delta t_{(1-2)}\right) &= z_1^c - z_2^c, \\ \frac{\partial}{\partial b}\left(\Delta t_{(2-3)}\right) &= z_2^c - z_3^c, \text{ etc} \end{aligned} \tag{5.15}$$

and

$$\begin{aligned} \frac{\partial}{\partial c}\left(\Delta t_{(1-2)}\right) &= b \ln\left(z_1^c\right) - b \ln\left(z_2^c\right), \\ \frac{\partial}{\partial c}\left(\Delta t_{(2-3)}\right) &= b \ln\left(z_2^c\right) - b \ln\left(z_3^c\right), \text{ etc.} \end{aligned} \tag{5.16}$$

The first design matrix of the least squares adjustment, A, is then derived as:

$$A = \begin{pmatrix} z_1^c - z_2^c & b \ln\left(z_1^c\right) - b \ln\left(z_2^c\right) \\ z_2^c - z_3^c & b \ln\left(z_2^c\right) - b \ln\left(z_3^c\right) \\ z_3^c - z_4^c & b \ln\left(z_3^c\right) - b \ln\left(z_4^c\right) \\ z_4^c - z_5^c & b \ln\left(z_4^c\right) - b \ln\left(z_5^c\right) \end{pmatrix} \tag{5.17}$$

Each temperature probe on the thermistor pole is calibrated daily using the same procedures and thus each is assumed to be of the same accuracy. The weight matrix is then represented by an identity matrix:

$$P = \begin{pmatrix} 1 & 0 & 0 & 0 \\ 0 & 1 & 0 & 0 \\ 0 & 0 & 1 & 0 \\ 0 & 0 & 0 & 1 \end{pmatrix} \tag{5.18}$$

The observation vector is composed of measured temperature differences,

$$\Delta t = \begin{pmatrix} \Delta t_{1-2} \\ \Delta t_{2-3} \\ \Delta t_{3-4} \\ \Delta t_{4-5} \end{pmatrix} \tag{5.19}$$

Values for b and c at each instrument setup can thus be obtained. The error associated with refraction can then be estimated using Equations (3.9) to (3.22).

5.3 Standards, Specifications and Procedures for Densification and Elevation Transfer

Densification schemes are designed to include sufficient redundancy to ensure reliability and accuracy. For reasons of economy, simple concrete monuments are used at service areas, it is therefore necessary to perform densification shortly before the elevation transfer process. The densification network includes at least three monuments on the service area that are connected to three existing PVCN benchmarks from which the appropriate elevations and variance-covariance information is obtained. Vertical densification also includes at least two temporary monuments on the collar of the shaft. This allows a quick transfer process from the surface to the tunnel. A typical densification network is shown on Figures 5.1.

The transfer of elevations is integrated into the horizontal control transfer and therefore accomplished during the same survey. The methodology includes the use of industrial metrology equipment, namely the Taylor-Hobson Sphere, which is an interchangeable sphere/reflector that defines a point in space and may be oriented in any

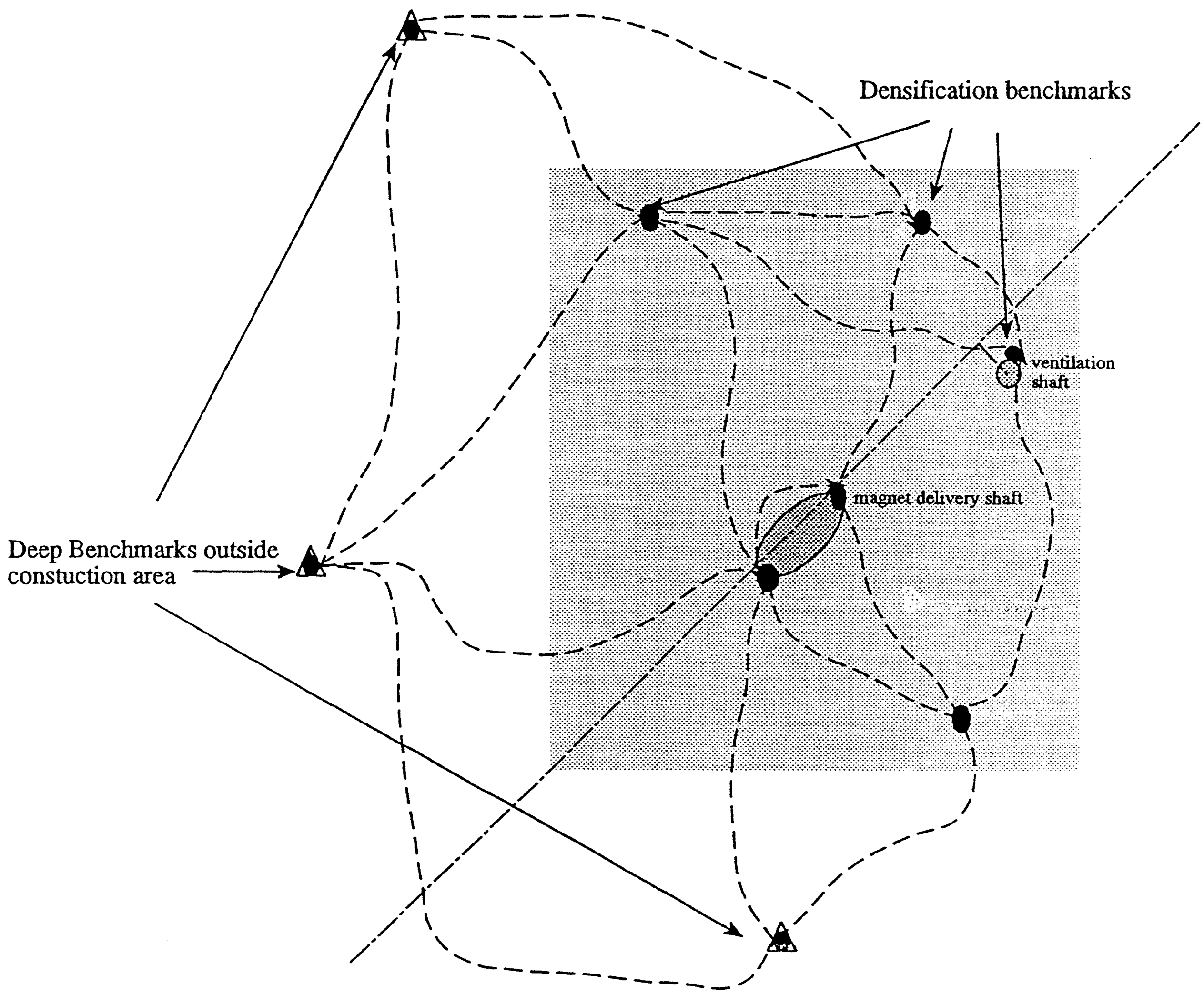

Figure 5.1
Typical Denification Scheme

direction. On the surface, a precise level with a parallel plate micrometer (Zeiss JENA Ni002A) is used in conjuction with a tripod with an elevating head to enable the level to be raised or lowered so that the Taylor-Hobson sphere center is within the micrometer range. The elevation is then transferred from the benchmarks on the collar to the Taylor-Hobson spheres (Figure 5.2). An estimated accuracy of 0.3 mm is expected using this method [Chrzanowski, et al., 1992].

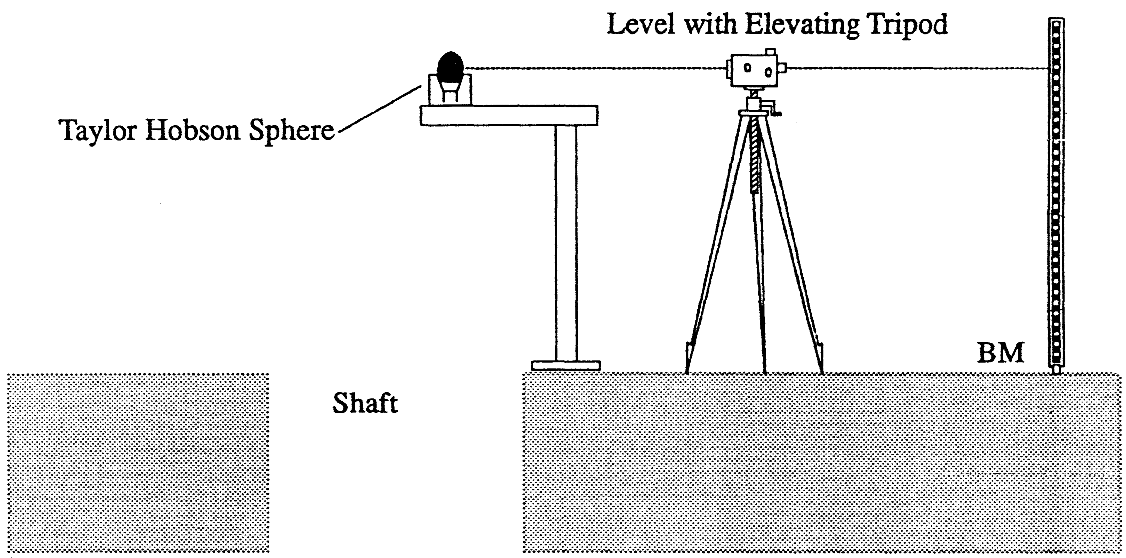

Figure 5.2
Elevation Transfer from Shaft Collar to
Taylor-Hobson Spheres

The heights are transferred by observing vertical distances using an Electronic Optical Distance Measuring Instrument (EODMI). A zenith plummet along with the Kern centering system (Kern tripod with centering rod) with translation stage is used for the purpose of locating the direct plumb down the shaft. The Taylor-Hobson spheres are replaced by a sphere with a precise prism insert (reflector) which serves as a retro reflector. The plummet is replaced by a coaxial precision total station (e.g., Wild/Leica TC2002). The telescope of the coaxial precision total station is pointed vertically to the prism and the vertical distance is measured in at least three sets with independent repointings between the sets. With repeated electronic pointings and proper calibration, the elevation transfer can be expected to have an accuracy of:

$$\sigma_{e.t.} = \sqrt{(0.5\ \text{mm})^2 + (2.0\ \text{ppm})^2} \tag{5.17}$$

Control transfer from the total station to the nearest benchmarks in the adit or tunnel is accomplished in a similiar manner. Instead of using Taylor-Hobson spheres, the trunnion axis of the theodolite is used as the target. The eccentricity of the dot representing the trunnion axis is expected to be less than 0.2 mm. The accuracy of the step is estimated to be 0.4 mm [Chrzanowski, et al., 1992]. The overall elevation transfer scheme is shown in Figure 5.3.

In the underground surveys, at least three benchmarks are established from the elevation transfer. Temporary BMs are established in the tunnel adit in case any tunnel BMs are destroyed during construction as well as to add strength to the geometry of the tunnel network. The proposed design of the survey from the shaft stations to the main tunnel depends on the type of shaft (ventilation, personnel/utility, magnet delivery) as well as obstacles caused by construction. Proposed design for elevation transfer is shown in Figures 5.4.

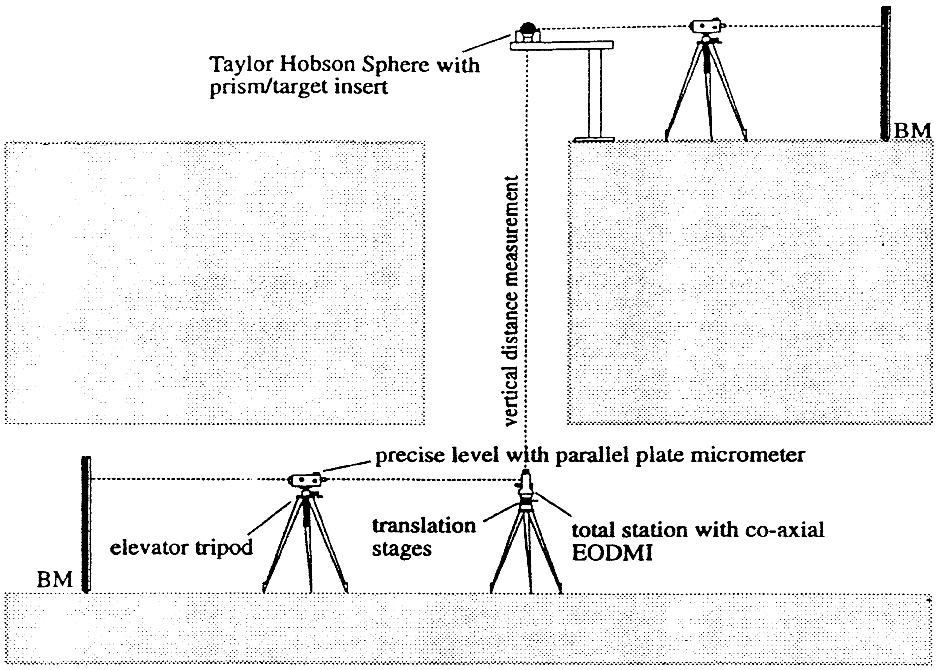

Figure 5.3

Elevation Transfer [Greening, et al., 1992]

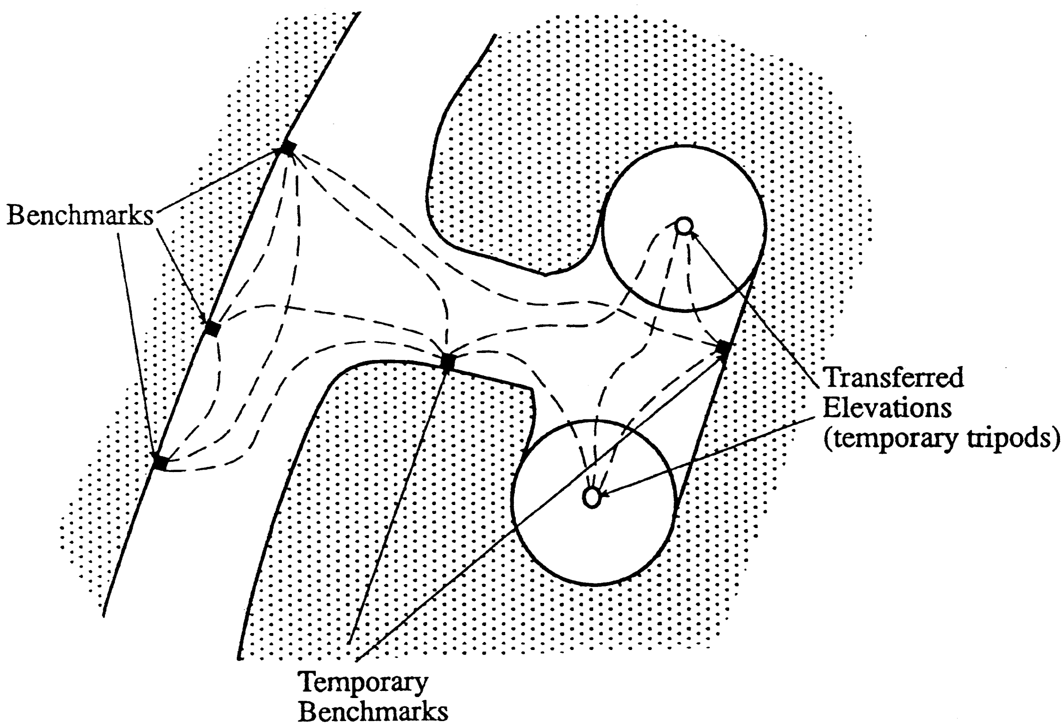

Figure 5.4

Shaft Transfer Design (Personnel/Utility Shaft)

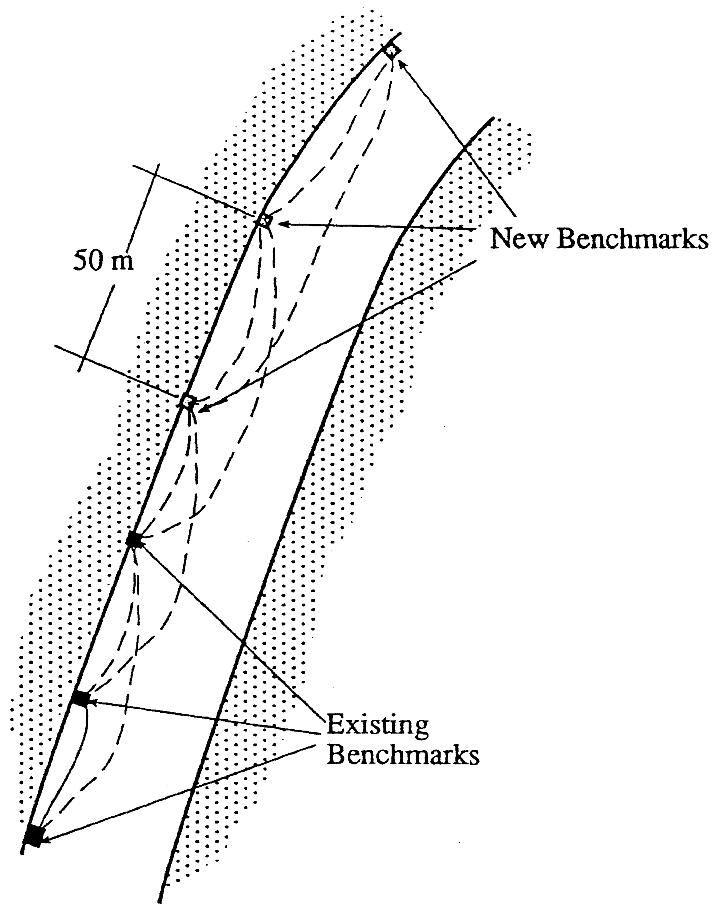

Figure 5.5
Vertical Control Extension

CHAPTER 6
POST ANALYSIS

A complete and thorough post-analysis is required to ensure the highest accuracy is achieved. The analysis of the Primary Vertical Control Network accuracy includes section and loop closures, and analysis of the least-squares adjustment. Geodetic reductions for atmospheric refraction and orthometric effect are analyzed and their effect on the elevations determined. A Minimum Norm Quadratic Estimation (MINQE) is performed to determine the proper weightings based on the variance-covariance of the observations differences are used in the final adjustment.

A complete analysis of the results of elevation transfers at the N15, N20, N25, N30, N35, N40 and N45 and tunnel control in the five completed half sectors of the A610, A611, A650 and A670 contracts is also described. The results of the breakthrough are included.

6.1. Section and Loop Closures of the Primary Vertical Control Network

The Primary Vertical Control Network commenced in early September, 1992 and was completed in April, 1993. Minor changes to the design of the network were necessary during the levelling campaign for reasons of safety and economics. The completed network can be seen in Figure 6.1.

Throughout this period the author calculated section closures as in Equation (5.8) when the data became available to ensure the standards were being achieved. Each section closure that was not within the allowable tolerance was relevelled. Economic considerations resulted in five sections being accepted even though they were slightly outside the derived PB/MK tolerance. Of the five sections that were outside the PB/MK section closure tolerance, three were within the FGCC First Order Class I tolerances and the remaining within FGCC First Order Class II. A total of 5 percent of the sections had to be relevelled. The actual and allowable section closures were plotted against the distance of the section together with the Federal Geodetic Control Commision (FGCC) First-Order Class I limits (Figure 6.2). The section closures are listed in Appendix A.

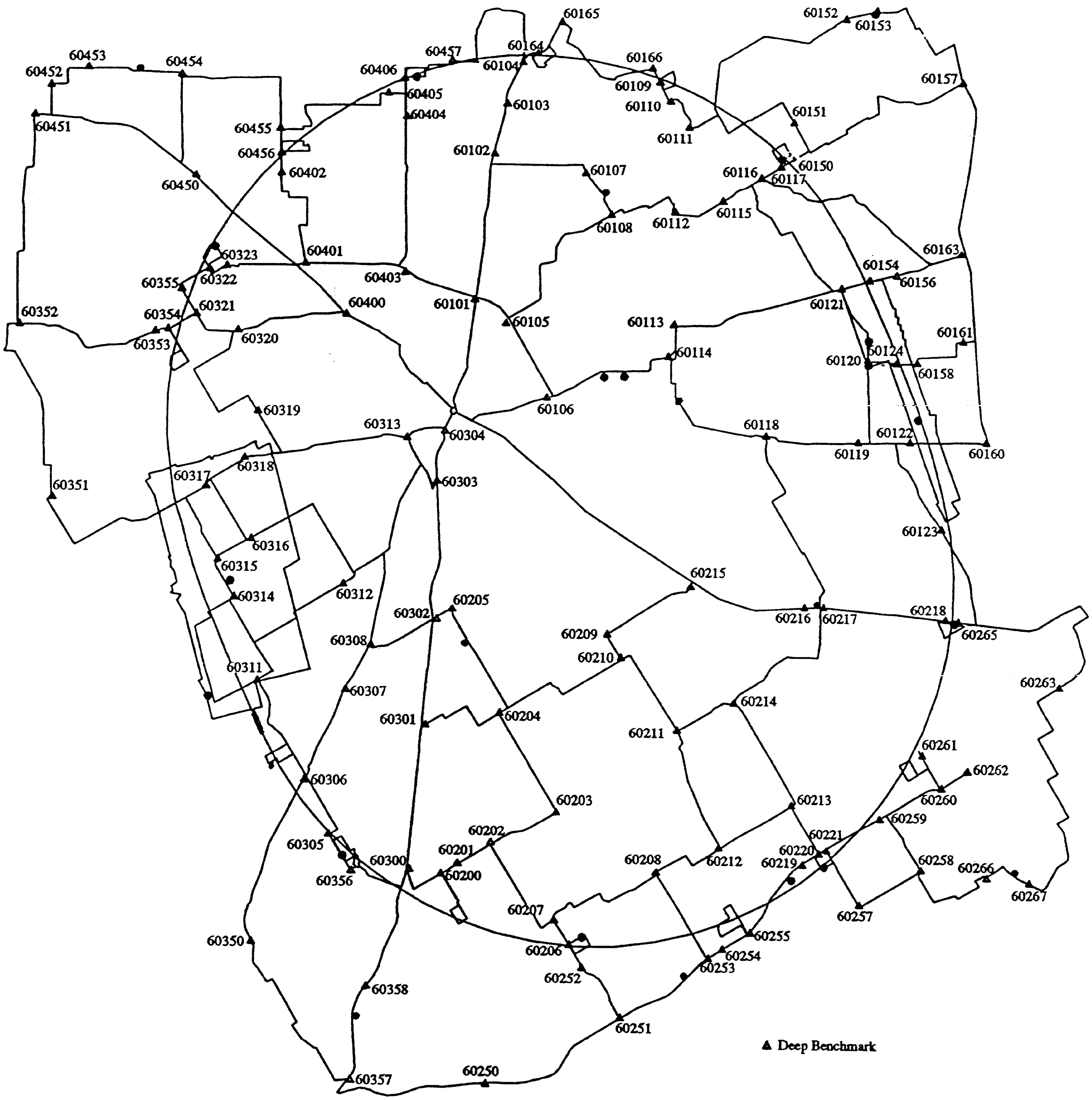

Figure 6.1
Primary Vertical Control Network

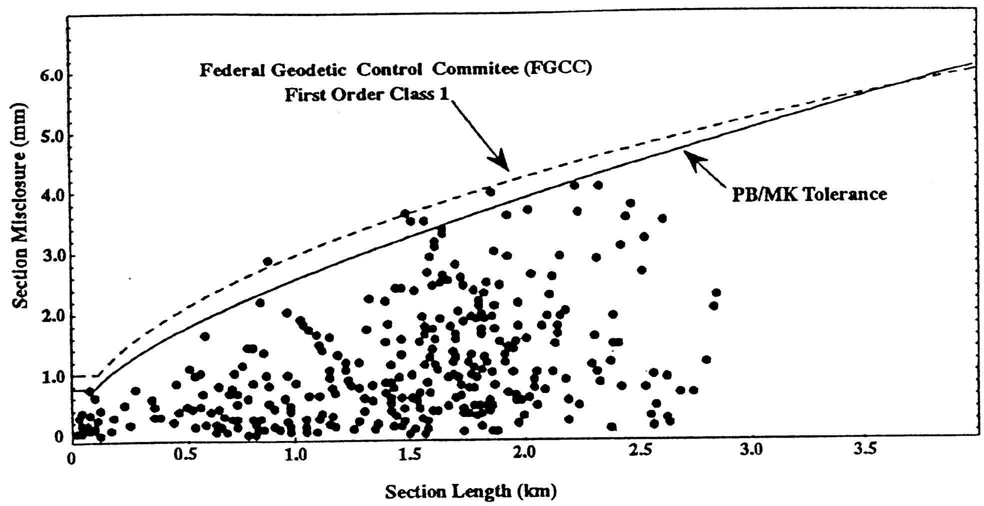

Figure 6.2
Section Closures

Loop closures were determined on a regular basis to guard against gross errors and temporary benchmark unstability between reoccupations. A total of forty-one loops were included in the PVCN. Loop closures were tested against Equation (5.10) and are shown in Table 6.1. Loop closures were also plotted against distance (See Figure 6.3). There were no loop closure outside the allowable tolerance.

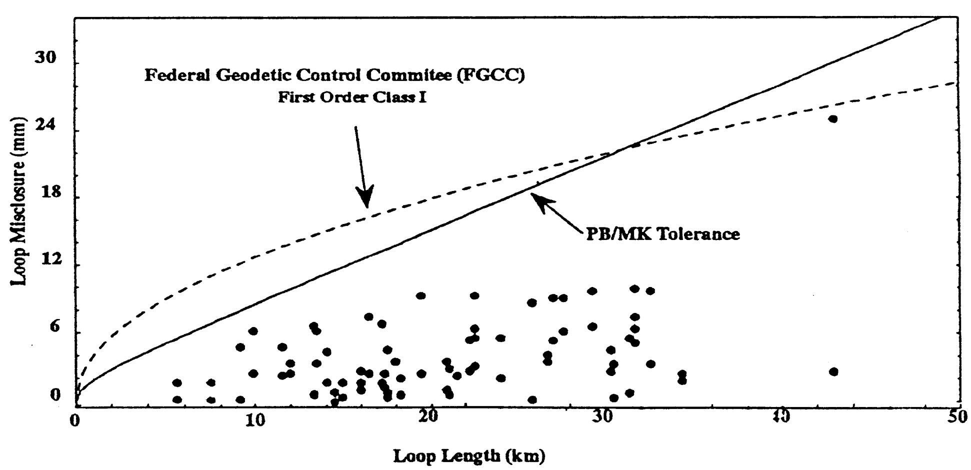

Figure 6.3
Loop Closures

Table 6.1
Loop Closures

Loop	Clockwise Misclosure (mm)	Counter Clockwise Misclosure (mm)	Allowed (mm)	Length (km)
1	5.1	7.4	22.6	31.6
2	3.3	-0.5	21.9	30.4
3	0.8	0	11.4	14.5
4	2.5	9.4	14.6	19.3
5	6.3	3.3	10.7	13.4
6	4.5	0.5	6.8	7.5
7	8.8	-0.3	18.9	25.8
8	2.6	1.7	12.4	15.9
9	-3.1	9.3	16.7	22.5
10	0.8	2.3	13.4	17.4
11	5.4	-2.7	16.5	22.2
12	9.1	5.3	19.7	27.2
13	4.6	2.6	21.7	30.4
14	-2.1	-0.6	14	18.2
15	-2.3	4.8	9.4	11.5
16	-0.8	5.8	22.4	31.2
17	6.7	-9.8	21.1	29.2
18	-0.7	6.7	10.6	13.2
19	1.1	-1.4	12.4	15.9
20	7.4	2.4	12.6	16.3
21	0.2	4.8	7.9	9.1
22	0.2	1.6	6.8	7.5
23	2.6	25	29.9	42.8
24	3	-0.7	15.7	21
25	3.6	1	15.6	20.9
26	4.2	-3.6	19.4	26.6
27	3.6	3.5	13.7	17.8
28	6.5	9.9	22.6	31.5
29	2.5	-1.3	13.3	17.3
30	3.4	2.4	9.7	11.9
31	9.2	6.2	20	27.5
32	6.5	5.5	16.7	22.4
33	1.7	6.9	13.2	17.1
34	9.7	3.3	23.2	32.5
35	-2.2	-2.1	16	21.4
36	4.4	-1.6	11.1	14
37	-1.6	0.4	11.7	14.9
38	1.8	2.4	24.3	34.2
39	2.1	5.6	17.7	24
40	-0.2	1.6	5.4	5.5
41	6.2	2.5	8.3	9.8

6.2 Preliminary Adjustment of the Primary Vertical Control Netwok

An adjustment of the PVCN was performed by the author on observed elevation differences in order to determine the initial accuracy of the Primary Vertical Control Network. The minimally constrained adjustment, using Geolab^{tm} (Version 2.4c), was carried out holding deep BM 60314 on the west campus fixed. Benchmark 60314 was used as the minimum constraint on the PVCN datum because of its location near the LINAC facility which is the origin of the SSC accelerators (design and alignment of the SSC is based relative to the LINAC).

Using a Tau Max distribution, there were no flagged residuals. A histogram of the standardized residuals is shown in Figure 6.4. There is a slight shift (-0.27) of the histogram from the normal distribution. This could be due to unmodelled systematic effects (refraction, orthometric correction, sinking of turning points and instrument, etc.) present in the observations. Further analysis is required to confirm this hypothesis.

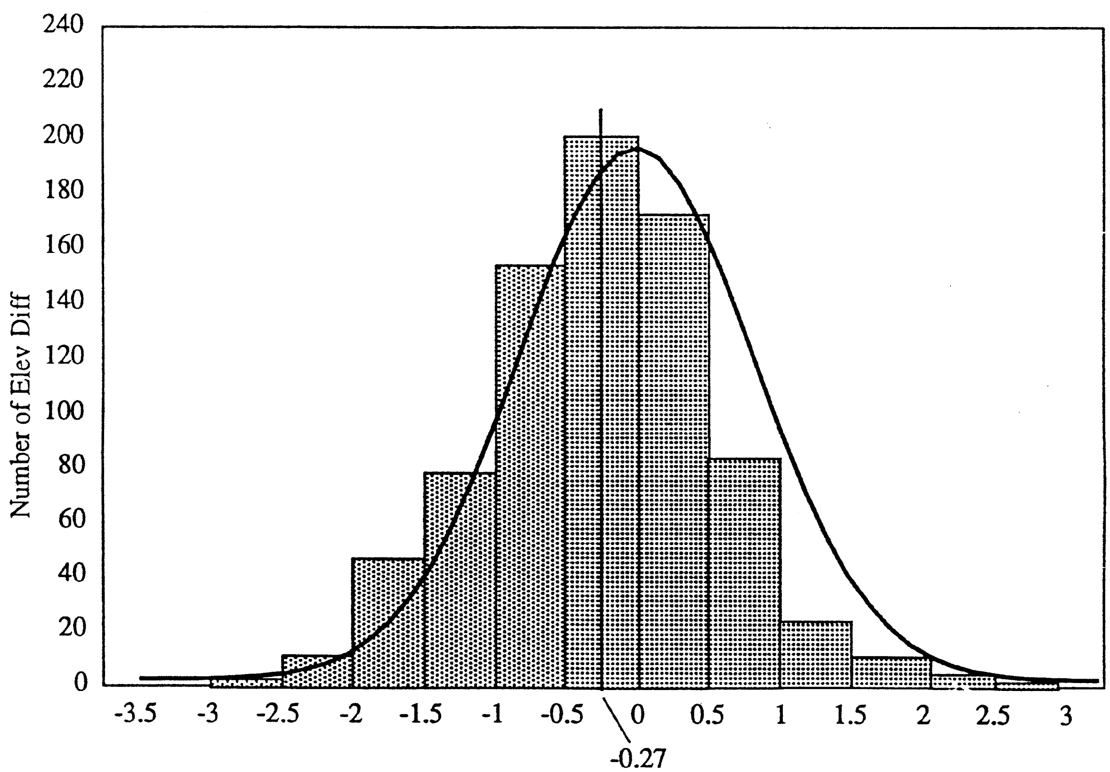

Figure 6.4
Histogram of Minimally Constrained Adjustment
Using One-Way Elevation Differences

The *a posteriori* variance factor from the adjustment is 0.757 which fails the "Chi-Square Test on the Variance Factor". As the levelling was performed under almost ideal conditions, it could be expected that the initial estimate of the standard deviation of the elevation differences were pessimistic. This assumption is further borne out by the small loop closures. The variance-covariance matrix of the adjusted non-rigorous heights were scaled accordingly.

The initial accuracy across the SSC Project ring was initially estimated to be 7.0 mm at the 99 percent level of confidence (Section 2.3). After preliminary adjustment, the scaled accuracy across the main collider ring between BMs 64130 and 64175 has a relative uncertainty of 5.4 mm at the same level of confidence. Table 6.2 shows the adjusted preliminary elevations and their associated standard deviations.

6.3 Application of Geodetic Corrections and Reductions

The relevant geodetic corrections and reductions deemed necessary were carefully analyzed to ensure accurate and reliable elevations are obtained. The corrections discussed include the effect of atmospheric refraction and the conversion from preliminary elevation differences to othometric heights. Tidal effects were not applied as they were previously found to contribute insignificantly to the results (Section 4.1).

6.3.1 Correction for Vertical Atmospheric Refraction

During the levelling campaign, temperatures were continuously measured at five different heights above the terrain (0.3 m, 0.7 m, 1.2 m, 1.8 m and 3.0 m). Approximately fifteen percent of the acquired data was not usable due to hardware problems. The missing temperature data was interpolated from the good data. The temperatures were averaged over ten measurement intervals (200 seconds) for each height above the terrain. Estimates for the the unknowns b and c in Equations (3.9) to (3.22d) were determined using the rigorous methodology described in Sections 3.2.8 and 5.2 and the non-linear parametric adjustment package Statistica™. Pressure was measured directly in the field. The effect of refraction on the elevation differences was estimated over a section length and applied for each instrument setup.

Table 6.2

Preliminary Adjusted Elevations and Associated Standard Deviations

BM	Preliminary Elevation (m)	Preliminary Std Dev (m)	BM	Preliminary Elevation (m)	Preliminary Std Dev (m)	BM	Preliminary Elevation (m)	Preliminary Std Dev (m)	BM	Preliminary Elevation (m)	Preliminary Std Dev (m)
60101	189.4841	0.0016	60157	138.9960	0.0022	60251	159.0859	0.0019	60318	208.6451	0.0013
60102	184.5825	0.0019	60158	141.0982	0.0021	60252	166.7402	0.0019	60319	205.9108	0.0015
60103	187.6866	0.0019	60160	151.8283	0.0021	60253	144.0407	0.0019	60320	216.9525	0.0016
60104	172.0514	0.0020	60161	136.4702	0.0020	60254	134.8247	0.0019	60321	222.9511	0.0017
60105	180.4891	0.0017	60163	141.2848	0.0020	60255	133.4997	0.0019	60322	212.3023	0.0017
60106	170.1078	0.0016	60164	163.2107	0.0020	60257	139.4653	0.0021	60323	210.2063	0.0017
60107	180.2845	0.0020	60165	169.3616	0.0021	60258	139.8608	0.0021	60350	175.5330	0.0019
60108	176.5114	0.0019	60166	166.5166	0.0022	60259	145.1001	0.0021	60351	224.1697	0.0017
60109	165.6779	0.0022	60200	161.9400	0.0017	60260	136.1184	0.0023	60352	252.7933	0.0018
60110	156.5558	0.0022	60201	167.6694	0.0017	60261	140.8819	0.0023	60353	231.9863	0.0017
60111	145.2664	0.0022	60202	164.0588	0.0017	60262	135.7282	0.0023	60354	232.9296	0.0017
60112	168.2277	0.0020	60203	158.6279	0.0017	60263	151.9317	0.0024	60355	220.4404	0.0017
60113	160.0718	0.0020	60204	166.5544	0.0015	60265	143.8606	0.0020	60356	158.7043	0.0015
60114	157.1676	0.0019	60205	189.3553	0.0014	60266	135.5059	0.0023	60357	168.1346	0.0019
60115	160.6638	0.0020	60206	155.2999	0.0019	60267	132.5944	0.0024	60358	166.4956	0.0018
60116	149.4463	0.0020	60207	154.5071	0.0018	60300	160.6689	0.0015	60400	174.6058	0.0016
60117	150.8693	0.0020	60208	149.8531	0.0019	60301	180.6819	0.0015	60401	182.8620	0.0016
60118	160.1742	0.0019	60209	168.4506	0.0018	60302	189.0671	0.0013	60402	213.2881	0.0019
60119	154.7177	0.0020	60210	163.7785	0.0017	60303	183.2441	0.0013	60403	194.1568	0.0017
60120	145.0010	0.0020	60211	156.6884	0.0018	60304	164.6070	0.0014	60404	211.7746	0.0019
60121	145.7111	0.0020	60212	148.9705	0.0019	60305	167.5325	0.0015	60405	216.4398	0.0019
60122	152.3210	0.0020	60213	152.3310	0.0019	60306	183.7156	0.0013	60406	210.4370	0.0020
60123	148.7786	0.0021	60214	160.5151	0.0018	60307	198.3555	0.0014	60450	197.0192	0.0019
60124	142.7059	0.0020	60215	150.8958	0.0018	60308	198.5954	0.0013	60451	228.0881	0.0020
60150	150.8480	0.0020	60216	149.5372	0.0018	60311	193.2554	0.0009	60452	224.7156	0.0020
60151	152.5398	0.0021	60217	153.9322	0.0018	60312	201.9998	0.0011	60453	224.2912	0.0020
60152	148.7421	0.0024	60218	140.7136	0.0020	60313	185.2895	0.0014	60454	220.6304	0.0020
60153	148.4260	0.0024	60219	145.8125	0.0019	60314	215.7090	0.0000	60455	219.4779	0.0019
60154	144.9495	0.0020	60220	147.0659	0.0019	60315	224.0623	0.0008	60456	218.1020	0.0019
60156	145.9948	0.0020	60221	148.2107	0.0019	60316	217.9603	0.0010	60457	198.1801	0.0021
60250	154.8945	0.0020	60317	225.6245	0.0011						

The elevation differences were re-adjusted once the refraction correction had been applied. The *a posteriori* variance factor of the adjustment is 0.748 which is a slight improvement from the preliminary adjustment. The differences between thc adjusted elevations with refraction correction and the adjusted elevations without refraction correction are as large as 4.8 mm. There appears to be a planar systematic trend of the refraction effect in the north-west to south-east direction that can be ignored. This trend can be approximated through least squares by the plane:

$$H^K - H = a_o + a_1\Delta x + a_2\Delta y, \tag{6.1}$$

where Δx is the difference in northing state plane coordinates (m),

Δy is the difference in easting state plane coordinates (m),

$a_o = -0.001916$ m,

$a_1 = 0.0000000610$, and

$a_2 = -\ 0.000000127$.

This effect causes a tilt of the SSC, due to the fact that the absolute position of the SSC Plane is arbitrarily chosen, it can therefore be safely ingored.

Results of the analysis are shown in Table 6.3. Deviations from the plane are less than half the correction which is within the noise level of the thermistor data. Correcting for the effect of refraction does not improve the accuracy of the preliminary elevations.

6.3.2 Application of Orthometric Correction

The orthometric corrections were applied to ensure elevation differences are adjusted in the same frame of reference. Levelled height differences are converted to geopotential number differences, also known as dynamic heights, because geopotential numbers are holonomic while observed height differences are not. To convert elevation differences to geopotential numbers, surface gravity along the levelling line is required. As mentioned in Section 4.2, the existing NGS gravity data is suitable for ensuring requirements are met. Geopotential differences maybe calculated by Equation (4.21). However, the following is used to determine an estimate of the geopotential number differences,

Table 6.3

Comparison of Preliminary Adjusted Elevations and Adjusted Elevations Corrected for Refraction

BM	Preliminary Elevation (m)	Elev with Refract Corr (m)	Difference Elevation (mm)	Residual (mm)	BM	Preliminary Elevation (m)	Elev with Refract Corr (m)	Difference Elevation (mm)	Residual (mm)	BM	Preliminary Elevation (m)	Elev with Refract Corr (m)	Difference Elevation (mm)	Residual (mm)
60101	189.4841	189.4855	-1.4	-0.1	60203	158.6279	158.6315	-3.6	-1.2	60306	183.7156	183.7177	-2.1	-0.7
60102	184.5825	184.5843	-1.8	-1.0	60204	166.5544	166.5577	-3.3	-0.5	60307	198.3555	198.3571	-1.6	-0.1
60103	187.6866	187.6881	-1.5	-0.8	60205	189.3553	189.3572	-1.9	0.8	60308	198.5954	198.5971	-1.7	-0.4
60104	172.0514	172.0539	-2.5	-1.2	60206	155.2999	155.3036	-3.7	-1.1	60311	193.2554	193.2570	-1.6	-0.5
60105	180.4891	180.4907	-1.6	-0.4	60207	154.5071	154.5107	-3.6	-1.0	60312	201.9998	202.0011	-1.3	0.0
60106	170.1078	170.1096	-1.8	-0.2	60208	149.8531	149.8566	-3.5	-0.7	60313	185.2895	185.2917	-2.2	-1.3
60107	180.2845	180.2867	-2.2	-0.7	60209	168.4506	168.4528	-2.2	0.1	60314	215.7090	215.7090	0.0	0.6
60108	176.5114	176.5136	-2.2	-0.8	60210	163.7785	163.7808	-2.3	0.2	60315	224.0623	224.0618	0.5	0.9
60109	165.6779	165.6803	-2.4	-0.9	60211	156.6884	156.6914	-3.0	0.0	60316	217.9603	217.9602	0.1	0.8
60110	156.5558	156.5584	-2.6	-1.0	60212	148.9705	148.9741	-3.6	-0.2	60317	225.6245	225.6239	0.6	1.0
60111	145.2664	145.2695	-3.1	-1.5	60213	152.3310	152.3344	-3.4	0.0	60318	208.6451	208.6462	-1.1	-0.5
60112	168.2277	168.2303	-2.6	-0.8	60214	160.5151	160.5179	-2.8	0.3	60319	205.9108	205.9120	-1.2	-0.6
60113	160.0718	160.0742	-2.4	-0.4	60215	150.8958	150.8988	-3.0	-0.6	60320	216.9525	216.9529	-0.4	-0.2
60114	157.1676	157.1701	-2.5	-0.3	60216	149.5372	149.5403	-3.1	-0.1	60321	222.9511	222.9511	0.0	0.0
60115	160.6638	160.6665	-2.7	-0.7	60217	153.9322	153.9352	-3.0	0.2	60322	212.3023	212.3030	-0.7	-0.5
60116	149.4463	149.4490	-2.7	-0.5	60218	140.7136	140.7162	-2.6	1.1	60323	210.2063	210.2073	-1.0	-1.1
60117	150.8693	150.8719	-2.6	-0.5	60219	145.8125	145.8161	-3.6	0.0	60350	175.5330	175.5345	-1.5	0.0
60118	160.1742	160.1765	-2.3	0.4	60220	147.0659	147.0696	-3.7	0.1	60351	224.1697	224.1688	0.9	0.7
60119	154.7177	154.7200	-2.3	0.8	60221	148.2107	148.2143	-3.6	0.3	60352	252.7933	252.7909	2.4	1.5
60120	145.0010	145.0038	-2.8	0.3	60250	154.8945	154.8989	-4.4	-1.5	60353	231.9863	231.9853	1.0	0.9
60121	145.7111	145.7138	-2.7	-0.9	60251	159.0859	159.0887	-2.8	0.3	60354	232.9296	232.9286	1.0	0.7
60122	152.3210	152.3232	-2.2	1.3	60252	166.7402	166.7425	-2.3	0.8	60355	220.4404	220.4407	-0.3	-0.5
60123	148.7786	148.7811	-2.5	1.0	60253	144.0407	144.0442	-3.5	-0.1	60356	158.7043	158.7074	-3.1	-1.3
60124	142.7059	142.7088	-2.9	0.0	60254	134.8247	134.8284	-3.7	-0.2	60357	168.1346	168.1382	-3.6	-1.3
60150	150.8480	150.8506	-2.6	-0.6	60255	133.4997	133.5035	-3.8	-0.4	60358	166.4956	166.4981	-2.5	-0.7
60151	152.5398	152.5425	-2.7	-0.6	60257	139.4653	139.4693	-4.0	0.1	60400	174.6058	174.6081	-2.3	-1.7
60152	148.7421	148.7453	-3.2	-0.9	60258	139.8608	139.8649	-4.1	0.1	60401	182.8620	182.8637	-1.7	-1.5
60153	148.4260	148.4292	-3.2	-1.0	60259	145.1001	145.1042	-4.1	-0.4	60402	213.2881	213.2878	0.3	0.5
60154	144.9495	144.9523	-2.8	0.1	60260	136.1184	136.1232	-4.8	-0.8	60403	194.1568	194.1579	-1.1	-0.5
60156	145.9948	145.9975	-2.7	0.2	60261	140.8819	140.8864	-4.5	-0.5	60404	211.7746	211.7742	0.4	0.8
60157	138.9960	139.0002	-4.2	-2.1	60262	135.7282	135.7330	-4.8	-0.6	60405	216.4398	216.4389	0.9	1.3
60158	141.0982	141.1012	-3.0	0.2	60263	151.9317	151.9333	-1.6	0.7	60406	210.4370	210.4368	0.2	0.5
60160	151.8283	151.8307	-2.4	1.0	60265	143.8606	143.8630	-2.4	1.6	60450	197.0192	197.0200	-0.8	-0.9
60161	136.4702	136.4734	-3.2	0.2	60266	135.5059	135.5102	-4.3	0.0	60451	228.0881	228.0873	0.8	-0.4
60163	141.2848	141.2879	-3.1	0.0	60267	132.5944	132.5988	-4.4	1.0	60452	224.7156	224.7148	0.8	-0.1
60164	163.2107	163.2132	-2.5	-1.2	60300	160.6689	160.6722	-3.3	-1.5	60453	224.2912	224.2903	0.9	0.1
60165	169.3616	169.3640	-2.4	-1.2	60301	180.6819	180.6838	-1.9	-0.3	60454	220.6304	220.6297	0.7	0.1
60166	166.5166	166.5190	-2.4	-1.0	60302	189.0671	189.0689	-1.8	-0.1	60455	219.4779	219.4772	0.7	0.8
60200	161.9400	161.9434	-3.4	-1.2	60303	183.2441	183.2459	-1.8	-0.4	60456	218.1020	218.1015	0.5	0.6
60201	167.6694	167.6723	-2.9	-0.8	60304	164.6070	164.6094	-2.4	-1.1	60457	198.1801	198.1804	-0.3	-0.2
60202	164.0588	164.0621	-3.3	-0.9	60305	167.5325	167.5353	-2.8	-1.4					

$$C_j - C_i = \sum_{k=i}^{j} g_k \Delta h_k, \tag{6.2}$$

where g_k is the mean gravity between points k and k-1,

Δh_k is the observed elevation difference, and

g_k is the mean gravity calculated as the average value of surface gravity at point k and k-1.

All levelled height differences are first converted to geopotential number differences according to Equation (6.2). Geopotential number differences were subsequently scaled by the reciprocal of the mean value of gravity for the area of concern (1/g = 1/979,460 [mGal]). The UNB Engineering Surveys Research Group performed the necessary conversions [Grodecki, et al., 1993].

Dynamic height differences resulting from the conversion of levelled height differences were adjusted in Geolab™ (Version 2.4c). Point 60314 was held fixed with a dynamic height of 215.7090 m. The maximum discrepancy between non-rigorous adjusted heights and dynamic heights did not exceed 0.9 mm [Grodecki, et al., 1993].

The adjusted dynamic heights are then converted to Helmert orthometric heights. The converted orthometric height of point 60314 was corrected by -0.00301 m to conform to the original minimal constraint (215.7090 m). Differences of up to 7 mm occurred between non-rigorous adjusted heights and orthometric heights. A contour map and a plot of the surface describing the differences between the final orthometric heights and the non-rigorous adjusted heights is shown in Figures 6.5.

There is a systematic trend of the orthometric correction in the south-west to north-east direction. This trend can be approximated by the plane,

$$H^o - H = a_o + a_1 \Delta x + a_2 \Delta y, \tag{6.3}$$

where $a_o = 0.00285$ m,

$a_1 = 0.000000107$, and

$a_2 = 0.000000208$.

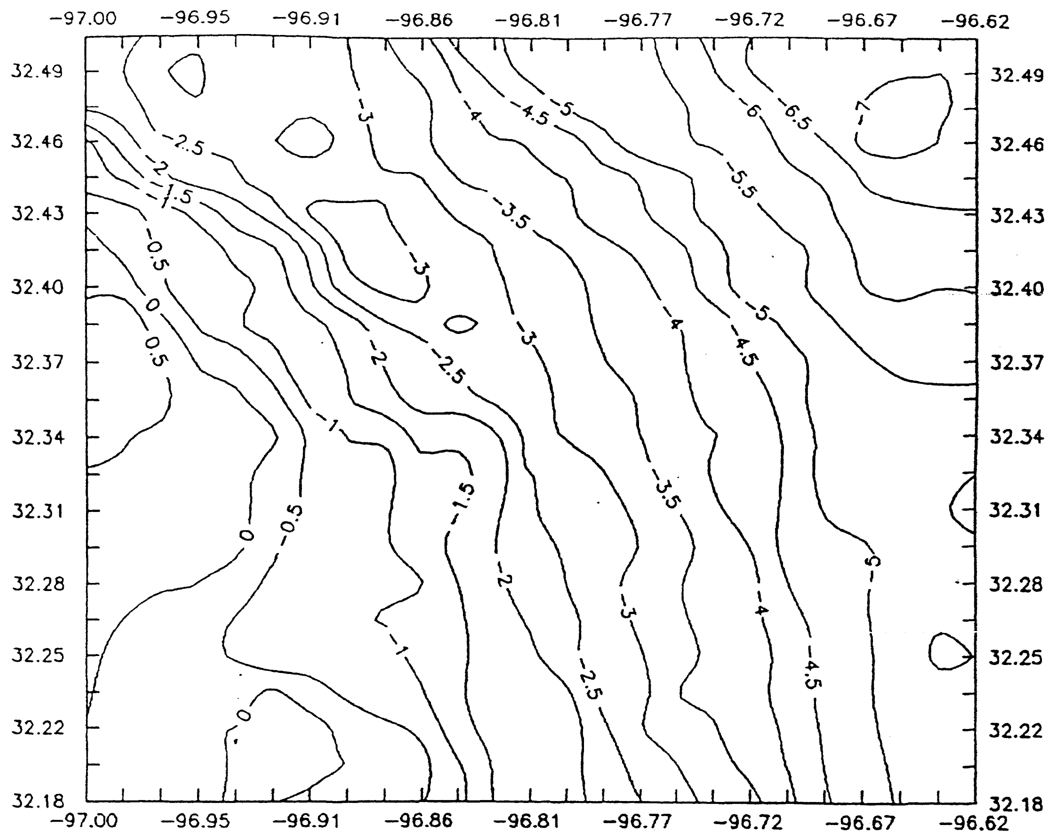

Figure 6.5
Differences in Non-Rigorous Heights and Orthometric Heights [mm] [Grodecki, et al., 1993]

The maximum deviation of the higher order effects is determined from the residual of the plane-fitting function. The maximum deviation is 1.3 mm which may be caused by the randomness of the prediction of the gravity. Results of the comparison of preliminary elevations, geopotential numbers and final orthometric heights are shown in Table 6.4.

It can be concluded that the conversion of levelled height differences to dynamic heights does not bring any significant improvements of accuracy as the differences are less than one millimetre which is well within the noise of the levelling observations. The analysis of the geodetic corrections show insignificant loss of accuracy if these corrections are not applied. The collider plane is slightly tilted and since it is arbitrarily chosen, the orthometric effect is not applied.

Table 6.4

Comparison of Preliminary Adjusted Elevation, Adjusted Geopotential Numbers and Orthometric Heights

BM	Preliminary Elevation (m)	Geopotential Number	Orthometric Height (m)	Differences		Residual* (mm)	BM	Preliminary Elevation (m)	Geopotential Number	Orthometric Height (m)	Differences		Residual* (mm)
				Pre-Geo (mm)	Pre-Orth (mm)						Pre-Geo (mm)	Pre-Orth (mm)	
60101	189.4841	189.4846	189.4812	-0.5	2.9	-0.3	60163	141.2848	141.2852	141.2785	-0.4	6.3	-0.6
60102	184.5825	184.5831	184.5785	-0.6	4.0	0.3	60164	163.2107	163.2111	163.2054	-0.4	5.3	-0.6
60103	187.6866	187.6871	187.6824	-0.5	4.2	0.4	60165	169.3616	169.3621	169.3564	-0.5	5.2	0.8
60104	172.0514	172.0519	172.0465	-0.5	4.9	0.4	60166	166.5166	166.5171	166.5113	-0.5	5.3	0.4
60105	180.4891	180.4897	180.4861	-0.6	3.0	0.3	60200	161.9400	161.9408	161.9388	-0.8	1.2	0.1
60106	170.1078	170.1084	170.1047	-0.6	3.1	0.3	60201	167.6694	167.6700	167.6682	-0.6	1.2	0.5
60107	180.2845	180.2851	180.2804	-0.6	4.1	0.4	60202	164.0588	164.0595	164.0572	-0.7	1.6	0.3
60108	176.5114	176.5120	176.5074	-0.6	4.1	0.4	60203	158.6279	158.6286	158.6258	-0.7	2.1	0.5
60109	165.6779	165.6784	165.6726	-0.5	5.3	0.5	60204	166.5544	166.5550	166.5523	-0.6	2.1	0.1
60110	156.5558	156.5563	156.5504	-0.5	5.4	0.5	60205	189.3553	189.3558	189.3541	-0.5	1.2	-0.6
60111	145.2664	145.2668	145.2607	-0.4	5.7	0.6	60206	155.2999	155.3006	155.2981	-0.7	1.8	0.5
60112	168.2277	168.2283	168.2233	-0.6	4.4	0.6	60207	154.5071	154.5078	154.5052	-0.7	1.9	0.8
60113	160.0718	160.0724	160.0678	-0.6	4.0	0.5	60208	149.8531	149.8538	149.8504	-0.7	2.7	0.5
60114	157.1676	157.1682	157.1636	-0.6	4.0	0.4	60209	168.4506	168.4512	168.4481	-0.6	2.5	-0.1
60115	160.6638	160.6644	160.6590	-0.6	4.8	0.4	60210	163.7785	163.7791	163.7758	-0.6	2.7	-0.4
60116	149.4463	149.4467	149.4408	-0.4	5.5	0.5	60211	156.6884	156.6891	156.6855	-0.7	2.9	-0.1
60117	150.8693	150.8697	150.8637	-0.4	5.7	0.6	60212	148.9705	148.9713	148.9673	-0.8	3.2	0.3
60118	160.1742	160.1748	160.1702	-0.6	4.0	-0.9	60213	152.3310	152.3317	152.3273	-0.7	3.7	0.5
60119	154.7177	154.7183	154.7131	-0.6	4.6	-0.9	60214	160.5151	160.5158	160.5119	-0.7	3.2	-0.5
60120	145.0010	145.0014	144.9956	-0.4	5.4	-0.3	60215	150.8958	150.8964	150.8922	-0.6	3.6	0.1
60121	145.7111	145.7115	145.7057	-0.4	5.4	0.0	60216	149.5372	149.5378	149.5330	-0.6	4.2	0.0
60122	152.3210	152.3216	152.3159	-0.6	5.1	-0.8	60217	153.9322	153.9328	153.9280	-0.6	4.2	-0.5
60123	148.7786	148.7792	148.7734	-0.6	5.2	-0.1	60218	140.7136	140.7141	140.7083	-0.5	5.3	0.4
60124	142.7059	142.7063	142.7003	-0.4	5.6	-0.1	60219	145.8125	145.8132	145.8087	-0.7	3.8	0.8
60150	150.8480	150.8484	150.8423	-0.4	5.8	0.0	60220	147.0659	147.0667	147.0621	-0.8	3.8	0.3
60151	152.5398	152.5403	152.5340	-0.5	5.8	0.1	60221	148.2107	148.2114	148.2068	-0.7	3.9	0.3
60152	148.7421	148.7425	148.7355	-0.4	6.6	-0.2	60250	154.8945	154.8953	154.8936	-0.8	0.9	0.6
60153	148.4260	148.4264	148.4193	-0.4	6.7	0.1	60251	159.0859	159.0866	159.0841	-0.7	1.9	0.6
60154	144.9495	144.9499	144.9439	-0.4	5.6	-0.4	60252	166.7402	166.7408	166.7388	-0.6	1.4	-0.1
60156	145.9948	145.9952	145.9890	-0.4	5.8	-0.6	60253	144.0407	144.0415	144.0379	-0.8	2.8	0.9
60157	138.9960	138.9963	138.9891	-0.3	6.9	-0.3	60254	134.8247	134.8254	134.8213	-0.7	3.4	0.7
60158	141.0982	141.0986	141.0924	-0.4	5.8	-0.4	60255	133.4997	133.5004	133.4961	-0.7	3.6	1.0
60160	151.8283	151.8289	151.8225	-0.6	5.8	-0.2	60257	139.4653	139.4660	139.4611	-0.7	4.2	0.6
60161	136.4702	136.4705	136.4639	-0.3	6.3	0.0	60258	139.8608	139.8614	139.8561	-0.6	4.7	0.3

Table 6.4 (Continued)

Comparison of Preliminary Adjusted Elevation, Adjusted Geopotential Numbers and Orthometric Heights

BM	Preliminary Elevation (m)	Geopotential Number	Orthometric Height (m)	Differences		Residual* (mm)	BM	Preliminary Elevation (m)	Geopotential Number	Orthometric Height (m)	Differences		Residual* (mm)
				Pre-Geo (mm)	Pre-Orth (mm)						Pre-Geo (mm)	Pre-Orth (mm)	
60259	145.1001	145.1008	145.0957	-0.7	4.4	0.4	60321	222.9511	222.9511	222.9499	0.0	1.2	-0.2
60260	136.1184	136.1190	136.1134	-0.6	5.0	0.7	60322	212.3023	212.3025	212.3005	-0.2	1.8	0.6
60261	140.8819	140.8825	140.8770	-0.6	4.9	0.1	60323	210.2063	210.2066	210.2045	-0.3	1.8	0.3
60262	135.7282	135.7288	135.7231	-0.6	5.1	0.0	60350	175.5330	175.5335	175.5331	-0.5	-0.1	0.4
60263	151.9317	151.9324	151.9263	-0.7	5.4	-0.4	60351	224.1697	224.1697	224.1704	0.0	-0.7	-0.5
60265	143.8606	143.8612	143.8554	-0.6	5.2	0.0	60352	252.7933	252.7926	252.7936	0.7	-0.3	-0.2
60266	135.5059	135.5065	135.5009	-0.6	5.0	0.1	60353	231.9863	231.9862	231.9858	0.1	0.6	-0.6
60267	132.5944	132.5949	132.5891	-0.5	5.3	0.4	60354	232.9296	232.9295	232.9291	0.1	0.5	-0.4
60300	160.6689	160.6697	160.6678	-0.8	1.1	0.6	60355	220.4404	220.4405	220.4390	-0.1	1.4	0.5
60301	180.6819	180.6824	180.6807	-0.5	1.2	0.0	60356	158.7043	158.7052	158.7034	-0.9	0.9	0.4
60302	189.0671	189.0675	189.0658	-0.4	1.3	-0.5	60357	168.1346	168.1352	168.1344	-0.6	0.2	0.7
60303	183.2441	183.2446	183.2420	-0.5	2.1	-0.4	60358	166.4956	166.4962	166.4954	-0.6	0.2	0.4
60304	164.6070	164.6076	164.6040	-0.6	3.1	0.3	60400	174.6058	174.6063	174.6025	-0.5	3.3	0.9
60305	167.5325	167.5332	167.5316	-0.7	0.9	0.8	60401	182.8620	182.8625	182.8589	-0.5	3.1	1.1
60306	183.7156	183.7161	183.7150	-0.5	0.6	0.1	60402	213.2881	213.2883	213.2857	-0.2	2.4	0.1
60307	198.3555	198.3557	198.3550	-0.2	0.5	-0.4	60403	194.1568	194.1572	194.1539	-0.4	2.9	0.2
60308	198.5954	198.5957	198.5948	-0.3	0.7	-0.3	60404	211.7746	211.7750	211.7715	-0.4	3.2	0.1
60311	193.2554	193.2559	193.2550	-0.5	0.4	0.1	60405	216.4398	216.4401	216.4366	-0.3	3.2	-0.3
60312	201.9998	202.0000	201.9989	-0.2	0.9	-0.4	60406	210.4370	210.4373	210.4334	-0.3	3.6	0.4
60313	185.2895	185.2900	185.2873	-0.5	2.3	0.1	60450	197.0192	197.0196	197.0165	-0.4	2.7	1.0
60314	215.7090	215.7090	215.7090	0.0	0.0	-0.3	60451	228.0881	228.0880	228.0860	0.1	2.1	1.4
60315	224.0623	224.0621	224.0625	0.2	-0.2	-0.6	60452	224.7156	224.7156	224.7130	0.0	2.6	1.5
60316	217.9603	217.9602	217.9599	0.1	0.4	-0.6	60453	224.2912	224.2912	224.2886	0.0	2.7	1.2
60317	225.6245	225.6243	225.6244	0.2	0.1	-0.8	60454	220.6304	220.6305	220.6279	-0.1	2.5	0.8
60318	208.6451	208.6453	208.6441	-0.2	1.0	0.0	60455	219.4779	219.4781	219.4755	-0.2	2.4	-0.1
60319	205.9108	205.9110	205.9094	-0.2	1.4	0.1	60456	218.1020	218.1022	218.0995	-0.2	2.5	0.0
60320	216.9525	216.9526	216.9512	-0.1	1.3	-0.4	60457	198.1801	198.1806	198.1768	-0.5	3.3	0.8

* Residual from plane fitting function

The final elevations can then be determined without the correction for vertical atmospheric refraction or the application of orthometric corrections.

6.4 Minimum Norm Quadratic Estimation of PVCN

Knowledge of variances and covariances of observations is crucial for obtaining the best estimation of the adjusted elevations and their accuracies. The preliminary least squares adjustment of the PVCN used an *a priori* weighting scheme based on a deterministic estimation (from the known sources of errors) of the observations. This may have led to an inappropriate distribution of weights in the least squares adjustment and hence a distortion of the values of the final elevations and their error estimates. One such statistical method that has been developed which uses an *a posteriori* determination of the variance-covariance components for the identification of the most appropriate model of observation errors, is the Minimum Norm Quadratic Estimation (MINQE) method [Chen et al., 1990].

The PVCN has been subjected to the MINQE analysis in order to provide the best possible estimation of the weight matrix components for a final adjustment and accuracy evaluation of the networks. The MINQE analysis was performed by the University of New Brunswick Engineering Surveys Research Group and is summarized below [Chrzanowski, et al., 1993].

Two evaluations have been performed:

- one using all single line levellings as independent observations in the network is used in the preliminary adjustment, and
- a second using mean values of the single (forward and backward) levellings.

In the first case, the MINQE analysis utilizes discrepancies between individual levellings of the same sections and loop misclosures. In the second analysis, only loop misclosures could be used in the accuracy evaluation.

6.4.1 Evaluation Using Single One Way Levellings

The following error model (variance model), similiar to Equation (5.4), was used in the evaluation,

$$\sigma^2 = a\,L + b\,L^2, \qquad (6.4)$$

where a and b are the unknown parameters describing the random and systematic components of the one-way elevation difference, and
L is the length of the levelling sections in kilometres.

The MINQE estimation resulted in [Chrzanowski, et al., 1993],

$a = 0.56 \pm 0.09$ (mm^2/km) and

$b = 0.14 \pm 0.07$ (mm^2/km^2)

for one way levellings.

In comparison with the *a priori* estimation for one-way elevation differences (Equation 5.6), the MINQE model shows smaller influence of random errors (0.56 compared to 0.77) and a good agreement in the systematic component (0.14 compared to 0.11).

As can be expected, due to the similiarity between the *a priori* and MINQE determined standard deviations, the least squares adjustment with the weights of observations obtained from the MINQE evaluation yielded differences in adjusted heights within the submillimetre range compared to the preliminary adjustment.

6.4.2 Evaluation Using Mean Elevation Differences

The second analysis included mean values of the repeated levellings of each section. The same error model (Equation 6.3) as in the first analysis was used in the MINQE evaluation. The analysis indicated that the error model was not correct because the value of b became statistically insignificant. Therefore, the MINQE analysis was repeated using the model containing only parameter a (representing random errors) [Chrzanowski, et al., 1993],

$$\sigma^2 = a\,L \tag{6.5}$$

which yielded a value for a of 0.59 for mean values of the leveling sections.

Since most of the levelling sections were observed twice (with some lines re-observed 3 times), the variance of the one way levelling could be approximated by:

$$\sigma^2 = 2\,a\,L = 1.18\,L. \tag{6.6}$$

Thus, in comparison with the deterministic variance model (Equation 5.6) the actual influence of random errors seems to be larger than expected. On the other hand, the insignificance of the b parameter in the MINQE model indicates that by taking the mean value of repeated levellings, the influence of the systematic errors is canceled out. This could be explained if the main source of the systematic errors is an accumulation of sinking errors of the backward rod when waiting for the instrument to move forward to the next set-up. The sinking of the rod would have to be about 0.036 mm at each set-up to give $b = 0.13$ over 10 set-ups (L=1 km) in Equation (6.3). This amount is close to what was initially expected (0.03 mm at each setup) (Section 3.2.6).

The levelling network has been re-adjusted using the mean elevation differences and their associated standard deviations (Equation 6.5). Table 6.5 shows differences in the adjusted heights from the MINQE mean elevation differences adjustment in comparison with the preliminary adjustment.

The differences are less than 1.5 mm. A comparison of the standard deviations of the adjusted heights shows that the adjustment with the MINQE derived weights gives standard deviations of up to 1.5 mm larger than originally expected.

The histogram of the standardized residuals (Figure 6.6) shows a small shift of the mean (-0.02), as opposed to the preliminary adjustment (-0.27). This tends to bear out the initial assumption that the preliminary adjustment contains the systematic effect of turning plate sinking. It is necessary that the mean elevation differences with their associated standard deviations determined from MINQE be used for the adjustment of the final elevations for the PVCN.

Table 6.5

Comparison of Preliminary Adjusted Elevations and Mean MINQE Elevations

BM	Preliminary		MINQE (mean 1 par)		Differences		BM	Preliminary		MINQE (mean 1 par)		Differences	
	Elevation (m)	Std Dev (m)	Elevation (m)	Std Dev (m)	Elevation (mm)	Std Dev (mm)		Elevation (m)	Std Dev (m)	Elevation (m)	Std Dev (m)	Elevation (mm)	Std Dev (mm)
60101	189.4841	0.0016	189.4847	0.0018	-0.6	-0.2	60163	141.2848	0.0020	141.2860	0.0023	-1.2	-0.3
60102	184.5825	0.0019	184.5832	0.0021	-0.7	-0.2	60164	163.2107	0.0020	163.2115	0.0023	-0.8	-0.3
60103	187.6866	0.0019	187.6875	0.0022	-0.9	-0.3	60165	169.3616	0.0021	169.3625	0.0023	-0.9	-0.2
60104	172.0514	0.0020	172.0522	0.0022	-0.8	-0.2	60166	166.5166	0.0022	166.5180	0.0025	-1.4	-0.3
60105	180.4891	0.0017	180.4900	0.0019	-0.9	-0.2	60200	161.9400	0.0017	161.9403	0.0019	-0.3	-0.2
60106	170.1078	0.0016	170.1086	0.0018	-0.8	-0.2	60201	167.6694	0.0017	167.6696	0.0019	-0.2	-0.2
60107	180.2845	0.0020	180.2845	0.0022	0.0	-0.2	60202	164.0588	0.0017	164.0590	0.0019	-0.2	-0.2
60108	176.5114	0.0019	176.5119	0.0021	-0.5	-0.2	60203	158.6279	0.0017	158.6278	0.0019	0.1	-0.2
60109	165.6779	0.0022	165.6793	0.0025	-1.4	-0.3	60204	166.5544	0.0015	166.5545	0.0017	-0.1	-0.2
60110	156.5558	0.0022	156.5572	0.0025	-1.4	-0.3	60205	189.3553	0.0014	189.3558	0.0016	-0.5	-0.2
60111	145.2664	0.0022	145.2680	0.0025	-1.6	-0.3	60206	155.2999	0.0019	155.3001	0.0021	-0.2	-0.2
60112	168.2277	0.0020	168.2283	0.0022	-0.6	-0.2	60207	154.5071	0.0018	154.5071	0.0020	0.0	-0.2
60113	160.0718	0.0020	160.0727	0.0022	-0.9	-0.2	60208	149.8531	0.0019	149.8536	0.0021	-0.5	-0.2
60114	157.1676	0.0019	157.1686	0.0021	-1.0	-0.2	60209	168.4506	0.0018	168.4512	0.0020	-0.6	-0.2
60115	160.6638	0.0020	160.6649	0.0023	-1.1	-0.3	60210	163.7785	0.0017	163.7793	0.0019	-0.8	-0.2
60116	149.4463	0.0020	149.4475	0.0022	-1.2	-0.2	60211	156.6884	0.0018	156.6891	0.0020	-0.7	-0.2
60117	150.8693	0.0020	150.8706	0.0023	-1.3	-0.3	60212	148.9705	0.0019	148.9710	0.0021	-0.5	-0.2
60118	160.1742	0.0019	160.1754	0.0022	-1.2	-0.3	60213	152.3310	0.0019	152.3318	0.0021	-0.8	-0.2
60119	154.7177	0.0020	154.7188	0.0022	-1.1	-0.2	60214	160.5151	0.0018	160.5161	0.0021	-1.0	-0.3
60120	145.0010	0.0020	145.0021	0.0022	-1.1	-0.2	60215	150.8958	0.0018	150.8969	0.0020	-1.1	-0.2
60121	145.7111	0.0020	145.7124	0.0022	-1.3	-0.2	60216	149.5372	0.0018	149.5381	0.0020	-0.9	-0.2
60122	152.3210	0.0020	152.3220	0.0022	-1.0	-0.2	60217	153.9322	0.0018	153.9330	0.0020	-0.8	-0.2
60123	148.7786	0.0021	148.7799	0.0023	-1.3	-0.2	60218	140.7136	0.0020	140.7143	0.0022	-0.7	-0.2
60124	142.7059	0.0020	142.7068	0.0023	-0.9	-0.3	60219	145.8125	0.0019	145.8130	0.0022	-0.5	-0.3
60150	150.8480	0.0020	150.8495	0.0023	-1.5	-0.3	60220	147.0659	0.0019	147.0666	0.0022	-0.7	-0.3
60151	152.5398	0.0021	152.5417	0.0024	-1.9	-0.3	60221	148.2107	0.0019	148.2113	0.0022	-0.6	-0.3
60152	148.7421	0.0024	148.7429	0.0027	-0.8	-0.3	60250	154.8945	0.0020	154.8949	0.0023	-0.4	-0.3
60153	148.4260	0.0024	148.4266	0.0027	-0.6	-0.3	60251	159.0859	0.0019	159.0864	0.0021	-0.5	-0.2
60154	144.9495	0.0020	144.9509	0.0022	-1.4	-0.2	60252	166.7402	0.0019	166.7406	0.0021	-0.4	-0.2
60156	145.9948	0.0020	145.9962	0.0023	-1.4	-0.3	60253	144.0407	0.0019	144.0411	0.0021	-0.4	-0.2
60157	138.9960	0.0022	138.9967	0.0025	-0.7	-0.3	60254	134.8247	0.0019	134.8251	0.0022	-0.4	-0.3
60158	141.0982	0.0021	141.0992	0.0023	-1.0	-0.2	60255	133.4997	0.0019	133.5005	0.0022	-0.8	-0.3
60160	151.8283	0.0021	151.8293	0.0023	-1.0	-0.2	60257	139.4653	0.0021	139.4662	0.0024	-0.9	-0.3
60161	136.4702	0.0020	136.4711	0.0023	-0.9	-0.3	60258	139.8608	0.0021	139.8617	0.0024	-0.9	-0.3

Table 6.5 (Continued)
Comparison of Preliminary Adjusted Elevations and Mean MINQE Elevations

BM	Preliminary		MINQE (mean 1 par)		Differences		BM	Preliminary		MINQE (mean 1 par)		Differences	
	Elevation (m)	Std Dev (m)	Elevation (m)	Std Dev (m)	Elevation (mm)	Std Dev (mm)		Elevation (m)	Std Dev (m)	Elevation (m)	Std Dev (m)	Elevation (mm)	Std Dev (mm)
60259	145.1001	0.0021	145.1011	0.0024	-1.0	-0.3	60321	222.9511	0.0017	222.9511	0.0019	0.0	-0.2
60260	136.1184	0.0023	136.1189	0.0026	-0.5	-0.3	60322	212.3023	0.0017	212.3023	0.0020	0.0	-0.3
60261	140.8819	0.0023	140.8824	0.0026	-0.5	-0.3	60323	210.2063	0.0017	210.2068	0.0020	-0.5	-0.3
60262	135.7282	0.0023	135.7290	0.0026	-0.8	-0.3	60350	175.5330	0.0019	175.5325	0.0021	0.5	-0.2
60263	151.9317	0.0024	151.9322	0.0027	-0.5	-0.3	60351	224.1697	0.0017	224.1692	0.0019	0.5	-0.2
60265	143.8606	0.0020	143.8613	0.0023	-0.7	-0.3	60352	252.7933	0.0018	252.7924	0.0020	0.9	-0.2
60266	135.5059	0.0023	135.5068	0.0026	-0.9	-0.3	60353	231.9863	0.0017	231.9863	0.0020	0.0	-0.3
60267	132.5944	0.0024	132.5949	0.0027	-0.5	-0.3	60354	232.9296	0.0017	232.9296	0.0019	0.0	-0.2
60300	160.6689	0.0015	160.6691	0.0017	-0.2	-0.2	60355	220.4404	0.0017	220.4406	0.0019	-0.2	-0.2
60301	180.6819	0.0015	180.6819	0.0017	0.0	-0.2	60356	158.7043	0.0015	158.7047	0.0017	-0.4	-0.2
60302	189.0671	0.0013	189.0675	0.0015	-0.4	-0.2	60357	168.1346	0.0019	168.1346	0.0021	0.0	-0.2
60303	183.2441	0.0013	183.2446	0.0015	-0.5	-0.2	60358	166.4956	0.0018	166.4958	0.0021	-0.2	-0.3
60304	164.6070	0.0014	164.6078	0.0015	-0.8	-0.1	60400	174.6058	0.0016	174.6063	0.0018	-0.5	-0.2
60305	167.5325	0.0015	167.5327	0.0017	-0.2	-0.2	60401	182.8620	0.0016	182.8625	0.0018	-0.5	-0.2
60306	183.7156	0.0013	183.7160	0.0014	-0.4	-0.1	60402	213.2881	0.0019	213.2883	0.0021	-0.2	-0.2
60307	198.3555	0.0014	198.3559	0.0015	-0.4	-0.1	60403	194.1568	0.0017	194.1575	0.0019	-0.7	-0.2
60308	198.5954	0.0013	198.5959	0.0014	-0.5	-0.1	60404	211.7746	0.0019	211.7745	0.0022	0.1	-0.3
60311	193.2554	0.0009	193.2560	0.0011	-0.6	-0.2	60405	216.4398	0.0019	216.4397	0.0021	0.1	-0.2
60312	201.9998	0.0011	202.0000	0.0012	-0.2	-0.1	60406	210.4370	0.0020	210.4369	0.0022	0.1	-0.2
60313	185.2895	0.0014	185.2902	0.0015	-0.7	-0.1	60450	197.0192	0.0019	197.0199	0.0021	-0.7	-0.2
60314	215.7090	0.0000	215.7090	0.0000	0.0	0.0	60451	228.0881	0.0020	228.0876	0.0022	0.5	-0.2
60315	224.0623	0.0008	224.0626	0.0009	-0.3	-0.1	60452	224.7156	0.0020	224.7150	0.0022	0.6	-0.2
60316	217.9603	0.0010	217.9610	0.0011	-0.7	-0.1	60453	224.2912	0.0020	224.2907	0.0022	0.5	-0.2
60317	225.6245	0.0011	225.6247	0.0012	-0.2	-0.1	60454	220.6304	0.0020	220.6305	0.0022	-0.1	-0.2
60318	208.6451	0.0013	208.6453	0.0014	-0.2	-0.1	60455	219.4779	0.0019	219.4778	0.0021	0.1	-0.2
60319	205.9108	0.0015	205.9109	0.0017	-0.1	-0.2	60456	218.1020	0.0019	218.1020	0.0021	0.0	-0.2
60320	216.9525	0.0016	216.9525	0.0018	0.0	-0.2	60457	198.1801	0.0021	198.1802	0.0023	-0.1	-0.2

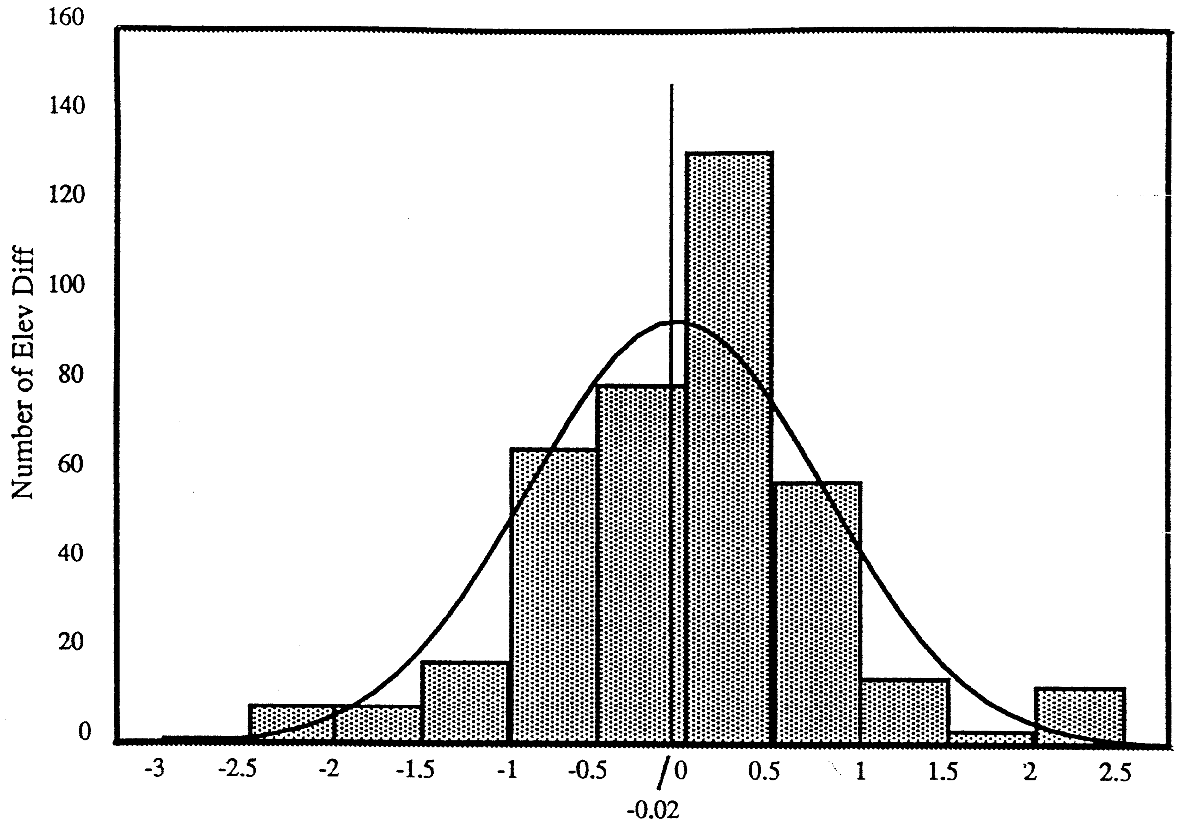

Figure 6.6
Histogram of Adjustment Using Mean Elevation
Differences and MINQE Determined Weights

6.5 Analysis of the Densifications, Elevation Transfers, Tunnel Control and Breakthroughs

Analysis of the densification, elevation transfer and vertical tunnel control is required to ensure accuracy requirements are achieved. The report describes the five completed tunnel half sectors which form the A610 and A611 contracts and the first half sectors of the A650 and A670 contracts (N15 through N35 and N40 to N45).

The densification at each service area had to be carried out a few days before the elevation transfer to ensure stability of the monuments. Reconaissance was performed a few days prior to the elevation transfer survey to ensure the densification and elevation transfer is performed according to the design scheme. The design scheme allows for reliability and accuracy. The transfer of elevations was performed using at least two vertical distances for redundancy. The vertical distances were corrected for prism calibration and atmospheric effects. The elevations and their associated accuracies from densification and shaft transfer are shown on Table 6.6. The accuracy for densfication (deep BM to shaft collar) ranges from 1.7 to 3.0 mm at the 99 percent level of confidence, and the accuracy for shaft transfer (shaft collar to tunnel BM) ranges from 1.8 to 4.2 mm at the 99 percent level of confidence. Both densification and shaft transfer are well within the initial estimated accuracy as mentioned in Section 2.3, and compatible with the *a priori* estimates given in Section 5.4.

The vertical tunnel control commenced after elevations were transferred to at least three benchmarks in the tunnel. From these three benchmarks, elevations were extended to within 330 metres (1000') of the trailing gear of the TBM following the procedures described in Section 5.4. Full variance-covariance information was propagated from the PVCN, to densification survey, elevation transfers, and finally through each tunnel (Figure 6.7). This allows for the determination of the tunnel BM elevations using the correct accuracy estimates. When control extension in the tunnel was required it included re-surveying three existing BMs to ensure stability of the tunnel BMs. The accuracy of the final tunnel BMs prior to breakthrough with the next shaft range from 5.4 mm to 10.8 mm at the 99 percent level of confidence.

The vertical survey error associated with the tunnel breakthrough was calculated as the average difference between elevations of benchmarks determined during the tunnel drive with common benchmarks from the elevation transfer accomplished at the next shaft. In the A610 breakthrough (N15 to N20 half sector), the vertical breakthrough was approximately -1.9 mm, in the A611 contract (N20 to N25 half sector), the vertical breakthrough was calculated as -4.5 mm, in the A650 contract (N25 to N30 half sector), the vertical breakthrough was determined to be -2.1 mm, in the A650 contract (N30 to N35 half sector), the vertical breakthrough was computed as -12.5 mm and in the A670 contract (N40 to N45), the vertical breakthrough was 2.1 mm. All are well within the allowable survey error for tunnel control of 108 mm. The largest breakthrough is A650 (N30 to N35) which was explained by the upheavel in the invert causing BM unstability because of long intervals between tunnel extensions.

The determination of the final elevations of the BMs in the tunnel was accomplished by a simultaneous adjustment using the connecting shaft transfers at both ends of the

Table 6.6
Densification and Shaft Transfer Elevations and Associated Standard Deviations

Service Area	BM	Description	Elevation (m)	Std Dev (m)	Service Area	BM	Description	Elevation (m)	Std Dev (m)
N15	90005	Densification	233.2480	0.0014	N25	90203	Densification	209.6506	0.0020
N15	90015	Densification	234.4272	0.0014	N25	90204	Densification	212.8297	0.0020
N15	90016	Densification	234.3860	0.0014	N25	90205	Densification	210.6644	0.0020
N15	90017	Densification	232.1646	0.0013	N25	90206	Densification	207.6301	0.0020
N15	90018	Densification	232.1356	0.0013	N25	90208	Densification	207.5936	0.0020
N15	90086	Taylor Hobson	233.8769	0.0013	N25	90259	Taylor Hobson	209.3044	0.0020
N15	90087	Taylor Hobson	233.7974	0.0013	N25	90261	Taylor Hobson	209.2749	0.0020
N15	90088	Taylor Hobson	235.6905	0.0014	N25	95218	Temporary	168.3988	0.0021
N15	95014	Temporary	163.0832	0.0015	N25	95219	Temporary	168.2849	0.0021
N15	95021	Temporary	163.0870	0.0015	N25	95220	Temporary	167.1595	0.0021
N15	95037	Temporary	164.4162	0.0015	N25	95221	Temporary	167.7087	0.0021
N15	95067	Tripod	164.5479	0.0015	N25	95222	Temporary	167.0296	0.0021
N15	95068	Tripod	164.4876	0.0015	N25	95223	Temporary	166.8729	0.0021
N15	95072	Tripod	164.8831	0.0015	N25	95253	Tripod	168.7803	0.0021
N15	70001	Tunnel	163.9512	0.0015	N25	95254	Tripod	168.9075	0.0021
N15	70002	Tunnel	163.9848	0.0015	N25	70401	Tunnel	167.4706	0.0022
N15	70003	Tunnel	164.0773	0.0015	N25	70402	Tunnel	167.5410	0.0022
N20	90101	Densification	226.4871	0.0022	N25	70403	Tunnel	167.4052	0.0022
N20	90102	Densification	221.0828	0.0022	N30	90301	Densification	218.2947	0.0021
N20	90103	Densification	222.2847	0.0022	N30	90302	Densification	213.5769	0.0022
N20	90104	Densification	219.6897	0.0022	N30	90303	Densification	215.3011	0.0022
N20	90105	Densification	220.0697	0.0022	N30	90306	Densification	215.2491	0.0022
N20	90165	Taylor Hobson	221.7706	0.0022	N30	90307	Densification	215.2395	0.0022
N20	90166	Taylor Hobson	221.7822	0.0022	N30	90357	Taylor Hobson	216.9146	0.0022
N20	95109	Temporary	168.1553	0.0027	N30	90358	Taylor Hobson	216.1816	0.0022
N20	95110	Temporary	168.3436	0.0027	N30	95308	Temporary	162.0643	0.0022
N20	95111	Temporary	170.0414	0.0026	N30	95309	Temporary	162.2822	0.0022
N20	95112	Temporary	170.0593	0.0026	N30	95310	Temporary	162.1157	0.0022
N20	95159	Tripod	168.7612	0.0024	N30	95311	Temporary	161.8377	0.0022
N20	95160	Tripod	168.7275	0.0024	N30	95353	Tripod	162.6547	0.0022
N20	70201	Tunnel	168.1703	0.0027	N30	95354	Tripod	162.6487	0.0022
N20	70202	Tunnel	168.1297	0.0027	N30	70606	Tunnel	161.7765	0.0024
N20	70204	Tunnel	168.8308	0.0027	N30	70609	Tunnel	161.3384	0.0024
					N30	70612	Tunnel	161.0344	0.0024

Table 6.6 (Continued)

Densification and Shaft Transfer Elevations and Associated Standard Deviations

Service Area	BM	Description	Elevation (m)	Std Dev (m)	Service Area	BM	Description	Elevation (m)	Std Dev (m)
N35	90404	Densification	211.5096	0.0014	N40	90569	Taylor Hobson	170.2725	0.0024
N35	90405	Densification	208.4369	0.0014	N40	90570	Taylor Hobson	170.3003	0.0024
N35	90406	Densification	204.7610	0.0014	N40	95511	Temporary	134.2701	0.0024
N35	90410	Densification	209.9686	0.0013	N40	95512	Temporary	135.1660	0.0024
N35	90411	Densification	209.8765	0.0013	N40	95513	Temporary	134.8683	0.0025
N35	90412	Densification	209.9382	0.0013	N40	95554	Tripod	135.3885	0.0025
N35	90413	Densification	209.9132	0.0013	N40	95555	Tripod	135.4413	0.0025
N35	90457	Taylor Hobson	211.6138	0.0014	N40	71001	Tunnel	134.8611	0.0029
N35	90458	Taylor Hobson	211.5582	0.0015	N40	71002	Tunnel	134.4903	0.0029
N35	95406	Temporary	149.9567	0.0016	N40	71003	Tunnel	134.3764	0.0029
N35	95407	Temporary	149.9877	0.0016	N45	90601	Densification	168.3078	0.0023
N35	95408	Temporary	150.0994	0.0016	N45	90602	Densification	168.0470	0.0023
N35	95455	Tripod	150.8140	0.0016	N45	90603	Densification	166.8018	0.0023
N35	95456	Tripod	150.8230	0.0016	N45	90609	Densification	168.7054	0.0023
N35	70804	Tunnel	149.7823	0.0017	N45	90610	Densification	168.5458	0.0023
N35	70805	Tunnel	149.7786	0.0017	N45	90654	Taylor Hobson	170.3054	0.0023
N35	70806	Tunnel	149.5499	0.0017	N45	90655	Taylor Hobson	170.1395	0.0023
N40	90501	Densification	175.7569	0.0023	N45	95606	Temporary	118.9873	0.0024
N40	90502	Densification	177.1240	0.0023	N45	95607	Temporary	118.9179	0.0024
N40	90503	Densification	171.3043	0.0023	N45	95608	Temporary	119.1536	0.0024
N40	90508	Densification	168.3423	0.0023	N45	95655	Tripod	119.8325	0.0024
N40	90509	Densification	168.2535	0.0023	N45	95656	Tripod	119.9218	0.0024

tunnel. The combined adjustment yields the highest vertical control for setting out the final invert.

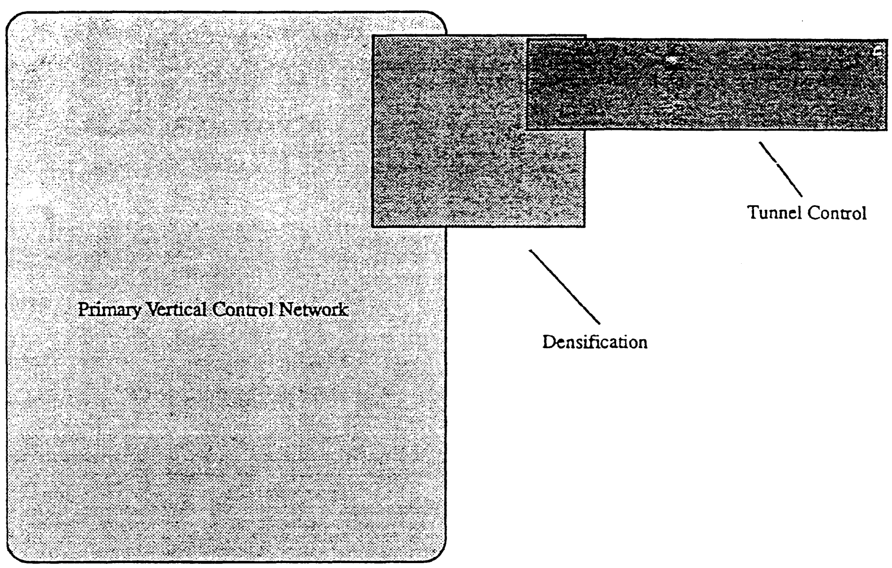

Figure 6.7
Schematic Diagram Showing Propogation of Full-Variance-Covariance
Information from PVCN to Tunnel Control

6.6 Combined Adjustment and Final Elevations

The highest accuracy is achieved by adjusting tunnel benchmarks using elevations transferred from the surface through shafts at each end of the tunnel drive. This will increase the accuracy and reliabilty of the tunnel BMs for the final invert requirements.

The effect of the combined adjustment on the the elevations of the tunnel BMs depend primarily on the accuracy of the tunnel breakthrough. The A610, A611, A650 and

A670 final elevations are compared to the elevations prior to breakthrough for BMs located at 250 m intervals along the tunnel are shown in Table 6.7.

Results of the analysis show an increase in accuracy of up to 6.1 mm at the 99 percent confidence level when connections to the surface are from two shaft transfers (about 4.0 km apart). The maximum difference in elevation before and after the breakthrough is 4.5 mm.

The combined adjustment ensures higher accuracy and reliability. Initial investigation shows that the final invert accuracy can be increased to 6.5 mm at the 99 percent level of confidence for the completed tunnel BMs (estimated to be as low as 8 mm at the 99 percent level of confidence for the tunnel furthest away from the West Campus), however the elevations must be corrected for the effect of geoid undulations. This will further hinder the accuracy of the final elevations. To minimize the influence of geoid undulations on the final invert a micro-geoid is needed.

Table 6.7

Tunnel Elevations Before and After Breakthrough

Tunnel Contract	BM	Location (km)	Elevation Before (m)	Std Dev (m)	Elevation After (m)	Std Dev (m)	Difference (mm)	Tunnel Contract	BM	Location (km)	Elevation Before (m)	Std Dev (m)	Elevation After (m)	Std Dev (m)	Difference (mm)
A610	70005	0.00	164.3147	0.0015	164.3153	0.0015	-0.6	A611	70247	2.00	168.8678	0.0030	168.8712	0.0022	-3.4
A610	70010	0.25	164.5501	0.0015	164.5508	0.0015	-0.7	A611	70252	2.25	168.8949	0.0030	168.8983	0.0022	-3.4
A610	70015	0.50	165.1486	0.0016	165.1494	0.0015	-0.8	A611	70257	2.50	168.5757	0.0030	168.5792	0.0022	-3.5
A610	70020	0.75	165.3530	0.0016	165.3539	0.0015	-0.9	A611	70262	2.75	168.5743	0.0030	168.5780	0.0022	-3.7
A610	70025	1.00	165.7772	0.0016	165.7780	0.0016	-0.8	A611	70267	3.00	168.4580	0.0031	168.4618	0.0022	-3.8
A610	70030	1.25	166.1209	0.0017	166.1219	0.0016	-1.0	A611	70272	3.25	168.2118	0.0031	168.2158	0.0022	-4.0
A610	70036	1.50	166.5124	0.0017	166.5135	0.0016	-1.1	A611	70273	3.50	168.2695	0.0031	168.2735	0.0022	-4.0
A610	70041	1.75	166.7114	0.0018	166.7125	0.0016	-1.1	A611	70282	3.75	167.9725	0.0032	167.9770	0.0021	-4.5
A610	70046	2.00	167.0517	0.0018	167.0529	0.0016	-1.2	A650-I	70404	0.00	167.8514	0.0023	167.8513	0.0021	0.1
A610	70051	2.25	167.2755	0.0019	167.2767	0.0016	-1.2	A650-I	70409	0.25	167.7646	0.0023	167.7648	0.0021	-0.2
A610	70058	2.50	167.5227	0.0019	167.5241	0.0016	-1.4	A650-I	70414	0.50	167.3551	0.0023	167.3554	0.0022	-0.3
A610	70064	2.75	167.6576	0.0019	167.6591	0.0016	-1.5	A650-I	70419	0.75	167.1015	0.0023	167.1021	0.0022	-0.6
A610	70069	3.00	167.9523	0.0020	167.9538	0.0016	-1.5	A650-I	70424	1.00	166.7993	0.0024	166.8000	0.0022	-0.7
A610	70074	3.25	168.1475	0.0020	168.1491	0.0016	-1.6	A650-I	70429	1.25	166.4230	0.0024	166.4238	0.0022	-0.8
A610	70079	3.50	168.3008	0.0020	168.3024	0.0016	-1.6	A650-I	70434	1.50	166.5126	0.0024	166.5135	0.0022	-0.9
A610	70084	3.75	168.4448	0.0021	168.4465	0.0016	-1.7	A650-I	70439	1.75	166.0257	0.0024	166.0269	0.0022	-1.2
A610	70089	4.00	168.6468	0.0021	168.6486	0.0016	-1.8	A650-I	70444	2.00	165.5305	0.0025	165.5319	0.0022	-1.4
A610	70091	4.25	168.7188	0.0021	168.7207	0.0016	-1.9	A650-I	70449	2.25	165.1679	0.0025	165.1694	0.0022	-1.5
A611	70207	0.00	169.2343	0.0027	169.2364	0.0022	-2.1	A650-I	70454	2.50	164.8916	0.0025	164.8933	0.0022	-1.7
A611	70212	0.25	168.5535	0.0028	168.5558	0.0022	-2.3	A650-I	70459	2.75	164.2212	0.0025	164.2231	0.0022	-1.9
A611	70217	0.50	168.5964	0.0028	168.5988	0.0022	-2.4	A650-I	70464	3.00	163.8349	0.0026	163.8369	0.0022	-2.0
A611	70222	0.75	168.6601	0.0028	168.6627	0.0022	-2.6	A650-I	70469	3.25	163.1607	0.0026	163.1629	0.0022	-2.2
A611	70227	1.00	168.8302	0.0029	168.8329	0.0022	-2.7	A650-I	70474	3.50	162.6853	0.0026	162.6876	0.0022	-2.3
A611	70232	1.25	168.8153	0.0029	168.8182	0.0022	-2.9	A650-I	70479	3.75	162.2748	0.0027	162.2775	0.0022	-2.7
A611	70237	1.50	168.8752	0.0029	168.8782	0.0022	-3.0	A650-I	70483	4.00	161.7708	0.0027	161.7737	0.0021	-2.9
A611	70242	1.75	168.8678	0.0029	168.8710	0.0022	-3.2								

Table 6.7 (Continued)
Tunnel Elevations Before and After Breakthrough

Tunnel Contract	BM	Location (km)	Elevation Before (m)	Std Dev (m)	Elevation After (m)	Std Dev (m)	Difference (mm)	Tunnel Contract	BM	Location (km)	Elevation Before (m)	Std Dev (m)	Elevation After (m)	Std Dev (m)	Difference (mm)
A650-II	70613	0.00	160.8929	0.0024	160.8961	0.0023	-3.2	A670	71004	0.00	134.1903	0.0029	134.1891	0.0025	1.2
A650-II	70618	0.25	160.7297	0.0025	160.7334	0.0023	-3.7	A670	71010	0.25	133.3525	0.0029	133.3513	0.0025	1.2
A650-II	70623	0.50	160.0640	0.0025	160.0681	0.0023	-4.1	A670	71015	0.50	132.5629	0.0029	132.5617	0.0025	1.2
A650-II	70628	0.75	159.4702	0.0025	159.4746	0.0024	-4.4	A670	71020	0.75	131.6518	0.0030	131.6506	0.0025	1.2
A650-II	70633	1.00	158.9062	0.0026	158.9108	0.0024	-4.6	A670	71025	1.00	130.5973	0.0030	130.5961	0.0025	1.2
A650-II	70638	1.25	158.2650	0.0026	158.2699	0.0024	-4.9	A670	71030	1.25	129.6416	0.0030	129.6402	0.0025	1.4
A650-II	70643	1.50	157.6718	0.0026	157.6771	0.0024	-5.3	A670	71035	1.50	128.6798	0.0030	128.6783	0.0025	1.5
A650-II	70648	1.75	157.0379	0.0027	157.0437	0.0024	-5.8	A670	71040	1.75	127.8287	0.0030	127.8271	0.0025	1.6
A650-II	70653	2.00	156.4134	0.0027	156.4195	0.0025	-6.1	A670	71045	2.00	126.8075	0.0030	126.8061	0.0025	1.4
A650-II	70658	2.25	155.6343	0.0028	155.6410	0.0025	-6.7	A670	71050	2.25	125.1839	0.0031	125.1822	0.0025	1.7
A650-II	70663	2.50	155.2023	0.0029	155.2098	0.0025	-7.5	A670	71055	2.50	124.6733	0.0031	124.6716	0.0025	1.7
A650-II	70668	2.75	154.4587	0.0029	154.4668	0.0025	-8.1	A670	71060	2.75	123.5862	0.0031	123.5844	0.0025	1.8
A650-II	70673	3.00	153.4210	0.0029	153.4294	0.0025	-8.4	A670	71065	3.00	122.6796	0.0031	122.6778	0.0025	1.8
A650-II	70679	3.25	152.7172	0.0030	152.7259	0.0025	-8.7	A670	71070	3.25	121.8198	0.0031	121.8179	0.0025	1.9
A650-II	70684	3.50	151.8858	0.0030	151.8950	0.0025	-9.2	A670	71075	3.50	120.8437	0.0031	120.8416	0.0025	2.1
A650-II	70689	3.75	151.1591	0.0030	151.1686	0.0025	-9.5	A670	71080	3.75	119.8548	0.0031	119.8526	0.0025	2.2
A650-II	70694	4.00	150.6251	0.0031	150.6359	0.0026	-10.8	A670	71084	4.00	119.1258	0.0032	119.1237	0.0025	2.1
A650-II	70699	4.25	149.7943	0.0032	149.8068	0.0025	-12.5								

CHAPTER 7
DETERMINATION OF MICRO-GEOID

The SSC is designed to be set out in a plane in space. The location of the plane relative to the real world depends on numerous practical considerations such as geology, politics and economics. From a geodetic engineering perspective, the location of the SSC plane is determined in relation to the reference ellipsoid while the orthometric heights are referenced to the geoid. To ensure that the elevations are referenced to a plane in space, careful consideration must be given for determining the geoid undulations N, which are the separation between the ellipsoid and the geoid (Figure 7.1).

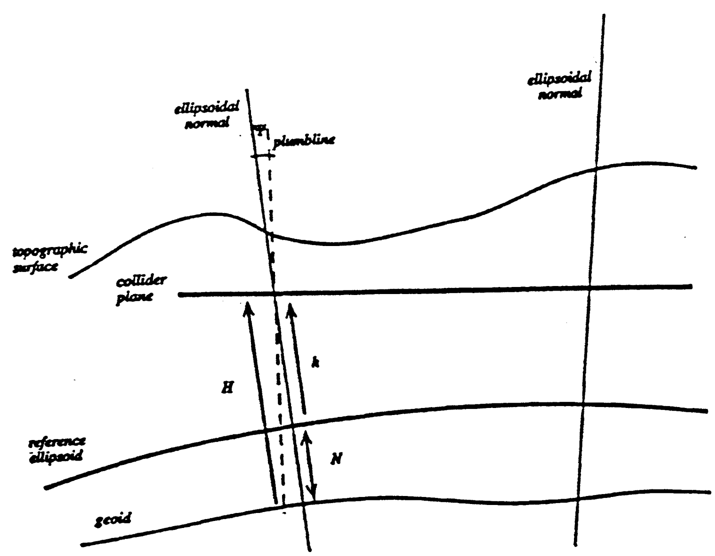

Figure 7.1
Relationship of SSC Plane, Ellipsoid and Geoid

The Global Positioning System (GPS) allows for ellipsoidal heights to be determined quite accurately and economically. Geoid undulations can be estimated throughout the SSC Project by comparing ellipsoidal heights with those obtained from the PVCN. The differences between the elevations obtained from the PVCN and those obtained from GPS can be modelled by appropriate polynomials to obtain accurate geoid undulations throughout the SSC Project. The design of an accurate GPS network and the methodology of the least squares fitting of a polynomial to estimate the geoid undulations necessary for SSC tunnel construction and final invert positioning is presented.

7.1 Geoidal Network Design

Initial estimates of the geoidal heights in the SSC Project area was determined using existing control and its associated variance-covariance information, comprised of orthometric heights and GPS heights. The trend of the geoid undulations in the SSC Project area was best fitted by a plane. This was determined to be sufficiently accurate for construction of the tunnels, yet for final invert elevations, a more accurate model for the geoidal trend was required. A preliminary investigation of the local geoid over the SSC was determined by the UNB Engineering Surveys Research Group [Kuang and Chrzanowski, 1992b]. A preanalysis was performed over 39 well spaced points to give a well balanced representation of the geoid. Initial investigation suggested that the geoidal heights can be expressed by the following:

$$\begin{aligned} N_i = h_i - H_i = a_0+a_1(x_i-x_0)+a_2(y_i-y_0)+a_3(x_i-x_0)^2+ \\ a_4(x_i-x_0)(y_i-y_0)+a_5(y_i-y_0)^2 \end{aligned} , \tag{7.1}$$

where h_i is the GPS height at one of the common points,

H_i is the orthometric height at the same point,

x_i and y_i are the plane coordinates of the common point, and

x_0 and y_0 are the origin of the area being modelled for geiod undulations (center of the SSC main collider ring.

The levelling accuracies determined from FGCC First-Order Class I (Equation 2.4) and those for GPS derived heights, based on a previous GPS survey, were used, as [Miles, et al, 1992]:

$$\sigma_h = \sqrt{(5\ \text{mm})^2+(1.5\ \text{ppm}\ S)^2}, \tag{7.2}$$

where S is the baseline distance.

Fitting a second order polynomial, suggests a micro-geoid can be determined to an accuracy of 5 mm at the standard level of confidence. At the 99 percent level of confidence, the micro-geoid can thus be determined to an accuracy of 13 mm.

The Geoidal Modeling GPS Network was observed over six days between March 3 and March 12, 1993. Six Ashtech P-XII dual frequency p-code recievers were used. The network comprised of 55 stations (as opposed to initially 39 due to the fact that the survey was a multi-purpose survey) for which elevations were obtained from the PVCN. The main design considerations for the geoidal network were strong geometry for the GPS survey so short baselines were observed to minimize the effect of the distance dependent component. The final design of the geoidal network is shown in Figure 7.2.

To ensure the compatibilty of the variance-covariance, the PVCN and the GPS (geoid) network were readjusted by the author using the same minimally constrained point (60005). The final adjusted ellipsoidal heights and preliminary orthometric heights and their associated variance-covariances were used for the polynomial fitting of the geoid undulations

7.2 Determination of the Model Through Least Squares

A model was developed from the 55 benchmarks using the least squares technique. To ensure proper statistical propagation, the modeling software incorporated the variance-covariance information from the PVCN and Geoid Network adjustments.

The author chose two polynomials for possibly modelling the geoid undulations, a plane and a third-order polynomial. The results are shown on Table 7.1. The plane does not fit well with an *a posteriori* variance factor of 26.97. and the largest residual of 33 mm. A third-order polynomial was attempted of the form:

$$\begin{gathered} N_i = h_i - H_i = a_0+a_1(x_i-x_0)+a_2(y_i-y_0)+a_3(x_i-x_0)^2+ \\ a_4(x_i-x_0)(y_i-y_0)+a_5(y_i-y_0)^2+a_6(x_i-x_0)^3+a_7(x_i-x_0)^2(y_i-y_0)+a_8(x_i-x_0)(y_i-y_0)^2+a_9(y_i-y_0)^3 \end{gathered} \quad (7.3)$$

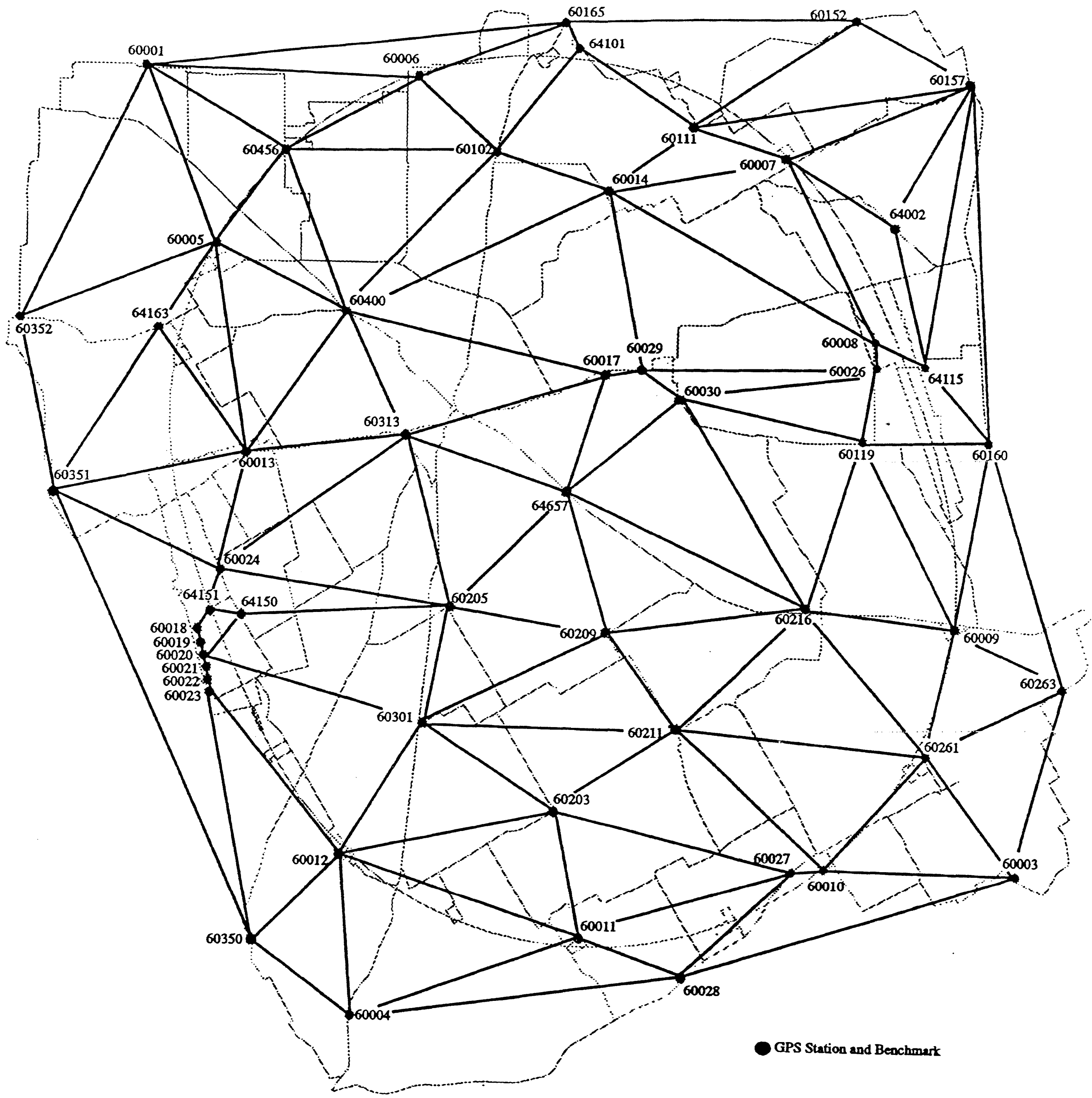

Figure 7.2
GPS Network for Geoidal Modelling

Table 7.1
Results of Geoidal Models

Geoidal Model	Coefficients (m)		Conf @ 95% (m)	Signifcance of Parameters 99%	95%	90%	80%	70%	Largest Residual (m)
N = a0+a1X+a2Y	a0 =	-27.1200	0.0344	Pass	Pass	Pass	Pass	Pass	0.0331
	a1 =	-3.043E-06	7.858E-07	Pass	Pass	Pass	Pass	Pass	
	a2 =	2.601E-05	8.530E-07	Pass	Pass	Pass	Pass	Pass	
N = a0+a1X+a2Y+a3XX +a4XY+a5YY+a7XXY	a0 =	-27.1500	0.0128	Pass	Pass	Pass	Pass	Pass	0.0148
	a1 =	-2.451E-06	3.426E-07	Pass	Pass	Pass	Pass	Pass	
	a2 =	2.590E-05	3.668E-07	Pass	Pass	Pass	Pass	Pass	
	a3 =	1.055E-10	2.473E-11	Pass	Pass	Pass	Pass	Pass	
	a4 =	-8.811E-11	3.598E-11	Pass	Pass	Pass	Pass	Pass	
	a5 =	1.777E-10	2.428E-11	Pass	Pass	Pass	Pass	Pass	
	a7 =	4.365E-15	2.700E-15	Pass	Pass	Pass	Pass	Pass	
N = a0+a1X+a2Y+a3XX +a4XY+a5YY+a6XXX +a7XXY+a9YYY	a0 =	-27.1500	0.0128	Pass	Pass	Pass	Pass	Pass	0.0146
	a1 =	-2.231E-06	4.945E-07	Pass	Pass	Pass	Pass	Pass	
	a2 =	2.557E-05	6.308E-07	Pass	Pass	Pass	Pass	Pass	
	a3 =	8.588E-11	4.303E-11	Pass	Pass	Pass	Pass	Pass	
	a4 =	-8.712E-11	3.595E-11	Pass	Pass	Pass	Pass	Pass	
	a5 =	1.836E-10	2.643E-11	Pass	Pass	Pass	Pass	Pass	
	a6 =	-1.603E-15	2.700E-15	Fail	Fail	Fail	Fail	Pass	
	a7 =	5.314E-15	2.947E-15	Pass	Pass	Pass	Pass	Pass	
	a9 =	1.684E-15	2.741E-15	Fail	Fail	Fail	Fail	Pass	
N = a0+a1X+a2Y+a3XX +a4XY+a5YY+a6XXX +a8XYY+a7XXY+a9YYY	a0 =	-27.1500	0.0131	Pass	Pass	Pass	Pass	Pass	0.0147
	a1 =	-2.242E-06	5.612E-07	Pass	Pass	Pass	Pass	Pass	
	a2 =	2.556E-05	6.478E-07	Pass	Pass	Pass	Pass	Pass	
	a3 =	8.587E-11	4.353E-11	Pass	Pass	Pass	Pass	Pass	
	a4 =	-8.700E-11	3.647E-11	Pass	Pass	Pass	Pass	Pass	
	a5 =	1.841E-10	2.946E-11	Pass	Pass	Pass	Pass	Pass	
	a6 =	-1.592E-15	2.744E-15	Fail	Fail	Fail	Fail	Pass	
	a7 =	5.318E-15	2.983E-15	Pass	Pass	Pass	Pass	Pass	
	a8 =	1.334E-16	3.227E-15	Fail	Fail	Fail	Fail	Fail	
	a9 =	1.724E-15	2.934E-15	Fail	Fail	Fail	Fail	Pass	

The *a posteriori* variance factor was 3.47 and the largest residual to 14.7 mm. However, the coefficients, a_8 failed at 70 percent confidence. It was removed and the *a posteriori* variance factor was reduced to 3.39 and the largest residual to 14.6 mm. Two other polynomials failed at 80 percent and removed. It was decided to go with the polynomial with the least amount of coefficients. The final model is:

$$N_i = h_i - H_i = a_0 + a_1(x_i - x_0) + a_2(y_i - y_0) + a_3(x_i - x_0)^2 + a_4(x_i - x_0)(y_i - y_0) + a_5(y_i - y_0)^2 + a_7(x_i - x_0)^2(y_i - y_0) \quad (7.4)$$

The *a posteriori* variance factor of 3.42 could be explained by deviations of geoid undulations from the polynomial that are not modelled. The geoid undulations along the collider track are shown on Figure 7.3. The maximum discrepancy between the plane function and the third-order polynomial along the centerline is 4 cm. This effect can be seen in Figure 7.4.

The accuracy of the model is 4.4 mm at the standard confidence level. An accuracy of 5 mm (13 mm at 99 percent level of confidence) was initially estimated for a second order polynomial by the UNB consultants. The final invert can then be estimated to an accuracy range of 14 to 17 mm at the 99 percent level of confidence.

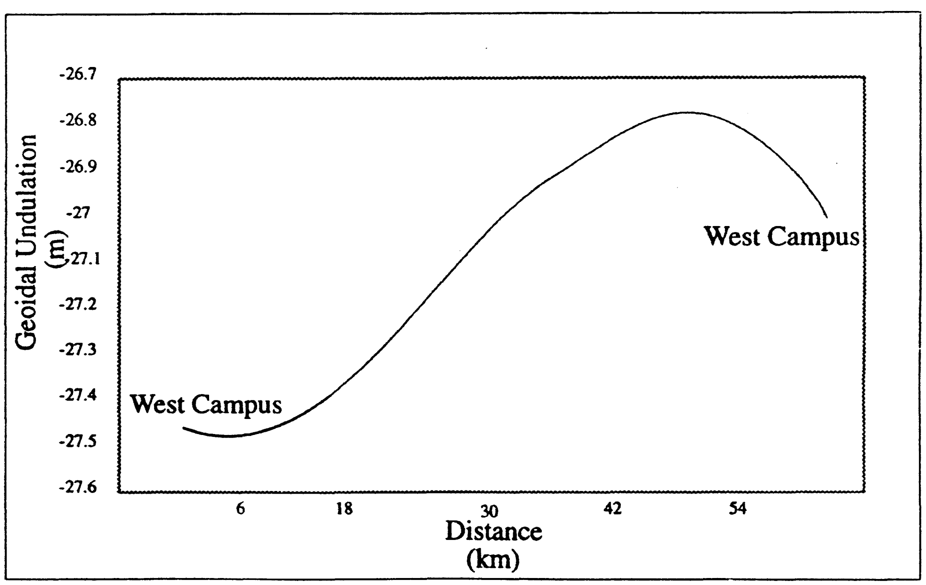

Figure 7.3

Geoid Separation Along the Main Collider Tunnel

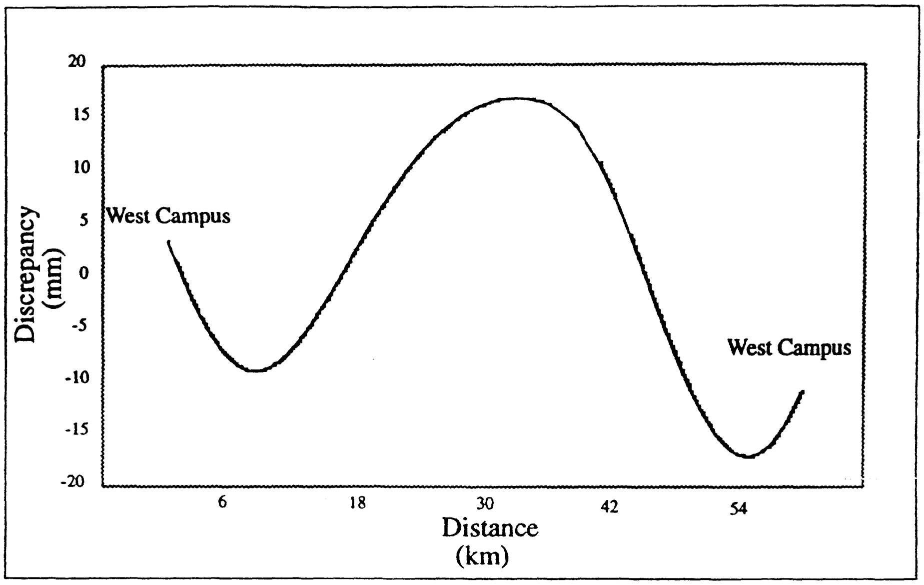

Figure 7.4
Effect of Discrepancy Between Plane and Third Order Polynomial

CHAPTER 8
CONCLUSIONS AND RECOMMENDATIONS

Upon the completion of the analysis of the first five tunnel half-sectors, certain conclusions can be drawn. Recommendations for the vertical positioning of the final invert are stated to ensure that the necessary accuracy is achieved.

8.1 Conclusions

The developed standards, specifications and procedures have ensured that the necessary accuracy requirements were achieved. The development of the standards, specifications and procedures required a thorough pre-analysis of all random and systematic errors, including instrument and turning plate sinking and rebound, vertical atmospheric refraction, tidal accelerations and orthometric corrections. Simulations of the estimated magnitude of the errors were determined using existing data, and their influences on the SSC plane were pre-analyzed. It was concluded that the effect of tidal accelerations causes a slight tilt of the SSC plane which is arbitrarily chosen in space, and therefore, this can be ignored.

The Primary Vertical Control Network was analyzed by section closures, loop closures and a minimally constrained adjustment which yielded a vertical accuracy of 5.4 mm at the 99 percent level of confidence as opposed to the initial estimate of 7.0 mm. The MINQE analysis of the variance-covariance components helped in determining an appropriate weighting scheme. Using the mean elevation differences, instead of the single-run elevation differences, minimized the effect of sinking of the turning plate and therefore mean elevation differences were used in the final adjustment.

Post-analysis of the influence of orthometric corrections concluded that by ignoring the corrections, a slight tilt of the SSC plane results, and therefore the orthometric correction can be safely ignored without adversely affecting the accuracy of the elevations. Analysis of the effect of the vertical atmospheric refraction concluded that refraction also causes a tilt of the collider plane and again can be safely ignored. Second-order effects were within the noise level of the thermistor data.

Developed procedures for densification of vertical control from the PVCN to the service areas, elevation transfer and tunnel control surveys ensured that the highest accuracy has been achieved. Adjustments of the first five tunnel half sectors confirm the high accuracy. The breakthrough errors of the first five tunnels are well within the allowed tolerance and ranged from -12.5 mm to 2.1 mm. The largest breakthrough error (-12.5 mm) was explained by the upheaval of the invert. The highest accuracy for the vertical tunnel control was achieved by adjusting each half-sector with connections from both shaft transfers.

The combination of GPS and precise levelling has been successfully used in the modelling of the geoid undulations in the area of the SSC Project. Geoid undulations have been determined to an accuracy of 13 mm at the 99 percent level of confidence.

The design and analysis of the vertical control was analyzed and it is estimated that the benchmarks in the tunnel can then be determined only to an accuracy range of 14 to 17 mm (depending on its location around the main collider ring) at the 99 percent level of confidence. This is larger than the allowable final invert accuracy invert of 6.25 mm.

8.2 Recommendations

Changes for design requirements of the final invert should be accomplished to accommodate the possible accuracy of the final invert elevations (17 mm at the 99 percent level of confidence).

To ensure the final invert is properly constructed, it is suggested that a stability analysis of the PVCN deep benchmarks be performed. The stability analysis should include all benchmarks around the main collider ring. The use of the Iterative Weighted Similiarity Transformation (IWST), developed by the Engineering Surveys Research Group will give a good depiction of the stability of the benchmarks.

Verification surveys should be performed on regular basis in the tunnel. This is especially important when upheaval is suspected or long periods pass between tunnel extensions. When movement of the tunnel benchmarks is suspected, overlapping of at least six existing BMs instead of three should be performed when tunnel extensions are performed.

References

Balazs, E., and G. Young (1982). *Corrections Applied by the National Geodetic Survey to Precise Levelling Observations,* NOAA Technical Memorandum NOS NGS 34, U.S. Department of Commerce, Rockville, Maryland, 12pp.

Chen, Y.Q., A. Chrzanowski, and M. Kavouras (1990). *Assessment of Observations Using Minimum Norm Quadratic Unbiased Estimation (MINQUE).* Canadian Institute of Surveying and Mapping, Vol. 44, No. 1, pp 39-46.

Chrzanowski, A. (1985). *Geodetic Survey Lecture Notes.* Professor of Surveying Engineering, University of New Brunswick, Fredericton, New Brunswick, Canada.

Chrzanowski, A., G. Robinson and T. Greening (1992). *Control Densification and Shaft Transfer for Superconducting Super Collider CPB-100191,* Parsons Brinckerhoff/Morrison Knudsen Document, for the Superconducting Super Collider Laboratory, under contract no. DE-AC02-89ER40486.

Chrzanowski, A., J. Grodecki, and M. Caissey (1993). *Evaluation of the GPS and Levelling Networks Using the Minimum Quadratic Estimation (MINQE) Analysis,* UNB Engineering Surveys Research Group for the Parsons Brinckerhoff/Morrison Knudsen Team for the Superconducting Super Collider Laboratory, under contract no. DE-AC02-89ER40486.

DeKrom, P., G. Robinson and T. Greening (1992a). *Standards and Specifications for Geodetic Leveling for Surface Network of Superconducting Super Collider CPB-100053,* Parsons Brinckerhoff/Morrison Knudsen Document, for the Superconducting Super Collider Laboratory, under contract no. DE-AC02-89ER40486.

DeKrom, P., G. Robinson and T. Greening (1992b). *Field Procedures for Geodetic Leveling for Surface Network of Superconducting Super Collider CPB-100053,* Parsons Brinckerhoff/Morrison Knudsen Document, for the Superconducting Super Collider Laboratory, under contract no. DE-AC02-89ER40486.

DeKrom, P., G. Robinson and T. Greening (1992c). *Standards, Specifications and Procedures for Tunnel Control for Main Collider Ring of Superconducting Super Collider CPB-100122* Parsons Brinckerhoff/Morrison Knudsen Document, for the Superconducting Super Collider Laboratory, under contract no. DE-AC02-89ER40486.

Federal Geodetic Control Committee (1984). *Standards and Specifications for Geodetic Control Networks.* National Geodetic Survey, National Oceanic Administration, Rockville, Maryland.

Greening, W.J.T. (1985). *Evaluation of Precision Trigonometric Methods,* Master of Science in Engineering, Department of Surveying Engineering, University of New Brunswick, Fredericton, New Brunswick.

Greening, W.J.T., A. Chrzanowski, and R.E. Ruland (1992). *Control Surveys for Tunnelling at the Superconducting Super Collider,* Seventh International Symposium on Deformation Measurements, Banff, Alberta.

Grodecki, J., G. Robinson and T. Greening (1992a). *Analysis of Influence of Tidal Phenomena on Vertical Control CPB-100014*, Parsons Brinckerhoff/Morrison Knudsen Document, for the Superconducting Super Collider Laboratory, under contract no. DE-AC02-89ER40486.

Grodecki, J., G. Robinson and T. Greening (1992b). *Analysis of Accuracy of Gravity Data on Vertical Control CPB-100083*, Parsons Brinckerhoff/Morrison Knudsen Document, for the Superconducting Super Collider Laboratory, under contract no. DE-AC02-89ER40486.

Grodecki, J. (1993). *Orthometric Heights for Superconducting Super Collider's Primary Vertical Control Network, CPB-100500,* Parsons Brinckerhoff/Morrison Knudsen Document, for the Superconducting Super Collider Laboratory, under contract no. DE-AC02-89ER40486.

Heiskanen, W.A. and H. Moritz (1984). *Physical Geodesy,* Reprint, Institute of Physical Geodesy, Technical University, Graz, 1984.

Kharaghani, G. (1987). *Propagation of Atmospheric Refraction on Trigonometric Levelling*, Technical Report 107, Department of Surveying Engineering, University of New Brunswick, Fredericton, New Brunswick.

Kuang, S-L and A. Chrzanowski (1992a). *Report on the Configuration Optimization of the SSC Levelling Network,* UNB Engineering Surveys Research Group for The Parsons Brinckerhoff/Morrison Knudsen Team, for the Superconducting Super Collider Laboratory, under contract no. DE-AC02-89ER40486,.

Kuang, S-L and A. Chrzanowski (1992b). *Accuracy Pre-Analysis of Geoidal Fitting in the SSC Area,* UNB Engineering Surveys Research Group for The Parsons Brinckerhoff/Morrison Knudsen Team, for the Superconducting Super Collider Laboratory, under contract no. DE-AC02-89ER40486,.

Miles, D., G. Robinson and T. Greening (1992). *Standards and Specifications for Global Positionning System for Fiducial Network of Superconducting Super Collider CPB-100056,* Parsons Brinckerhoff/Morrison Knudsen Document, for the Superconducting Super Collider Laboratory, under contract no. DE-AC02-89ER40486.

Pagiatakis, S. (1982). *Ocean Tide Loading, BodyTide and Polar Motion Effects on VLBI*, Technical Report 92, Department of Surveying Engineering, University of New Brunswick, Fredericton, New Brunswick.

Thomson, D.B. (1978). *Introduction to Geodetic Astronomy*, Lecture Notes 40, Department of Surveying Engineering, University of New Brunswick, Fredericton, New Brunswick.

Törge, W. (1980). *Geodesy*. Walter de Gruyter, New York.

Vanicek, P. and E. Krakiwsky (1986). *Geodesy - the Concepts*. North-Holland, New York.

Appendix A

Section Closures of the PVCN

From	To	Elev Diff (m)	Section Dist (km)	Section Closure (mm)	Allowed Section Closure (mm)
60002	60152	-0.56093	0.8537	0.81	2.38
60152	60002	0.56174	0.8545		
60002	60153	-0.87741	0.0745	0.09	0.77
60153	60002	0.87732	0.0745		
60266	60003	1.55904	1.1452	1.34	2.81
60003	60266	-1.55770	1.1606		
60003	60267	-4.46976	0.5568	0.68	1.89
60267	60003	4.46908	0.5570		
64551	60004	12.14571	1.0669	0.06	2.70
60004	64551	-12.14565	1.0688		
60004	64552	-2.22599	0.4869	0.47	1.76
64552	60004	2.22552	0.4889		
60005	60322	1.29131	0.7996	0.16	2.30
60322	60005	-1.29115	0.8225		
60405	60006	-6.92861	1.1812	0.87	2.86
60006	60405	6.92774	1.3971		
60007	60150	-2.33054	0.4555	0.40	1.69
60150	60007	2.33094	0.5724		
60008	60120	-2.89507	0.6592	0.30	2.07
60120	60008	2.89477	0.6690		
60206	60011	0.99329	0.5010	1.11	1.78
60011	60206	-0.99218	0.5066		
60013	60318	-6.00913	0.3758	0.32	1.53
60318	60013	6.00881	0.3760		
60014	60108	-7.02113	0.6671	0.05	2.08
60108	60014	7.02117	0.6683		
60016	60205	5.40466	1.2905	1.76	3.01
60205	60016	-5.40290	1.2916		
60029	60017	8.36891	1.0719	0.63	2.70
60017	60029	-8.36828	1.0727		

From	To	Elev Diff (m)	Section Dist (km)	Section Closure (mm)	Allowed Section Closure (mm)
60017	60106	-3.05359	1.9157	3.64	3.80
60106	60017	3.04995	1.9333		
60018	60019	-1.53900	0.2645	0.76	1.27
60019	60018	1.53976	0.2686		
60018	64151	-6.21101	1.0289	1.73	2.64
64151	60018	6.21274	1.0671		
60019	60020	-5.84476	1.0112	1.84	2.62
60020	60019	5.84659	1.0423		
60021	60020	0.63044	0.1135	0.41	0.83
60020	60021	-0.63003	0.1145		
60021	60022	-3.00096	0.5273	0.98	1.83
60022	60021	3.00194	0.5520		
60023	60022	1.13223	0.2164	0.51	1.15
60022	60023	-1.13172	0.2209		
64146	60023	8.42530	1.7057	2.02	3.54
60023	64146	-8.42328	1.7967		
60024	60315	-2.25610	0.8563	2.90**	2.38
60315	60024	2.25900	0.8631		
60025	60122	6.50344	1.0140	0.04	2.62
60122	60025	-6.50340	1.0420		
60026	60120	-1.11848	0.1580	0.07	0.98
60120	60026	1.11855	0.1595		
60027	60219	-2.96655	0.5745	1.67	1.92
60219	60027	2.96823	0.5794		
60253	60028	13.08923	0.9200	0.60	2.48
60028	60253	-13.08863	0.9238		
60114	60029	7.62481	1.7366	0.77	3.58
60029	60114	-7.62404	1.7438		
60030	60114	-6.97005	1.7800	1.94	3.63
60114	60030	6.96811	1.7822		

From	To	Elev Diff (m)	Section Dist (km)	Section Closure (mm)	Allowed Section Closure (mm)
60030	60564	-7.71670	1.6309	3.32	3.45
60564	60030	7.72002	1.6346		
60101	60105	-8.99422	1.3809	1.85	3.13
60105	60101	8.99607	1.3945		
60101	60538	9.41966	1.0889	0.33	2.73
60538	60101	-9.41932	1.0894		
60101	64611	-0.31914	0.5704	0.18	1.91
64611	60101	0.31897	0.5739		
60101	64612	-0.43353	0.9315	2.05	2.50
64612	60101	0.43148	0.9325		
60102	60103	3.10463	1.6562	1.78	3.48
60103	60102	-3.10286	1.6591		
60542	60102	-1.86258	2.1405	2.95	4.06
60102	60542	1.85963	2.1481		
64615	60102	-0.24912	0.1521	-0.02	0.68
60102	64615	0.24925	0.1524	-0.14	
64615	60102	-0.24894	0.1526	0.16	
64616	60103	-0.98222	0.0563	0.35	0.77
60103	64616	0.98187	0.0714		
60104	60164	-8.84062	0.6154	0.17	1.99
60164	60104	8.84079	0.6352		
60104	64100	0.40508	0.0154	0.05	0.77
64100	60104	-0.40504	0.0224		
60104	64616	16.61747	1.4681	0.01	3.24
64616	60104	-16.61748	1.4701		
60105	60539	-3.12412	1.6038	1.07	3.41
60539	60105	3.12519	1.6054		
60541	60105	0.06135	1.4699	0.02	3.24
60105	60541	-0.06133	1.4785		
60106	60539	7.25674	1.4475	0.22	3.21
60539	60106	-7.25696	1.4533		

From	To	Elev Diff (m)	Section Dist (km)	Section Closure (mm)	Allowed Section Closure (mm)
60106	64659	-7.97263	2.6727	0.69	4.67
64659	60106	7.97194	2.6901		
60108	60107	3.77412	1.6166	2.63	3.43
60107	60108	-3.77149	1.6233		
60107	60542	6.15904	1.4346	1.34	3.20
60542	60107	-6.15770	1.4349		
60108	60112	-8.28305	2.7408	0.67	4.75
60112	60108	8.28371	2.7688		
60540	60108	4.80462	1.9456	0.18	3.83
60108	60540	-4.80480	1.9665		
60109	60110	-9.12172	0.7138	0.66	2.16
60110	60109	9.12239	0.7186		
60109	64104	0.62804	0.0386	0.03	0.77
64104	60109	-0.62807	0.0446		
60111	60110	11.29012	1.4217	1.60	3.18
60110	60111	-11.28852	1.4344		
60571	60111	-14.21635	1.0228	0.65	2.63
60111	60571	14.21701	1.0292		
60111	60601	17.82071	1.7175	0.42	3.56
60601	60111	-17.82113	1.7611		
60115	60112	7.56519	1.8416	3.02	3.71
60112	60115	-7.56217	1.8547		
60114	60113	2.90420	1.2643	0.37	2.97
60113	60114	-2.90383	1.2796		
60563	60113	5.24343	1.7548	0.92	3.60
60113	60563	-5.24251	1.7722		
60115	60116	-11.21672	1.5732	1.29	3.38
60116	60115	11.21801	1.5964		
60117	60116	-1.42341	0.7871	-0.40	1.61
60116	60117	1.42323	0.7900	-0.22	
60117	60116	-1.42239	0.7922	0.62	

From	To	Elev Diff (m)	Section Dist (km)	Section Closure (mm)	Allowed Section Closure (mm)
60116	60561	11.64642	1.9024	1.31	3.78
60561	60116	-11.64511	1.9156		
60116	64109	-2.16249	1.9702	0.19	3.86
64109	60116	2.16268	1.9858		
60150	60117	0.02225	0.4894	-0.60	1.24
60150	60117	-0.02125	0.4907	0.39	
60117	60150	-0.02143	0.4908	0.21	
60558	60118	5.70799	1.4337	0.15	3.20
60118	60558	-5.70814	1.4384		
60559	60118	9.65369	2.5173	0.77	4.50
60118	60559	-9.65446	2.5221		
60564	60118	3.75442	1.7942	1.68	3.65
60118	60564	-3.75609	1.7985		
60122	60119	2.39709	1.7176	0.35	3.56
60119	60122	-2.39674	1.7222		
60544	60119	5.10170	1.3624	0.70	3.10
60119	60544	-5.10240	1.3702		
60558	60119	0.25048	1.7465	1.20	3.59
60119	60558	-0.25168	1.7481		
60543	60120	4.54478	1.5457	0.01	3.34
60120	60543	-4.54479	1.5481		
60544	60120	-4.61634	1.6862	2.80	3.52
60120	60544	4.61354	1.6864		
60120	64114	-2.26740	0.8978	0.11	2.45
64114	60120	2.26729	0.9004		
60121	60154	-0.76116	0.9460	0.45	2.52
60154	60121	0.76161	0.9469		
60562	60121	-5.95036	2.0822	0.74	4.00
60121	60562	5.94962	2.0877		
60121	60580	-1.07443	1.8496	4.00*	3.72
60580	60121	1.07843	1.8513		

From	To	Elev Diff (m)	Section Dist (km)	Section Closure (mm)	Allowed Section Closure (mm)
64111	60121	-0.15643	0.0300	0.18	0.77
60121	64111	0.15625	0.0305		
60545	60122	-2.35794	1.4876	0.60	3.27
60122	60545	2.35854	1.4879		
64117	60122	6.52801	0.7815	0.84	2.27
60122	64117	-6.52717	0.7836		
64119	60123	-0.34157	0.0243	0.12	0.77
60123	64119	0.34169	0.0246		
64120	60123	2.43652	0.9501	0.03	2.53
60123	64120	-2.43654	0.9503		
60124	60158	-1.60750	0.6851	0.76	2.11
60158	60124	1.60826	0.6853		
60124	64114	0.02811	0.0385	0.39	0.77
64114	60124	-0.02773	0.0397		
64108	60150	-0.23217	0.0258	0.01	0.77
60150	64108	0.23218	0.0445		
60151	64106	3.42412	1.8014	1.06	3.66
64106	60151	-3.42306	1.8127		
60151	64108	-1.46097	1.6099	2.53	3.42
64108	60151	1.45844	1.6176		
60572	60152	5.55496	1.9169	1.47	3.80
60152	60572	-5.55348	1.9189		
60153	60604	-4.90508	2.1731	2.06	4.10
60604	60153	4.90714	2.1770		
60154	64112	1.27718	0.0552	0.16	0.77
64112	60154	-1.27701	0.0558		
60156	60163	-4.71026	1.9978	1.60	3.90
60163	60156	4.70866	2.0081		
64112	60156	-0.23140	0.8688	0.43	2.40
60156	64112	0.23183	0.8726		

From	To	Elev Diff (m)	Section Dist (km)	Section Closure (mm)	Allowed Section Closure (mm)
60157	60605	3.12248	1.8142	2.35	3.67
60605	60157	-3.12013	1.8263		
60157	60606	-0.46901	1.5435	1.65	3.34
60606	60157	0.47066	1.5453		
60157	60609	-21.55445	1.7208	1.90	3.56
60609	60157	21.55635	1.7330		
60158	64115	0.03448	0.0156	0.02	0.77
64115	60158	-0.03447	0.0157		
60159	64150	9.95360	0.697	1.04	2.13
64150	60159	-9.95255	0.701		
60160	60546	-7.98975	1.2525	0.20	2.96
60546	60160	7.98955	1.2535		
60160	64117	-6.03449	1.7499	0.97	3.60
64117	60160	6.03546	1.7718		
60546	60161	-7.36822	2.4128	0.76	4.38
60161	60546	7.36898	2.4157		
60161	60547	3.04668	1.8850	2.49	3.76
60547	60161	-3.04419	1.8901		
60161	64115	4.66237	2.1334	1.48	4.06
64115	60161	-4.66385	2.1499		
60163	60547	-1.76827	1.5113	0.55	3.30
60547	60163	1.76882	1.5184		
60611	60163	-0.88847	1.4794	0.08	3.26
60163	60611	0.88839	1.4983		
64113	60163	-4.52090	1.4831	0.15	3.26
60163	64113	4.52104	1.4867		
64500	60164	-5.64523	1.2361	0.76	2.93
60164	64500	5.64599	1.2476		
64101	60165	2.20025	1.4649	1.52	3.24
60165	64101	-2.19873	1.5202		

From	To	Elev Diff (m)	Section Dist (km)	Section Closure (mm)	Allowed Section Closure (mm)
60165	64500	-0.50525	0.0948	0.15	0.77
64500	60165	0.50540	0.0962		
60166	64102	-1.67865	0.8471	0.99	2.37
64102	60166	1.67965	0.8506		
60166	64104	-0.21066	0.5305	0.14	1.84
64104	60166	0.21052	0.5307		
60200	60201	5.72941	0.9467	0.12	2.52
60201	60200	-5.72929	0.9504		
60200	60300	-1.27122	1.9937	0.32	3.89
60300	60200	1.27090	2.0530		
60202	60201	3.61009	0.9346	0.97	2.50
60201	60202	-3.61106	0.9383		
60203	60202	5.42975	2.4041	1.51	4.37
60202	60203	-5.43126	2.4046		
60202	60553	-11.36163	1.7102	2.59	3.55
60553	60202	11.35904	1.7111		
60556	60203	-0.78338	1.9622	1.80	3.85
60203	60556	0.78518	1.9674		
60549	60204	-10.10153	1.8170	0.39	3.68
60204	60549	10.10192	1.8323		
60204	60550	7.91853	1.5575	0.10	3.36
60550	60204	-7.91843	1.5634		
60551	60204	8.33712	2.3167	4.08	4.27
60204	60551	-8.33304	2.3293		
60204	60556	-7.14337	1.8468	1.03	3.71
60556	60204	7.14234	1.8507		
60205	60302	-0.28819	0.6386	0.14	2.03
60302	60205	0.28833	0.6672		
60205	60549	-12.70179	2.2505	-2.28	2.97
60549	60205	12.69716	2.2588	2.34	
60549	60205	12.69957	2.2565	-0.06	

From	To	Elev Diff (m)	Section Dist (km)	Section Closure (mm)	Allowed Section Closure (mm)
60206	64134	11.60035	0.8178	2.23	2.32
64134	60206	-11.59812	0.8179		
60206	64135	0.37990	0.1083	0.24	0.81
64135	60206	-0.38014	0.1088		
60553	60207	1.80831	1.9783	0.76	3.87
60207	60553	-1.80755	2.0297		
60207	64133	-8.51890	2.8267	2.09	4.84
64133	60207	8.51681	2.8365		
64135	60207	-1.17229	0.9644	0.84	2.55
60207	64135	1.17313	0.9670		
60212	60208	0.88258	2.5627	0.49	4.55
60208	60212	-0.88306	2.5698		
60208	64132	-5.48923	1.1356	0.77	2.79
64132	60208	5.48845	1.1403		
64133	60208	3.86274	1.5336	1.81	3.32
60208	64133	-3.86455	1.5417		
60209	60210	-4.67188	0.9454	0.40	2.52
60210	60209	4.67228	0.9497		
60548	60209	25.56951	1.7630	2.39	3.61
60209	60548	-25.56711	1.7683		
60210	60551	-5.56265	2.5168	2.67	4.50
60551	60210	5.55998	2.5387		
60210	60552	-3.57918	1.5391	1.16	3.33
60552	60210	3.58034	1.5403		
60214	60211	-3.82677	2.1582	0.22	4.09
60211	60214	3.82655	2.1887		
60211	60552	3.50938	1.8175	1.28	3.68
60552	60211	-3.50810	1.8205		
60211	60567	-6.61963	1.9490	0.57	3.84
60567	60211	6.62020	1.9615		

From	To	Elev Diff (m)	Section Dist (km)	Section Closure (mm)	Allowed Section Closure (mm)
60212	60213	3.36304	2.8391	2.31	4.86
60213	60212	-3.36073	2.8476		
60212	60567	1.09539	2.1824	0.53	4.11
60567	60212	-1.09593	2.1904		
60220	60213	5.26439	1.8498	0.48	3.72
60213	60220	-5.26392	1.8516		
60566	60213	3.30722	1.9956	-0.98	2.75
60213	60566	-3.30506	1.9970	1.18	
60213	60566	-3.30644	1.9983	-0.20	
60557	60214	11.59862	2.7879	1.18	4.80
60214	60557	-11.59979	2.7960		
60566	60214	11.49169	2.0458	1.00	3.95
60214	60566	-11.49069	2.0482		
60548	60215	8.01196	1.8238	2.51	3.69
60215	60548	-8.01447	1.8267		
60215	64654	3.84196	1.4078	0.75	3.16
64654	60215	-3.84271	1.4135		
64655	60215	-0.22658	0.5071	1.03	1.79
60215	64655	0.22761	0.5447		
60217	60216	-4.39538	0.8483	0.50	2.37
60216	60217	4.39488	0.8489		
64653	60216	-0.56743	1.5534	0.23	3.35
60216	64653	0.56766	1.5546		
60557	60217	5.01619	2.6110	0.96	4.60
60217	60557	-5.01523	2.6168		
60217	60560	7.17937	2.3774	1.21	4.34
60560	60217	-7.17816	2.3833		
60217	64122	-3.11321	1.7612	1.11	3.61
64122	60217	3.11210	1.7624		
60265	60218	-3.14681	0.5428	0.45	1.86
60218	60265	3.14727	0.5466		

From	To	Elev Diff (m)	Section Dist (km)	Section Closure (mm)	Allowed Section Closure (mm)
60218	64650	-3.40807	1.1420	0.70	2.80
64650	60218	3.40877	1.1482		
60220	60219	-1.25313	0.6970	0.51	2.13
60219	60220	1.25365	0.7152		
64130	60219	5.37695	2.4033	-2.75	3.42
60219	64130	-5.37335	2.4037	0.85	
60219	64130	-5.37079	2.4039	3.41	
64130	60219	5.37571	2.4053	-1.51	
60220	64129	2.64501	0.1811	0.31	1.05
64129	60220	-2.64531	0.1845		
60221	60257	-8.74462	2.1377	1.78	4.06
60257	60221	8.74640	2.1398		
60221	60259	-3.10886	2.1390	1.65	4.06
60259	60221	3.11051	2.1427		
60221	64129	1.50039	0.1219	0.00	0.86
64129	60221	-1.50039	0.1220		
60554	60250	-9.44009	2.6318	0.17	4.63
60250	60554	9.44026	2.6332		
60250	93022	-18.82047	1.7495	1.96	3.60
93022	60250	18.82242	1.7815		
60252	60251	-7.65482	2.2316	0.45	4.17
60251	60252	7.65437	2.2333		
60251	60555	-10.23455	2.0330	0.90	3.94
60555	60251	10.23545	2.0389		
60251	60565	-2.36890	1.7123	0.82	3.55
60565	60251	2.36808	1.7440		
60252	64134	0.15907	0.0883	0.11	0.77
64134	60252	-0.15896	0.0883		
60254	60253	9.21613	0.6212	0.04	2.00
60253	60254	-9.21609	0.6232		

From	To	Elev Diff (m)	Section Dist (km)	Section Closure (mm)	Allowed Section Closure (mm)
60565	60253	-12.67748	1.8460	0.03	3.71
60253	60565	12.67750	1.8465		
64131	60253	-4.42545	0.7487	1.45	2.21
60253	64131	4.42690	0.7565		
60254	60255	-1.32463	1.1223	1.06	2.78
60255	60254	1.32569	1.1250		
60255	64130	6.93821	0.4290	0.22	1.64
64130	60255	-6.93843	0.4330		
60258	60257	-0.39533	2.3594	0.09	4.32
60257	60258	0.39525	2.3703		
60590	60258	9.26397	1.5772	0.39	3.38
60258	60590	-9.26358	1.5820		
64128	60258	-6.01257	2.3762	1.50	4.34
60258	64128	6.01407	2.3859		
60616	60259	7.97280	1.9767	0.56	3.87
60259	60616	-7.97224	1.9822		
64128	60259	-0.77503	0.0582	0.10	0.77
60259	64128	0.77513	0.0694		
60262	60260	0.39071	0.9864	1.92	2.58
60260	60262	-0.38879	0.9886		
60260	64127	4.03728	0.7410	1.16	2.20
64127	60260	-4.03844	0.7423		
60260	64128	9.75815	2.2373	3.66	4.18
64128	60260	-9.75449	2.2412		
64126	60261	-0.46840	0.2488	0.19	1.23
60261	64126	0.46822	0.2500		
60261	64127	-0.72538	0.4377	0.17	1.66
64127	60261	0.72521	0.4383		
60617	60262	-2.64006	1.2290	0.08	2.92
60262	60617	2.63998	1.2308		

From	To	Elev Diff (m)	Section Dist (km)	Section Closure (mm)	Allowed Section Closure (mm)
60263	60612	-1.50728	2.4219	3.10	4.39
60612	60263	1.51037	2.4244		
64527	60263	0.32354	1.5532	2.67	3.35
60263	64527	-0.32087	1.5560		
64003	60265	-6.37960	0.3458	0.28	1.47
60265	64003	6.37989	0.3469		
60590	60266	4.91034	1.9062	0.63	3.79
60266	60590	-4.90970	1.9587		
60267	60615	-13.32606	1.4604	3.67**	3.23
60615	60267	13.32974	1.4627		
60300	64005	4.27187	1.3912	0.59	3.14
64005	60300	-4.27128	1.3964		
64139	60300	2.95891	1.0165	0.26	2.62
60300	64139	-2.95865	1.0177		
60300	64600	6.44086	1.4291	0.94	3.19
64600	60300	-6.44181	1.4305		
60550	60301	6.20924	1.7181	2.47	3.56
60301	60550	-6.20677	1.7195		
64601	60301	0.16599	1.6860	2.05	3.52
60301	64601	-0.16803	1.7016		
60301	64603	-0.18250	1.5357	1.95	3.33
64603	60301	0.18445	1.5381		
60302	60525	4.53070	1.2071	0.91	2.89
60525	60302	-4.52979	1.2078		
60302	64604	-3.66795	0.4420	0.84	1.67
64604	60302	3.66879	0.4423		
64605	60302	10.22447	1.4376	0.44	3.20
60302	64605	-10.22403	1.4471		
60303	60313	2.04476	2.0129	0.60	3.91
60313	60303	-2.04416	2.0457		

From	To	Elev Diff (m)	Section Dist (km)	Section Closure (mm)	Allowed Section Closure (mm)
60529	60303	-6.97155	1.3345	0.87	3.07
60303	60529	6.97242	1.3679		
60303	64606	-10.95173	1.6832	1.26	3.51
64606	60303	10.95299	1.6839		
64608	60303	15.46323	1.8094	0.55	3.67
60303	64608	-15.46268	1.8422		
60313	60304	-20.68200	1.5442	0.83	3.34
60304	60313	20.68283	1.5529		
60304	64608	3.17383	0.0940	0.63	0.77
64608	60304	-3.17446	0.0940		
60304	93015	6.88991	0.7188	0.27	2.17
93015	60304	-6.89018	0.7261		
60306	60305	-16.18153	2.3911	3.60	4.35
60305	60306	16.18513	2.4440		
60305	60356	-8.82871	1.3942	0.52	3.14
60356	60305	8.82818	1.4020		
60306	60524	7.20430	1.7505	1.31	3.60
60524	60306	-7.20300	1.7585		
64142	60306	9.12234	0.7525	0.00	2.22
60306	64142	-9.12233	0.7550		
64144	60306	2.84815	1.9545	2.16	3.84
60306	64144	-2.84598	1.9705		
60307	60524	-7.43696	1.5160	0.44	3.30
60524	60307	7.43652	1.5219		
60307	60530	-7.64461	1.1036	1.55	2.75
60530	60308	7.88406	0.5841		
60308	60307	-0.24100	1.6825		
60308	60525	-4.99770	1.3155	0.54	3.04
60525	60308	4.99824	1.3236		
60526	60308	-5.46979	1.3634	1.54	3.10
60308	60526	5.46825	1.3692		

From	To	Elev Diff (m)	Section Dist (km)	Section Closure (mm)	Allowed Section Closure (mm)
64144	60311	12.38744	1.7562	0.14	3.60
60311	64144	-12.38730	1.7991		
60311	64146	0.11542	0.0161	0.09	0.77
64146	60311	-0.11551	0.0161		
64147	60311	-7.69531	1.0849	1.39	2.72
60311	64147	7.69671	1.0893		
60526	60312	-2.06432	1.7287	0.35	3.57
60312	60526	2.06467	1.7320		
60528	60312	22.16023	1.9147	0.67	3.80
60312	60528	-22.16090	1.9217		
64149	60312	-1.24144	2.0955	1.96	4.01
60312	64149	1.24340	2.0960		
60313	60531	18.32182	2.3182	1.03	4.27
60531	60313	-18.32079	2.3545		
64150	60314	8.42231	1.1168	0.19	2.77
60314	64150	-8.42212	1.1247		
64151	60314	7.97765	1.1801	0.84	2.02
60314	64151	-7.97911	1.1815	-0.61	
60314	64151	-7.97872	1.1836	-0.23	
64152	60314	-8.33915	1.4514	3.53*	3.22
60314	64152	8.34268	1.4817		
60316	60315	6.10354	1.2750	2.26	2.99
60315	60316	-6.10128	1.3002		
64152	60315	0.01275	0.0248	0.32	0.77
60315	64152	-0.01243	0.0288		
60315	64153	3.72809	0.6844	0.25	2.11
64153	60315	-3.72834	0.6846		
60317	60316	-7.66409	2.6174	0.26	4.61
60316	60317	7.66383	2.6184		
60521	60316	24.62976	1.7600	0.49	3.61
60316	60521	-24.62927	1.7711		

From	To	Elev Diff (m)	Section Dist (km)	Section Closure (mm)	Allowed Section Closure (mm)
60318	60317	16.97816	1.5828	1.43	3.39
60317	60318	-16.97959	1.5838		
60317	64156	-0.19356	0.0245	0.04	0.77
64156	60317	0.19352	0.0245		
64155	60318	-0.39995	0.0265	-0.57	0.61
60318	64155	0.39908	0.0330	0.29	
64155	60318	-0.39932	0.0334	0.05	
60318	64155	0.39915	0.0382	0.22	
60501	60319	-3.31988	1.7087	0.63	3.55
60319	60501	3.32051	1.7088		
64154	60319	13.18264	1.7006	0.93	3.54
60319	64154	-13.18357	1.7009		
60320	60503	-16.62852	1.7827	0.28	3.64
60503	60320	16.62880	1.7842		
60320	64161	8.08973	1.2466	1.19	2.95
64161	60320	-8.08854	1.2474		
64164	60320	-5.73429	1.6110	2.55	3.42
60320	64164	5.73683	1.6526		
60354	60321	-9.97782	1.0542	1.67	2.68
60321	60354	9.97949	1.0692		
60321	60355	-2.50982	1.0705	1.51	2.70
60355	60321	2.51133	1.0796		
60321	64164	-0.26330	0.0418	0.05	0.55
64164	60321	0.26347	0.0435	-0.12	
64164	60321	0.26327	0.0497	0.08	
60322	60355	8.13850	1.2147	0.82	2.90
60355	60322	-8.13768	1.2280		
60322	64165	-2.14519	0.7882	1.45	2.28
64165	60322	2.14664	0.7966		
60323	60502	-29.96074	1.6772	1.37	3.51
60502	60323	29.96212	1.6911		

From	To	Elev Diff (m)	Section Dist (km)	Section Closure (mm)	Allowed Section Closure (mm)
60323	64165	-0.04946	0.0122	-0.07	0.66
60323	64165	-0.04934	0.0239	0.05	
60323	64165	-0.04928	0.0266	0.14	
64165	60323	0.04949	0.0400	-0.08	
60323	64165	-0.04939	0.0401	0.00	
60569	60350	-9.47330	2.2857	1.14	4.23
60350	60569	9.47443	2.2874		
60600	60350	25.89564	2.5999	3.53	4.59
60350	60600	-25.89211	2.6078		
60513	60351	-5.34304	1.2754	0.59	2.99
60351	60513	5.34363	1.2801		
60351	60514	-8.77592	1.5406	3.56	3.33
60514	60351	8.77947	1.5693		
60352	60510	1.02953	1.5921	1.59	3.40
60510	60352	-1.02794	1.5985		
60352	60511	-10.02531	1.6936	0.70	3.53
60511	60352	10.02461	1.7134		
60516	60352	11.50729	1.6393	0.95	3.46
60352	60516	-11.50824	1.6442		
60517	60353	3.94568	1.5921	1.16	3.40
60353	60517	-3.94685	1.5938		
64163	60353	-0.43945	0.0235	0.06	0.77
60353	64163	0.43951	0.0309		
60354	64163	-0.50362	0.3782	0.34	1.54
64163	60354	0.50396	0.3891		
64005	60356	-6.23657	1.1864	1.21	2.86
60356	64005	6.23536	1.1878		
60357	60568	12.79525	2.1190	1.04	4.04
60568	60357	-12.79628	2.2032		
64553	60357	-0.75657	0.0575	0.08	0.77
60357	64553	0.75665	0.0577		

From	To	Elev Diff (m)	Section Dist (km)	Section Closure (mm)	Allowed Section Closure (mm)
93023	60357	-1.95903	0.3326	0.61	1.44
60357	93023	1.95964	0.3348		
60358	64551	-0.28588	0.0162	0.09	0.77
64551	60358	0.28579	0.0179		
60358	93021	-22.38647	1.3869	1.17	3.13
93021	60358	22.38764	1.9862		
60400	60503	25.72014	1.8525	1.95	3.72
60503	60400	-25.71820	1.8822		
60400	64662	2.85011	0.5142	0.42	1.81
64662	60400	-2.84968	0.5145		
64663	60400	-1.19580	0.0688	0.49	0.54
60400	64663	1.19586	0.0680	0.27	
60400	64663	1.19657	0.0695	0.27	
60504	60401	-8.76203	1.3659	2.24	3.11
60401	60504	8.76427	1.3662		
60401	60537	5.81494	1.9396	1.05	3.83
60537	60401	-5.81390	1.9444		
60401	64665	-2.32382	0.3504	0.47	1.48
64665	60401	2.32336	0.3561		
60402	64168	0.04062	0.0174	0.08	0.77
64168	60402	-0.04054	0.0182		
64169	60402	-4.94420	0.6331	0.44	2.02
60402	64169	4.94375	0.6332		
60403	60536	14.38532	1.9069	1.18	3.79
60536	60403	-14.38650	1.9124		
60537	60403	5.47964	1.7462	0.78	3.59
60403	60537	-5.48042	1.7616		
60403	60538	4.74650	1.4178	0.28	3.18
60538	60403	-4.74622	1.4192		
60404	60405	4.66542	1.3391	0.17	3.07
60405	60404	-4.66525	1.3568		

From	To	Elev Diff (m)	Section Dist (km)	Section Closure (mm)	Allowed Section Closure (mm)
60535	60404	15.31365	1.8379	1.76	3.70
60404	60535	-15.31189	1.8647		
64172	60405	5.05226	1.3890	0.38	3.14
60405	64172	-5.05264	1.3905		
60405	64173	0.32820	0.0191	0.03	0.77
64173	60405	-0.32823	0.0191		
60457	60406	12.25665	1.9159	0.60	3.80
60406	60457	-12.25605	1.9719		
60406	64174	0.43427	0.0304	0.09	0.77
64174	60406	-0.43418	0.0307		
64007	60450	5.14027	1.6801	0.60	3.51
60450	64007	-5.13967	1.6822		
60450	64575	0.25262	0.0106	0.04	0.77
64575	60450	-0.25257	0.0120		
60508	60451	-19.51252	2.1647	0.89	4.09
60451	60508	19.51342	2.1719		
64578	60451	2.16201	0.8110	1.38	2.31
60451	64578	-2.16339	0.8249		
60453	60452	0.42499	1.6746	1.60	3.50
60452	60453	-0.42340	1.6890		
64578	60452	-1.20996	1.3014	0.80	3.02
60452	64578	1.20915	1.3066		
60507	60453	-0.26276	1.5565	0.23	3.35
60453	60507	0.26253	1.5630		
60506	60454	0.14984	1.7811	2.14	3.63
60454	60506	-0.14770	1.7901		
60507	60454	-3.92456	1.5948	0.39	3.40
60454	60507	3.92417	1.5974		
60455	60505	7.57817	2.1532	2.90	4.08
60505	60455	-7.57527	2.1673		

From	To	Elev Diff (m)	Section Dist (km)	Section Closure (mm)	Allowed Section Closure (mm)
60455	60533	-0.35708	2.5564	0.11	4.54
60533	60455	0.35696	2.5968		
64170	60455	0.13760	0.0162	0.04	0.77
60455	64170	-0.13764	0.0186		
60456	64169	0.12986		0.05	
64169	60456	-0.13000		0.08	
64169	60456	-0.12988		0.03	
60456	64170	1.23836	0.8065	0.09	2.31
64170	60456	-1.23845	0.8318		
64175	60457	0.05635	0.0187	0.14	0.77
60457	64175	-0.05621	0.0193		
60501	64160	14.40352	1.8622	2.13	3.73
64160	60501	-14.40139	1.8696		
64665	60502	-0.29416	1.1147	0.82	2.76
60502	64665	0.29335	1.1421		
60504	64167	19.88019	1.8046	0.34	3.66
64167	60504	-19.87985	1.8559		
60506	64575	-23.20770	1.5683	2.94	3.37
64575	60506	23.21065	1.5748		
60508	60509	-3.42370	1.6722	1.20	3.50
60509	60508	3.42490	1.6765		
60509	60510	9.64443	1.7861	0.46	3.64
60510	60509	-9.64489	1.8028		
60511	60512	11.33573	1.7301	1.19	3.57
60512	60511	-11.33692	1.7361		
60512	60513	-24.59031	2.1097	2.29	4.03
60513	60512	24.59259	2.1099		
60515	60514	-16.62862	2.1424	1.97	4.07
60514	60515	16.63059	2.1551		
64006	60515	3.24084	1.8298	0.58	3.69
60515	64006	-3.24026	1.8304		

From	To	Elev Diff (m)	Section Dist (km)	Section Closure (mm)	Allowed Section Closure (mm)
60516	60517	-13.24614	1.6193	0.45	3.43
60517	60516	13.24570	1.6213		
60519	64147	3.61786	0.6263	0.80	2.01
64147	60519	-3.61867	0.6278		
64148	60519	-0.84393	0.7893	0.01	2.28
60519	64148	0.84392	0.7904		
64150	60519	-9.95256	0.6972	1.05	2.13
60519	64150	9.95360	0.7018		
60528	60529	10.37728	2.3190	2.89	4.27
60529	60528	-10.37439	2.3382		
64154	60531	10.88401	2.0113	3.71	3.91
60531	64154	-10.88772	2.0137		
60533	64172	-7.73298	1.0193	0.30	2.63
64172	60533	7.73268	1.0214		
60534	64001	11.77713	2.5650	0.99	4.55
64001	60534	-11.77613	2.5692		
64176	60534	-23.20627	1.9149	2.93	3.80
60534	64176	23.20334	1.9210		
60535	60536	12.08147	1.4126	2.44	3.17
60536	60535	-12.07903	1.4135		
60540	60541	8.72272	2.3828	1.98	4.34
60541	60540	-8.72074	2.3833		
60543	64111	5.41215	1.1185	0.96	2.77
64111	60543	-5.41119	1.1202		
60545	64118	-7.83041	1.5859	3.21	3.39
64118	60545	7.83361	1.5860		
64553	60554	-4.55740	2.1799	0.86	4.11
60554	64553	4.55655	2.3294		
60555	93022	-12.77648	1.6166	1.92	3.43
93022	60555	12.77840	1.6187		

From	To	Elev Diff (m)	Section Dist (km)	Section Closure (mm)	Allowed Section Closure (mm)
60560	60559	-10.59058	1.9988	1.60	3.90
60559	60560	10.59219	2.0003		
60580	60561	16.45754	1.7824	2.24	3.64
60561	60580	-16.45530	1.7851		
60563	60562	-3.16878	2.0415	0.49	3.95
60562	60563	3.16829	2.0483		
60568	60569	4.07841	2.3002	1.63	4.25
60569	60568	-4.07678	2.3199		
64612	60570	1.12220	1.5727	1.75	3.37
60570	64612	-1.12395	1.5735		
64614	60570	5.94860	1.1482	0.14	2.81
60570	64614	-5.94875	1.1504		
60571	64106	-3.51968	1.8207	0.45	3.68
64106	60571	3.52013	1.8616		
60572	60602	14.18363	2.0601	0.49	3.97
60602	60572	-14.18412	2.0611		
60572	93055	-1.94961	0.0490	0.14	0.77
93055	60572	1.94975	0.0492		
60600	64142	24.95669	2.5270	3.23	4.51
64142	60600	-24.95346	2.5272		
60602	60601	5.71502	1.8727	0.05	3.75
60601	60602	-5.71506	1.8766		
60605	60604	1.40379	1.5823	3.43*	3.39
60604	60605	-1.40036	1.6289		
60606	60607	-1.44914	1.4836	0.99	3.26
60607	60606	1.44814	1.4892		
60607	60608	12.69855	2.2179	4.12	4.15
60608	60607	-12.69443	2.2208		
60608	64108	1.30719	1.8152	1.92	3.68
64108	60608	-1.30527	1.8275		

From	To	Elev Diff (m)	Section Dist (km)	Section Closure (mm)	Allowed Section Closure (mm)
60610	60609	0.22207	1.4951	2.39	3.28
60609	60610	-0.22446	1.4958		
60610	60611	24.95789	1.5938	3.13	3.40
60611	60610	-24.95475	1.5969		
60613	60612	6.01247	2.0180	2.65	3.92
60612	60613	-6.00981	2.0258		
60614	60613	7.93959	1.8341	0.83	3.70
60613	60614	-7.93876	1.8588		
60614	60615	-17.20896	1.3213	0.10	3.05
60615	60614	17.20907	1.3312		
64126	60616	-4.22255	1.7124	1.02	3.55
60616	64126	4.22153	1.7455		
64126	60617	-2.98358	1.1885	1.07	2.87
60617	64126	2.98252	1.1913		
64100	64001	11.22633	0.8690	0.12	2.40
64001	64100	-11.22646	0.8790		
64113	64002	-2.92501	1.8836	1.30	3.76
64002	64113	2.92631	1.9084		
64202	64002	-0.39572	0.0223	0.08	0.77
64002	64202	0.39564	0.0226		
64003	64121	2.77353	1.7969	1.73	3.65
64121	64003	-2.77180	1.8200		
64525	64003	3.76421	1.5635	0.16	3.36
64003	64525	-3.76438	1.5711		
64153	64006	0.99222	1.6235	1.68	3.44
64006	64153	-0.99054	1.6807		
64006	64156	-3.34872	1.1178	1.63	2.77
64156	64006	3.35036	1.1295		
64166	64007	3.81275	0.7789	0.26	2.26
64007	64166	-3.81250	0.7876		

From	To	Elev Diff (m)	Section Dist (km)	Section Closure (mm)	Allowed Section Closure (mm)
64008	64656	-14.64775	2.5476	0.31	4.53
64656	64008	14.64744	2.5902		
64008	64657	1.12200	1.8542	2.02	3.72
64657	64008	-1.11999	1.8552		
64102	64101	2.32577	2.1163	2.59	4.04
64101	64102	-2.32318	2.1175		
64110	64109	-0.06384	0.6718	0.70	2.09
64109	64110	0.06454	0.6739		
64202	64110	4.07243	1.5250	0.67	3.31
64110	64202	-4.07309	1.5253		
64119	64118	-2.27228	0.6910	0.27	2.12
64118	64119	2.27254	0.6917		
64121	64120	-6.67034	0.8179	0.27	2.32
64120	64121	6.67060	0.8197		
64650	64122	13.51506	0.9345	0.21	2.50
64122	64650	-13.51485	0.9356		
64131	64132	-4.10223	1.8247	1.17	3.69
64132	64131	4.10340	1.8270		
64139	93021	-13.60036	2.0682	1.80	3.98
93021	64139	13.60216	2.0752		
64149	64148	-5.06478	1.0126	0.11	2.62
64148	64149	5.06489	1.0207		
64154	64155	16.31690	1.0221	0.23	2.63
64155	64154	-16.31667	1.0235		
64160	64161	1.40742	0.5953	0.39	1.95
64161	64160	-1.40703	0.6104		
64666	64166	7.49104	0.7073	0.58	2.15
64166	64666	-7.49046	0.7589		
64168	64167	-1.82429	0.7043	0.12	2.14
64167	64168	1.82417	0.7112		

From	To	Elev Diff (m)	Section Dist (km)	Section Closure (mm)	Allowed Section Closure (mm)
64173	64174	-5.89661	0.9509	0.01	2.53
64174	64173	5.89663	0.9552		
64176	64175	3.01135	0.8357	0.10	2.35
64175	64176	-3.01125	0.8360		
93056	64525	-18.40858	2.4696	3.81	4.44
64525	93056	18.41239	2.4729		
93056	64527	-13.27879	1.9445	1.56	3.83
64527	93056	13.28034	1.9557		
64552	93023	-6.03541	1.4018	0.12	3.15
93023	64552	6.03553	1.4023		
64575	64576	7.46146	1.6468	0.49	3.47
64576	64575	-7.46194	1.6547		
64577	64576	-1.45328	1.4228	2.45	3.18
64576	64577	1.45083	1.4378		
64578	64577	-19.74079	1.8470	1.54	3.71
64577	64578	19.73926	1.8864		
64601	64600	-13.40404	1.7426	0.35	3.59
64600	64601	13.40369	1.7478		
64604	64603	-4.89864	1.4738	0.05	3.25
64603	64604	4.89860	1.4819		
64605	64606	-6.55288	1.5725	0.70	3.37
64606	64605	6.55218	1.5982		
64610	64611	1.98490	1.5744	2.48	3.38
64611	64610	-1.98242	1.5961		
64610	93015	-15.68387	1.9372	1.41	3.82
93015	64610	15.68528	1.9814		
64615	64614	-0.60560	1.0764	0.26	2.71
64614	64615	0.60587	1.0783		
64653	64654	4.63458	1.6697	1.00	3.50
64654	64653	-4.63357	1.7085		

From	To	Elev Diff (m)	Section Dist (km)	Section Closure (mm)	Allowed Section Closure (mm)
64655	64656	0.99639	1.3830	1.57	3.13
64656	64655	-0.99482	1.3833		
64658	64657	-3.44888	1.2549	0.80	2.96
64657	64658	3.44968	1.2572		
64658	64659	-9.20043	1.5350	0.27	3.33
64659	64658	9.20070	1.5356		
64659	93015	9.36220	0.6139	0.12	1.99
93015	64659	-9.36208	0.6404		
64661	64660	-1.05069	1.5406	0.88	3.33
64660	64661	1.05157	1.5538		
64660	93015	-0.04476	1.4419	0.61	3.21
93015	64660	0.04537	1.4441		
64661	64662	4.86408	1.5655	0.74	3.37
64662	64661	-4.86334	1.6465		
64663	64664	4.82557	1.1375	0.32	2.80
64664	64663	-4.82589	1.1410		
64665	64664	0.08942	0.8051	0.19	2.30
64664	64665	-0.08924	0.8053		
64665	64666	0.03673	1.7181	0.06	3.56
64666	64665	-0.03679	1.7225		

* Outside PB/MK derived tolerance, but within FGCC First-Order Class I

** Outside PB/MK derived tolerance, but within FGCC First-Order Class II

VITA

Name: Peter William DeKrom

Place and Date of Birth: Montreal, Quebec - November 7, 1965

Permanent Address:
8161 S. Poplar Way, Apt 101
Englewood, Colorado
80112

Universities Attended:
Bachelor of Science in Engineering (Surveying), 1990
University of New Brunswick

Publications:
Geodetic Aspects, Design Considerations and Surface
Control Implementations at the Superconducting Super Collider
Greg L. Robinson, Peter W. DeKrom and W.J. Trevor Greening
Presented at the Seventh International FIG Symposium
on Deformation Surveys, Banff, Alberta, 1993